R 116

THE AEROBRAKING SPACE TRANSFER VEHICLE

APRIL, 1990

VIRGINIA TECH AEROSPACE SENIOR DESIGN TEAM

THE AEROBRAKING SPACE TRANSFER VEHICLE

VIRGINIA TECH AEROSPACE SENIOR DESIGN TEAM
Glen Andrews
Brian Carpenter
Steve Corns
Robert Harris
Brian Jun
Bruce Munro
Eric Pulling
Amrit Sekhon
Walt Welton
Dr. A. Jakubowski

Abstract

With the advent of the Space Station and the proposed Geosynchronous Operation Support Center (GeoShack) in the early 21st century, the need for a cost-effective, reusable orbital transport vehicle has arisen. This transport vehicle will be used in conjunction with the Space Shuttle, the Space Station, and GeoShack. The vehicle will transfer mission crew and payloads between low earth and geosynchronous orbits with minimal cost. Recent technological advances in thermal protection systems such as those employed in the Space Shuttle have made it possible to incorporate an aerobrake on the transfer vehicle to further reduce transport costs. This report presents the research and final design configuration of the aerospace senior design team from Virginia Polytechnic Institute and State University working in conjunction with NASA and the direction of Dr. A. Jakubowski. The report addresses the topic of aerobraking and focuses on the evolution of an Aerobraking Space Transfer Vehicle (ASTV).

Table of Contents

NOMENCLATURE 1

1. INTRODUCTION 2
1.1 FOUNDATIONS OF THE ASTV 2
1.1.1 PROJECT BACKGROUND 2
1.1.2 RATIONALE FOR A SPACE BASED AEROBRAKING SYSTEM 2
1.2 DESIGN CRITERIA 3
1.3 MAJOR MISSION ASSUMPTIONS 3
1.4 MISSION SCENARIOS 4
1.5 EVOLUTION OF THE ASTV CONFIGURATION 5
1.5.1 AEROBRAKE SELECTION 5
1.5.2 VEHICLE LAYOUT 6
1.5.3 PRELIMINARY CONFIGURATION 9

2. FLIGHT DYNAMICS 17
2.1 ORBITAL MECHANICS 17
2.1.1 MINIMIZING TOTAL ΔV REQUIREMENTS 17
2.1.2 ΔV REQUIREMENTS 19
2.1.3 PROPELLANT REQUIREMENTS 22
2.1.4 AEROBRAKING VS. ALL-PROPULSIVE TRANSFER 24
2.2 AEROBRAKING MANEUVERS 25
2.2.1 AEROBRAKING PHASE 25
2.2.2 AEROBRAKE REQUIREMENTS 29
2.2.3 AEROBRAKE ANALYSIS 29
2.2.4 AERODYNAMIC FORCE CALCULATIONS 30
2.2.5 AEROBRAKE STABILITY AND CONTROL 32
2.2.6 LIMITATIONS ON CG POSITION DUE TO WAKE EFFECTS 36

3. PROPULSION 39
3.1 ASTV ENGINE DESIGN 39
3.1.1 DESIGN CONSIDERATIONS 39
3.1.2 ENGINE SPECIFICATIONS 39
3.1.3 ENGINE DIMENSIONS AND MASS 42
3.1.4 CONFIGURATION 44
3.2 PROPELLANT HANDLING 50
3.2.1 PROPELLANT ACQUISITION 50
3.2.2 PROPELLANT LINES 51

4. STRUCTURES 53
4.1 FRAME 53
4.1.1 MATERIALS 53
4.1.2 FRAME COMPONENTS 55
4.1.3 STRUCTURAL ANALYSIS 57
4.1.4 FRAME SPECIFICATIONS 59
4.1.5 EARTH-TO-ORBIT DELIVERY 60
4.2 AEROBRAKE 63
4.2.1 DIMENSIONS 63
4.2.2 GEOMETRICAL PROPERTIES 63

4.2.3 STRINGERS 65
4.2.4 THERMAL PROTECTION SYSTEM 65
4.3 CARGO MODULE 66
4.3.1 DIMENSIONS 66
4.3.2 CARGO MODULE DESIGN 68
4.4 CREW MODULE 74
4.4.1 DIMENSIONS/CONSTRUCTION 75
4.4.2 LIFE SUPPORT 78
4.5 PROPELLANT TANKS 80
4.5.1 DISPOSABLE TANKS 80
4.5.2 PERMANENT TANKS 85
4.5.3 INSULATION 86
4.5.4 IMPACT PROTECTION 86

5. RCS SYSTEM 89
5.1 MOMENTS OF INERTIA 89
5.2 SIZES 89
5.3 PROPELLANT TYPE 90
5.4 LOCATIONS 90
5.5 PROPELLANT REQUIREMENTS 93

6. GUIDANCE, NAVIGATION AND CONTROL 96
6.1 REQUIREMENTS 96
6.2 MAIN COMPONENTS 96

7. POWER SYSTEMS, COMMUNICATIONS AND DATA MANAGEMENT 98
7.1 POWER SYSTEMS 98
7.2 COMMUNICATIONS AND DATA MANAGEMENT 100
7.2.1 COMMUNICATIONS 100
7.2.2 DATA MANAGEMENT 100

8. DOCKING TO SPACE STATION, ASSEMBLY, AND MAINTENANCE 103
8.1 DOCKING 103
8.2 HANGAR AT SPACE STATION 103
8.3 GENERAL COST ANALYSIS 103

SUMMARY 105

Appendix A. : FLIGHT PLAN ANALYSIS 106

List of Illustrations

Figure 1. Typical ASTV Mission Scenario 4
Figure 2. Eight General Layouts of the ASTV 7
Figure 3. Disposable Tank Configuration - Top View 12
Figure 4. Disposable Tank Configuration - Side View 13
Figure 5. Disposable Tank Configuration - Front View 13
Figure 6. Disposable Tank Configuration - Isometric View 14
Figure 7. Bi-Elliptic Transfer 17
Figure 8. Combined Burn at GEO 18
Figure 9. ΔV Requirements 18
Figure 10. LEO to GEO Transfer 19
Figure 11. Ejection 20
Figure 12. De-Orbiting Burn at GEO 21
Figure 13. Burn to Circularize at Phasing Orbit 21
Figure 14. Transfer From Phasing Orbit to LEO 22
Figure 15. Propellant Requirements Per Mission 23
Figure 16. Atmospheric Deceleration 27
Figure 17. Heating Rate (Stagnation) 27
Figure 18. Total Heat Absorbed 28
Figure 19. Dynamic Pressure 28
Figure 20. Aerobrake Analysis 30
Figure 21. Determination of Overall Center of Pressure 32
Figure 22. Effect of Pitch Angle on Pitching Moment Coefficient 33
Figure 23. Flight Configuration of Aerobrake With Center of Pressure 34
Figure 24. Effect of Roll Angle on Roll Moment Coefficient 35
Figure 25. Effect of Yaw Angle on Yaw Moment Coefficient 36
Figure 26. Aerobrake Protection Zone 37
Figure 27. ASTV Engine Propellant Flow Diagram 41
Figure 28. Throat/Combustion Cooling Configuration 42
Figure 29. ASTV Engine Dimensions 43
Figure 30. Dual Engine Configuration Layout 46
Figure 31. Engines in Stowed Position 47
Figure 32. Thrust Vectoring through Extreme CG Locations 47
Figure 33. ASTV Engine Mount 48
Figure 34. Limitations on Engine Yaw Gimballing 49
Figure 35. Exhaust Impingement Problem Arising During Parallel Yaw 49
Figure 36. Propellant Flow Schematic 51
Figure 37. ASTV Frame 54
Figure 38. Material Characteristic Comparison 55
Figure 39. Typical Fiber Orientation 56
Figure 40. Frame Spine Member 56
Figure 41. Aluminum Endfitting and Aerobrake Connection Assembly 57
Figure 42. Deflections in Aerobrake Maneuver - Front View 58
Figure 43. Deflections in Aerobrake Maneuver - Side View 58
Figure 44. Deflections in Thrusting Maneuver - Bottom View 59
Figure 45. Deflections in Thrusting Maneuver - Side View 59
Figure 46. Frame Partitioning For Delivery 60
Figure 47. Frame Fore and Aft Section Joining 61
Figure 48. Frame Final Payload Configuration - Side View 61

Figure 49. Frame Final Payload Configuration - Front View 62
Figure 50. Frame Final Package in Payload Area 62
Figure 51. Aerobrake Geometry 64
Figure 52. Aerobrake Stringer Configuration 65
Figure 53. Radial Section View of Cargo Module 67
Figure 54. Transverse Section View of Cargo Module 67
Figure 55. Detail of Cargo Module Stringer 68
Figure 56. Detail of Cargo Module Edge 69
Figure 57. Detail of Rib and Foot 69
Figure 58. Cross Section of Rib and Foot 70
Figure 59. Automatic Positioning During Cargo Module Installation 71
Figure 60. Detail of Mounting Rail 71
Figure 61. Power Supply Outlet Locations 72
Figure 62. Payload Attachment Point Locations 73
Figure 63. Crew Module Layout - Top View 74
Figure 64. Crew Module Layout - Front View 75
Figure 65. Crew Module Structure - Side View 77
Figure 66. Crew Module Structure - Front View 78
Figure 67. External Schematic of Propellant Tank 82
Figure 68. External Side View of Propellant Tank 83
Figure 69. Tank Section View A-A 84
Figure 70. Tank Release Mechanism 85
Figure 71. Cross-Section of Permanent Tank 86
Figure 72. RCS Locations 91
Figure 73. RCS Package View 1 92
Figure 74. RCS Package View 2 92
Figure 75. RCS Retractor 93
Figure 76. Four Point Docking Grapple 104

List of Tables

Table 1. Comparison of Aerobrakes 5

Table 2. Comparison of Configurations 9

Table 3. Propellant Mass per Mission Phase 24

Table 4. Oxygen and Hydrogen Breakdown per Mission 24

Table 5. Aerobraking vs. All-Propulsive Transfer 25

Table 6. Variation of Cpmax during Aerobraking Pass 31

Table 7. Stability Derivatives at $\alpha = 13.25°$ 32

Table 8. ASTV Main Engine Parameters 40

Table 9. Factors Influencing Propellant Selection 44

Table 10. Comparisons of Single and Dual Engine Configurations 44

Table 11. Frame Material Candidates 54

Table 12. Frame Specifications 60

Table 13. Aerobrake Geometrical Properties 63

Table 14. Mass Estimate for Cargo Module 74

Table 15. Weight Summary of Crew Module 76

Table 16. Tanks 80

Table 17. Tank Shielding and Insulation 87

Table 18. Mass and Moments of Inertia 89

Table 19. RCS Dimensions 90

Table 20. Fuel Type Considerations 90

Table 21. RCS Angular and Linear Acceleration 91

Table 22. GN&C Main Equipment 97

Table 23. Electrical Power Subsystem Components(Manned Mission) 99

Table 24. Power Requirements 99

Table 25. Communications and Data Handling 101

NOMENCLATURE

ASTV	Aerobraking Space Transfer Vehicle
GEO	Geosynchronous Earth Orbit
GN&C	Guidance, Navigation and Control
LEO	Low Earth Orbit
MLI	Multilayer Insulation
OTV	Orbital Transfer Vehicle
RCS	Reaction Control System
SS	Space Station
TDRSS	Tracking Data Relay Satellite System
TPS	Thermal Protection System

1. INTRODUCTION

1.1 FOUNDATIONS OF THE ASTV

1.1.1 PROJECT BACKGROUND

In 1986, several ambitious projects were submitted by the U.S. National Commission on Space as a recommendation to the White House for the next 50 years. One of these endeavors involved stationing a Geosynchronous Operations Support Center at GEO for the purpose of servicing high value space structures at this orbit. This center would also serve as a base to support a crew for missions lasting a few days each. The crew and the payload would be delivered to GEO from LEO by an Aerobraking Space Transfer Vehicle based at the Space Station.

The 1990 senior class in the Aerospace and Ocean Engineering Department at Virginia Polytechnic Institute and State University engaged in the design of such a cost efficient, manned/unmanned transfer vehicle that would support GeoShack.

1.1.2 RATIONALE FOR A SPACE BASED AEROBRAKING SYSTEM

The concept for the ASTV evolves from the idea of using a space-based transportation system. The primary benefit of space-basing the vehicle is that it allows reuse of the upper stage, thus avoiding repeated expenditures with each trip. In addition, the structure can be of a lighter design since the earth launch acceleration will not be a factor. Another benefit of space-basing is that expended stages do not become orbital debris.

To minimize costs in delivering a payload to geosynchronous orbit, the ASTV design uses atmospheric drag of an aerobrake to slow the vehicle to the required LEO orbital velocity on its return leg from the higher energy orbit. This leads to an overall reduction of required propulsive ΔV. To justify the use of an aerobrake, several criteria were met in the design:

- The aerobrake must be able to protect the vehicle from atmospheric heating.
- The vehicle structure must be able to withstand the thermal loadings and the aerodynamic forces during the aeropass.
- The mass of the aerobrake must not exceed the mass of the fuel which would be saved by the aerobraking procedure.

1.2 DESIGN CRITERIA

A list of objectives was established as a guide throughout the ASTV design process. Several major design criteria of the ASTV include:

1. Minimize mission costs
2. Offer dependability and safety
3. Maximize flexibility

The ASTV is designed to save money. The vehicle is reusable, requires less propellant compared to expendable earth-launched vehicles, uses a fuel efficient engine, and incorporates a light but strong frame. These are only a few of several ways that mission costs will be reduced.

As with all high speed vehicles, there is always a possibility of catastrophic failure. The factor of safety is critical for a manned ASTV, and the design of the vehicle must therefore anticipate any worst case scenarios such as engine failure, power failure, or even a solar flare (in which a large factor of safety in the radiation shielding proves to be crucial to the safety of the crew).

The ASTV is also designed with maximum flexibility in the range of mission variations it can conduct. The vehicle meets and surpasses the following mission requirements:

1. Mission 1: Deliver 6,000 lbm round trip between the Space Station and GeoShack
2. Mission 2: Deliver 20,000 lbm to GeoShack and return empty
3. Mission 3: Deliver 28,000 lbm to GeoShack and dispose vehicle into a higher orbit

Furthermore, the configuration is designed to easily accommodate payloads consisting of cargo, a maximum crew of three, or a combination of cargo and crew.

In addition to delivering payloads to GEO, the vehicle can be used to retrieve satellites for maintenance at the GeoShack or Space Station. These types of missions would require several modifications, one being the installation of a remote manipulator arm.

1.3 MAJOR MISSION ASSUMPTIONS

For the purpose of this project it was assumed that GeoShack will be ready for deployment to GEO circa 2020, and that the Space Station will be fully operational in LEO to support the ASTV missions. Additional assumptions include:

- hangar space provided at SS to shield ASTV from radiation and debris
- airlock system provided at SS and at GeoShack
- propellant, maintenance, and replenishments supplied by SS
- remote manipulator arms at SS and at GeoShack to load and unload mission modules

Furthermore, the next few decades will see advancements primarily in the areas of materials/composites and engine design. All materials for the ASTV will be selected from current inventories; however, these materials have not been proven or tested in space. The engines for the ASTV have been designed with slightly higher specifications to account for future technology improvements.

1.4 MISSION SCENARIOS

The typical mission of the ASTV is to deliver a payload, possibly including a maximum crew of three, from LEO to GEO. Figure 1 on page 4 illustrates the overall mission profile. The baseline mission consists of four phases: traveling from LEO to GEO, unloading and returning to the Earth's atmosphere, making the aeropass, and finally docking at the Space Station.

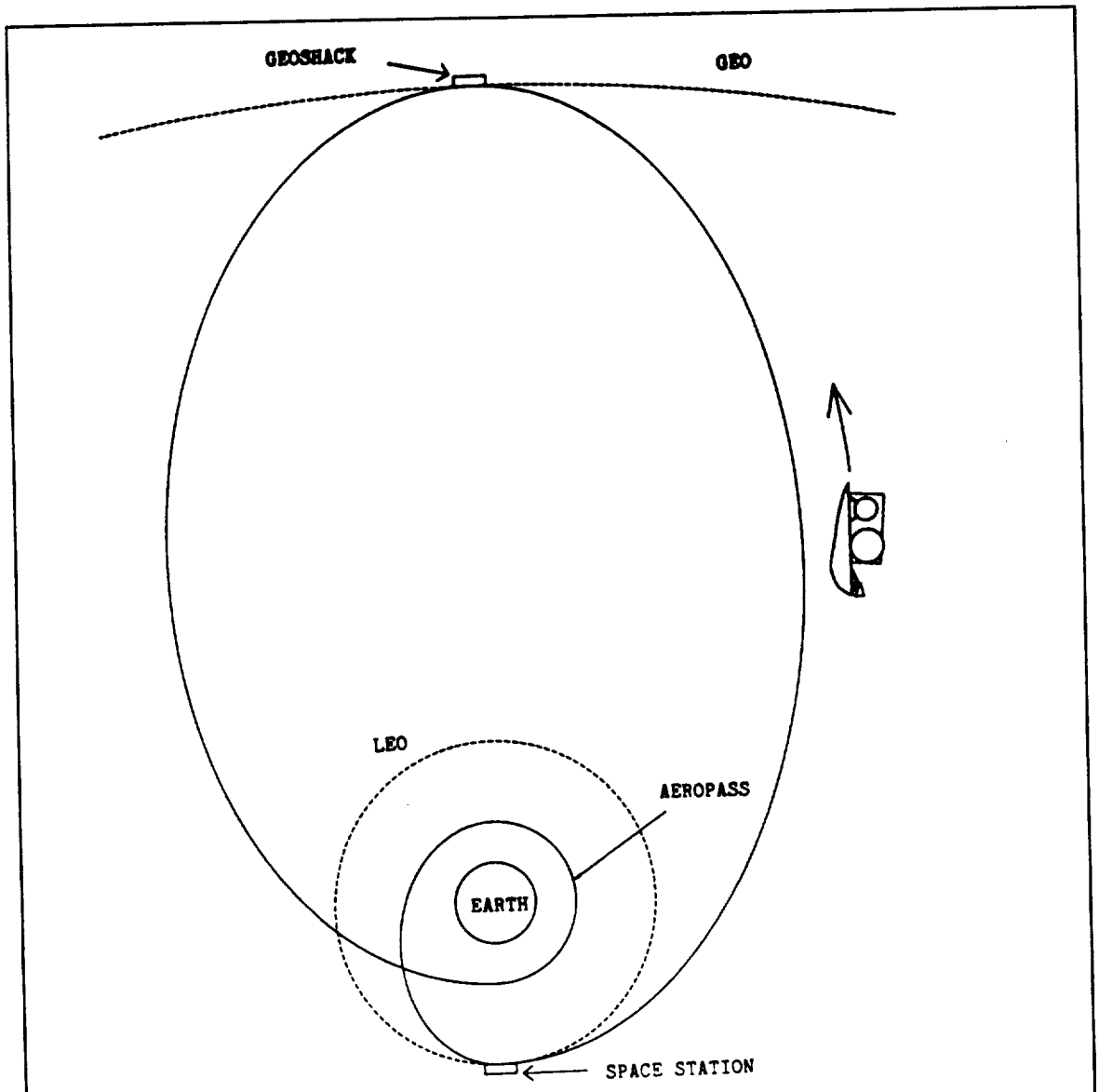

Figure 1. Typical ASTV Mission Scenario

The mission originates at the Space Station which is based in a low earth orbit (200 miles). The Space Station provides the propellant and other necessities to fulfill the mission requirement. At this point, the aerobrake can be removed from the vehicle if the mission is to deliver a payload to GEO with no return trip, thereby avoiding loss of the aerobrake. Once the cargo and/or crew has been transferred to the ASTV from the Space Station or the Space Shuttle, the ASTV disconnects from the Space Station, and slowly progresses to a safe distance to fire its main engines. The trajectory of the vehicle is a Hohmann transfer which places the vehicle at GEO.

Upon reaching GEO, the ASTV fires its main engines to circularize and change orbital planes at this orbit. The ASTV can then deploy the cargo if required, or it can rendezvous at GeoShack to unload and conduct extravehicular activities. Having fulfilled its mission at this orbit, the ASTV is either disposed into a higher orbit, or it returns back to the earth's upper atmosphere.

The aerobraking phase of the mission begins when the ASTV reaches an altitude of approximately 400,000 ft, and continues through to a perigee of approximately 277,000 ft. By using atmospheric drag, the ASTV is able to decelerate significantly so that upon exiting the atmosphere, the vehicle will be on a trajectory having an apogee of 350 miles. During this aeropass, the aerobrake not only shields the vehicle from excessive thermal heating, but also provides some lift, enabling the vehicle to make a small plane change.

After leaving the atmosphere, the vehicle's exit velocity carries it to an apogee at the phasing orbit altitude. Once any orbital corrections have been made at the phasing altitude, the vehicle proceeds to LEO. Rendezvous and docking with the Space Station concludes the mission.

1.5 EVOLUTION OF THE ASTV CONFIGURATION

Using the requirements and primary goals as a guide in the design process, the ASTV's configuration evolved through many changes to its final form. The justifications for the arrival at this configuration will now be discussed.

1.5.1 AEROBRAKE SELECTION

The first major task involved the selection of an aerobrake and its shape. The two candidates were a rigid aerobrake and a ballute aerobrake. The advantages and disadvantages are compared in Table 1. Based on this comparison a rigid aerobrake was selected.

Table 1. Comparison of Aerobrakes

Characteristics	Rigid Aerobrake	Ballute Aerobrake
Simplicity	+	
Weight	–	+
Potential to be a Lifting Body	+	
Durability	+	
Need for an Inflation System		–
Added Rigidity to Vehicle	+	
Reliability	+	

This rigid aerobrake has a raked cone shape. There were several reasons for selecting this type of aerobrake:

1. NASA has considered the raked cone aerobrake in some of its preliminary designs for an aerobraking space transfer vehicle. NASA has conducted wind tunnel tests of the aerobrake, and also plans to conduct an actual flight test of a vehicle utilizing the raked-cone aerobrake. This will provide valuable data on the performance of this type of aerobrake.

2. The unsymmetrical shape of the aerobrake gives it increased stability compared to a spherical aerobrake. The spherical aerobrake has no preferred trim angle of attack, and is therefore neutrally stable. Conversely, the raked cone aerobrake seeks a given trim angle of attack and is stable about that point. Such stability is desirable at the high velocities at which the aerobrake will enter the atmosphere. Sudden fluctuations in atmospheric density will therefore not cause loss of control.

3. This shape has a moderate lift-to-drag ratio which allows the vehicle to perform a greater range of flight maneuvers. One of these would be a plane change maneuver. Doing this maneuver within the atmosphere lowers overall mission propellant requirements.

1.5.2 VEHICLE LAYOUT

Having selected a rigid aerobrake, the vehicle's overall layout was chosen. The layout includes placement and alignment of the engine(s), mission module, and propellant tanks. Eight configurations were analyzed, and these are shown in Figure 2 on page 7.

Engine position was restricted to four locations:

- top mounted for firing opposite the aerobrake, and directly attached to the aerobrake structure; requires two engines for stability
- rear mounted for firing similar to the top mounted engines except they are centrally located behind the cargo modules
- bottom mounted for firing through the aerobrake, and located between the aerobrake and the cargo module
- side mounted for firing parallel to the plane of the aerobrake

The mission module alignment was allowed to be either longitudinal or transverse. For longitudinal alignment, the axis of the cylindrical module is parallel to the thrust vector except for the case of top mounted engines, where the axis is parallel to the line joining the two engines. For transverse alignment, the cylinder axis is perpendicular to the thrust vector, or, in the case of the top mounted engines, perpendicular to the line joining the two engines.

JUDGING CRITERIA

The previous configurations were judged based upon the following:

1. CG location (during thrusting and aerobraking)
2. Ease of cargo module loading
3. Ease of docking
4. Flexibility to handle combinations of crew or cargo module
5. Size and complexity of structure
6. Possibility of engine failure

CG LOCATION

Center of gravity location is an important factor for choosing the ASTV configuration. It affects the spacecraft's maneuverability, stability and structural stresses.

Propellant initially makes up the majority of the spacecraft's mass. Thus, the CG will initially be controlled by the position of the fuel tanks. During thrusting maneuvers, stability will be enhanced if the engines are located near the CG. The bottom-engine configurations share this feature, while the rear-engine and side-engine configurations do not. During the aerobraking phase stability becomes even more important, and the CG should be located reasonably close to the aerobrake. The rear-engine configurations and the bottom-engine/longitudinal configuration will have their CG located slightly further from the aerobrake than the other configurations, and thus will have a greater tendency to become unstable.

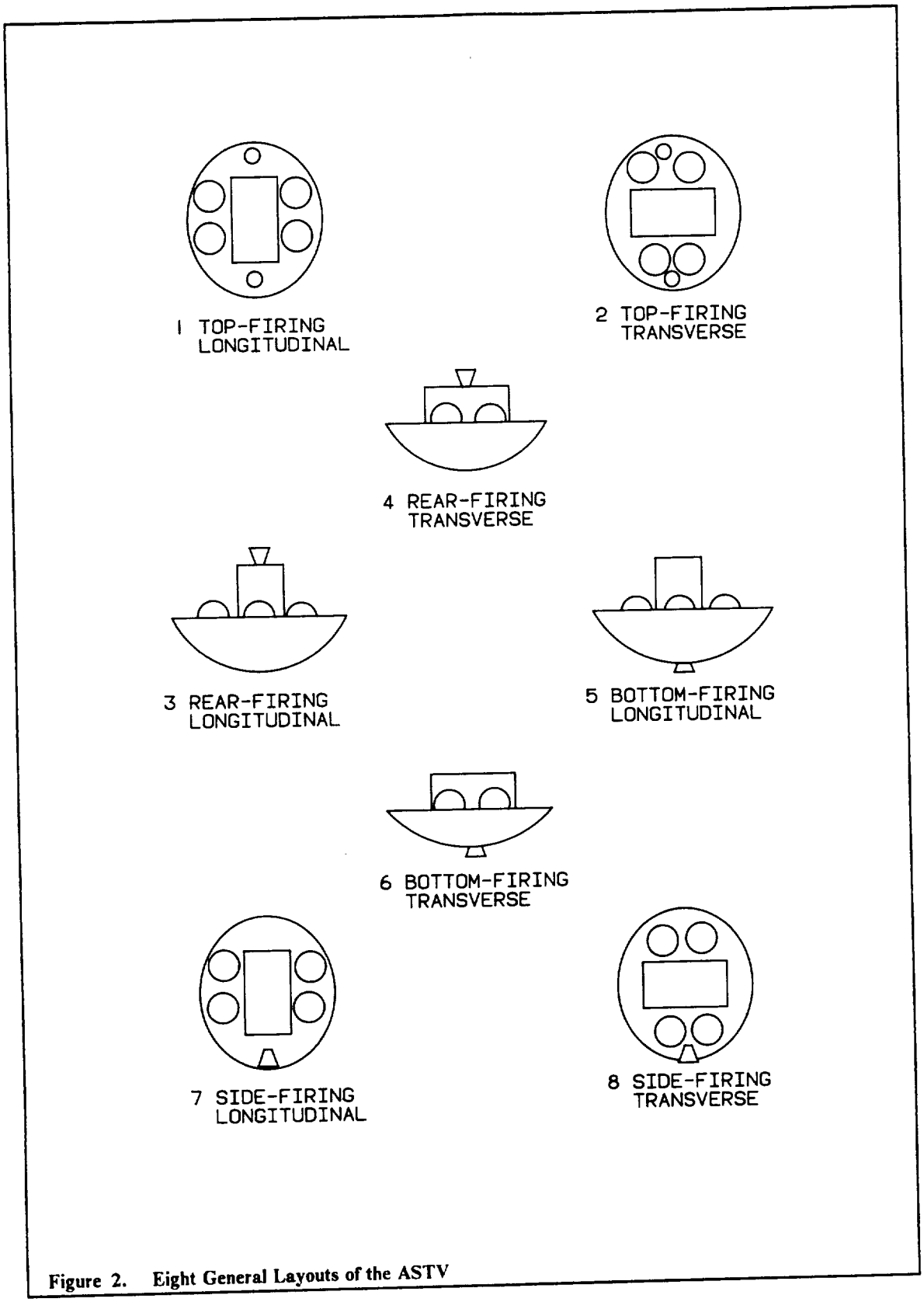

Figure 2. Eight General Layouts of the ASTV

EASE OF CARGO MODULE LOADING

The ASTV must be capable of accepting and transporting various sized mission modules. These modules must be easy to attach and remove. If astronauts perform this job, then the difficulties of working in the space environment must be considered. If robots perform the task, then the limitations of these machines will have to be considered. Thus, ease of installation and removal is essential in both cases.

Only the two configurations having rear mounted engines pose loading difficulties. In these two configurations, the structure connecting the engine and aerobrake restricts movement of the modules during loading. The module would have to be loaded from the side, and care would have to be taken so as not to strike the engine supporting structure.

In all other configurations, the modules can be loaded either from the side or from the top. The structures of these configurations are not protruding, and thus do not hinder the installation of the modules.

EASE OF DOCKING

The ASTV must be able to dock with both the Space Station and GeoShack via a standard Space Station docking interface. Thus, a strategically positioned ASTV docking port simplifies the task of docking and minimizes the amount of docking space used.

The bottom-engine/transverse configuration and both the top and side-engine configurations have relatively low profiles. The docking port would be positioned on the cargo module opposite the aerobrake. The ASTV could then be easily maneuvered and attached to the docking interface. The disadvantage of this set-up is that the aerobrake takes up a relatively large amount of docking space.

It is also possible to have the docking port positioned on one of the flat sides of the cargo module if the docking interfaces on the Space Station/GeoShack are long enough. All transverse configurations would support this set up, as well as the side-engine/longitudinal configuration. With such a set up, the ASTV could be rotated about the docking port to an optimum docking position.

The rear-engine/longitudinal configuration does not allow the ASTV to dock as a complete craft, unless, by some unlikely chance, the Space Station/GeoShack docking interfaces are long enough to extend over the aerobrake to the cargo module.

FLEXIBILITY TO HANDLE DIFFERENT COMPONENTS

The ability to add cargo modules, crew modules, or a combination of the two to fulfill the mission requirement should be weighed heavily when comparing configurations. In configurations 5 and 6 problems occur due to engine placement. In configurations 7 and 8, the bottom placement of the engine frees the top half for easy shifting of the modules. In configurations 7 and 4 the engine thrust vector passes through the mission module axis, thereby freeing the chore of balancing the center of gravity.

SIZE AND COMPLEXITY OF STRUCTURE

Having a simple yet sturdy structure helps decrease the empty mass of the ASTV. A simple structure also costs less to build and can be repaired more easily. The rear-engine and bottom-engine configurations have increased structural complexity due to positioning of the engines.

The structure for the rear-engine configurations must be designed to transfer the thrusting force from the engine down to the aerobrake, propellant tanks, and cargo module. This is analogous to having to support a heavy weight at the end of a long pole. The structure for these configurations will therefore tend to be bulky and complex.

The structural complexity of the bottom-engine configurations is increased because the aerobrake must have a panel which can be opened and closed. Actuators must open the panel during thrusting maneuvers to allow the engine to fire, and close it during reentry maneuvers to protect the engine nozzles. Such an aerobrake would not be as structurally reliable as a solid aerobrake. It may have fatal consequences in the event of a leak in the seal of these engine doors.

POSSIBILITY OF ENGINE FAILURE

There is always a possibility that a rocket engine will fail. Even though having two engines doubles the probability that an engine may fail, having two smaller engines as opposed to one larger engine is still beneficial. If one engine fails, then the other would still be able to transport the crew back to safety.

The bottom-engine configuration would most likely be limited to one engine in order to reduce the size of the panel which must be opened and closed. The side-engine/transverse configuration would probably also be limited to a single engine. The propellant tanks' positions do not allow two engines to be placed side by side. The option of stacking two engines is also eliminated because the upper engine would not be well protected by the aerobrake. All other configurations could have two engines.

The only configurations which actually require two engines are the top-engine configurations as shown in Figure 2 on page 7. The benefit of engine redundancy is lost in these cases because the craft is uncontrollable in an engine out scenario.

CONCLUSION ON LAYOUT

The rear-engine configurations had the most disadvantages relative to the others. Both rear-engine configurations were at a disadvantage when it came to ease of cargo module loading, CG location, and structural complexity. In addition, the rear-engine/longitudinal configuration did not support easy docking. The bottom-engine configurations had problems with component accessibility and structural complexity. Finally, the top and side-engine configurations did well in all but one category. The top-engine configurations had problems with engine failure, while the side-engine configurations had slightly worse CG locations.

Based on these judgements, the side-engine configurations appears to offer the most advantages. A summary of these comparisons is presented in Table 2.

Table 2. Comparison of Configurations

Judging Criteria	Configurations: 1	2	3	4	5	6	7	8
C.G. Locations: Thrusting							+	+
Aerobraking					−	−	−	−
Ease of Cargo Module Loading					−	−		
Ease of Docking				+	−	−	+	+
Flexibility				+	−	−	+	+
Size/Complexity of Structure					−	−	−	−
Accommodation of Two Engines		+		+				

(+) favorable
(−) unfavorable
( ) no benefits

1.5.3 PRELIMINARY CONFIGURATION

After selecting a general layout, the next task involved creating several preliminary proposals to base the final configuration on. These proposals were created based on four criteria.

1. Side-firing double engine configuration
2. Minimal cross-sectional area from the top view to reduce the size of the aerobrake, thereby reducing the overall vehicle weight and mission cost.

3. Relatively simple superstructure interconnecting the cargo module, crew module, fuel tanks, engines, and aerobrake. This allows the aerobrake to be detached for the expendable mission and the cargo or crew modules to be shifted to obtain a favorable center of gravity position for the aeropass.

4. Individual components such as propellant tanks, cargo module, and crew module must be size limited for the initial delivery to LEO using current volumetric launch capabilities (15 ft dia. x 60 ft).

Four different configurations were created. These are discussed next.

TORROIDAL AND ELLIPTICAL TANK CONFIGURATIONS

The torroidal design utilized a symmetric aerobrake with a radius of approximately 42 ft. One oxygen tank was placed in front of the mission module and two hydrogen tanks were placed on either side of the mission module. These tanks were torroidal in shape in order to conform to the edges of the aerobrake. It was necessary to split the tanks along the plane of symmetry and stretch them out to accommodate the required amount of propellant.

The elliptical design utilized a symmetric aerobrake with a diameter of 44 ft. Two hydrogen tanks and two oxygen tanks were placed on either side of the mission module, with the oxygen tank above the hydrogen tank. The shape of these tanks was selected by making the total tank height equal to the 14 foot diamter of the mission module. The tanks would run the length of the mission module, with the widths of each tank being equal to give them their elliptical cross-sections.

A disadvantage of the torroidal and elliptical designs was that the manufacturing costs of the tanks would greatly exceed the costs for conventional tanks. The tanks would also require a greater wall thickness compared to spherical cylindrical tanks. Furthermore, the frame design would also be complicated and would require more trusses than a conventional shape. For these reasons both of these configurations were discarded.

CYLINDRICAL TANK CONFIGURATION

This design utilized a raked cone aerobrake with a length of 45 ft and width of 34 ft. Four hydrogen tanks and two oxygen tanks were used. The oxygen tanks were placed in front of the mission module and were stacked one above the other. Two hydrogen tanks were placed on either side of the mission module and were also stacked one above the other. These tanks ran the length of the mission module.

DISPOSABLE TANK CONFIGURATION

The primary goal in designing the ASTV was to minimize costs. One method of reducing costs would be to use disposable propellant tanks. This involves having propellant cms tanks that would separate from the vehicle prior to the aeropass. The aerobrake would not be required to shield these tanks and therefore could be made considerably smaller and lighter. Also, the spherical shape of the tanks allows a minimal wall thickness to be used, again saving weight.

The disposable tanks carry the propellant needed for the transfer from LEO to GEO as well as the initial impulse for the trip to the earth's atmosphere. As the vehicle approaches the atmosphere, the tanks are ejected using small solid rockets and allowed to burn up in the atmosphere. This configuration also requires having permanent tanks to store the propellant needed to perform any burns after the aeropass. There are a total of five small hydrogen tanks and five small oxygen tanks in the vehicle shielded by the aerobrake.

The main disadvantage of this configuration is that the spherical tanks need to be replaced for each mission. However, the benefit gained by disposing the main tanks is that the initial vehicle mass is lighter due to the reduction in the size of the aerobrake. Propellant requirements are therefore reduced for each mission. At the present time, the cost of delivering one pound of cargo to LEO is very high. The savings obtained by using the disposable configuration far outweighs the cost of the tanks. The following analysis justifies the use of this configuration as opposed to the cylindrical configuration for the final ASTV design configuration

DISPOSABLE TANK CONFIGURATION VS. REUSABLE TANK CONFIGURATION

Estimated cost of delivery from Earth to LEO:

Present day (approx)	= $5,000 per lb
Projected for 2010	= $1,000 per lb

Comparison:

Configurations	Empty Weight	Required Fuel (Mission 2)
Reusable Tanks	17,160 lbs	76,930 lbs
Disposable Tanks	11,860 lbs	63,083 lbs
	Difference in propellant =	13,847 lbs

Savings in using the disposable tank configuration:

1) Initial savings of delivering to LEO:
17,160 - 11,860 = 5,300 lbs

-Present day	$26,500,000
-Projected	$5,300,000

2) Savings per mission:

-Present day	$69,235,000
-Projected	$13,847,000

Total Life Savings (delivery to LEO plus 30 trip duration):

-Present day	$2,103,550,000
-Projected	$420,710,000

Costs:
Two hydrogen tanks per mission
Two oxygen tanks per mission

Assuming the average approximate value of these tanks to be $1,000,000, and assuming that the price of these tanks will reduce as more tanks are manufactured, the total cost for the 30 mission life ASTV is approximately $96,000,000.

Savings:	Present day	Projected
	$2,103,550,000	$420,710,000
Costs	- $96,000,000	- $96,000,000
Total	+ $2,007,450,000	+ $324,710,000

Results:

The cost of manufacturing is minor in relation to the savings achieved through decreased weight of the vehicle. Also, the fuel supplied from the Earth to LEO could be transported in the actual fuel tanks and then attached to the vehicle when needed. These factors justified the use of the disposable tank configuration.

Another configuration derived from this disposable tank configuration was also studied. This vehicle would not only dispose empty tanks before the aeropass, but also dispose empty tanks at GEO to save fuel on the trip from GEO to the atmosphere. After analysis, this configuration was deemed unworthy since the extra tanks (two more hydrogen and oxygen tanks) would increase the initial mission weight. Also, the superstructure would be more complicated in accommodating the extra tanks.

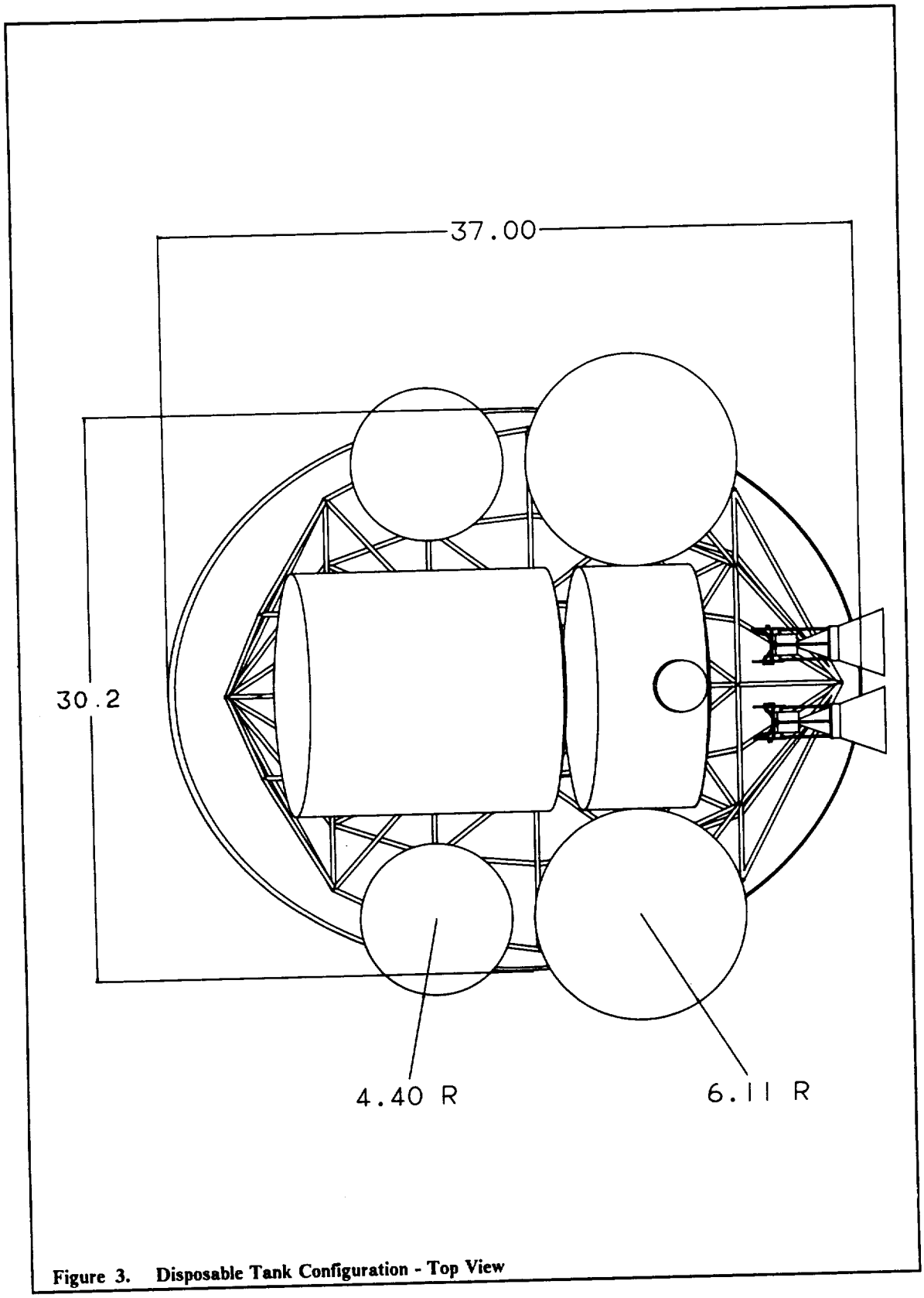

Figure 3. Disposable Tank Configuration - Top View

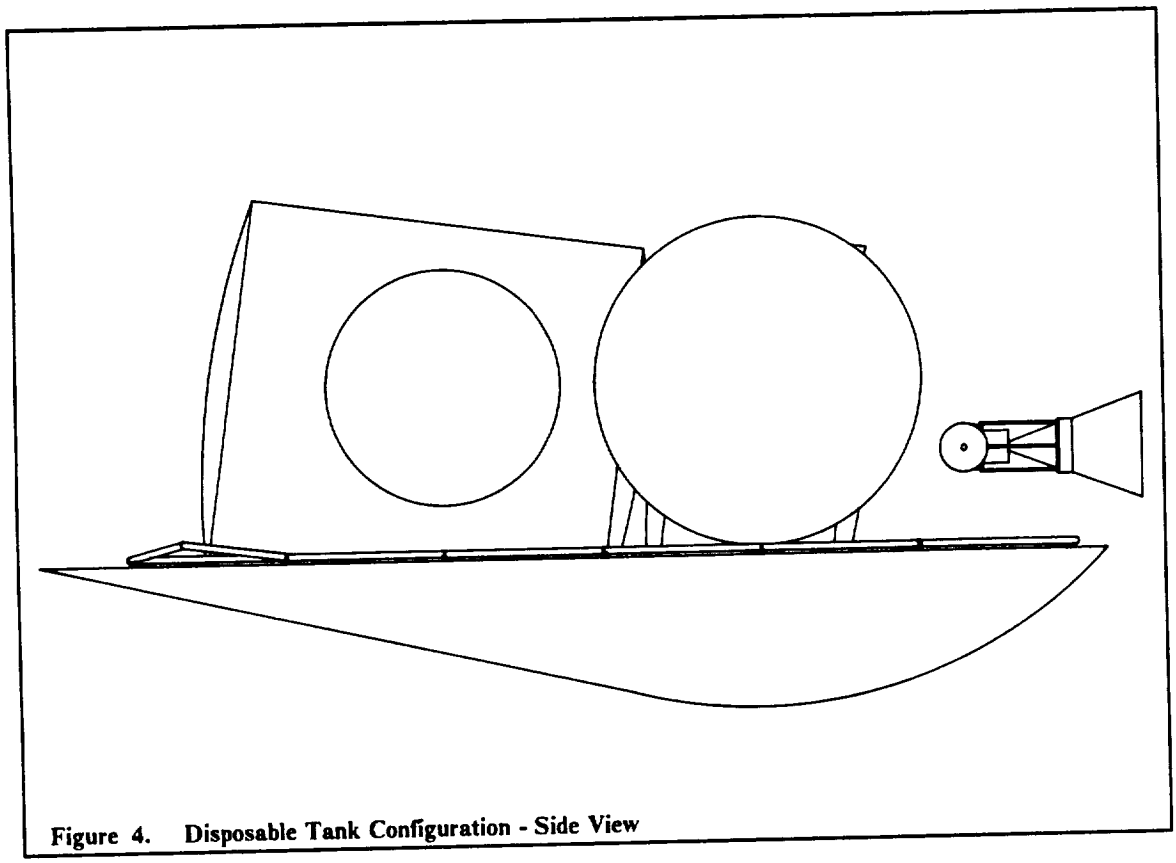

Figure 4. Disposable Tank Configuration - Side View

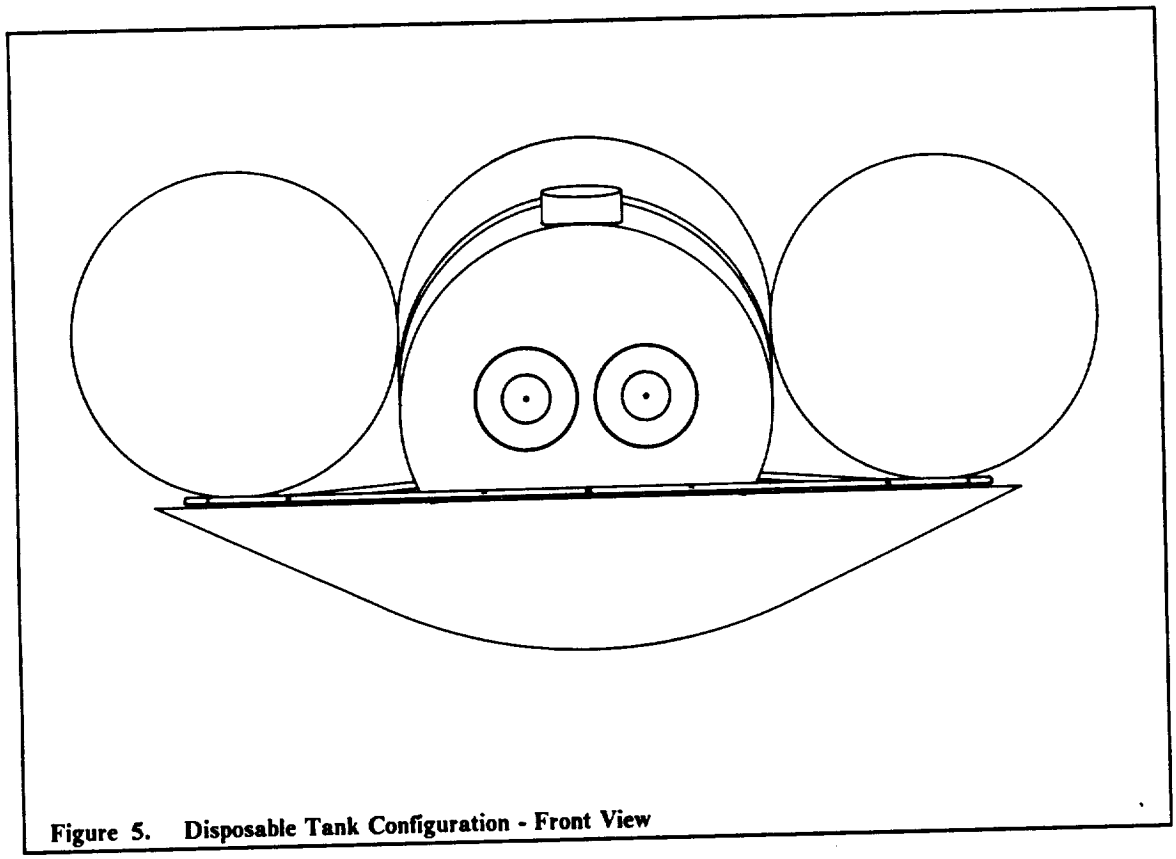

Figure 5. Disposable Tank Configuration - Front View

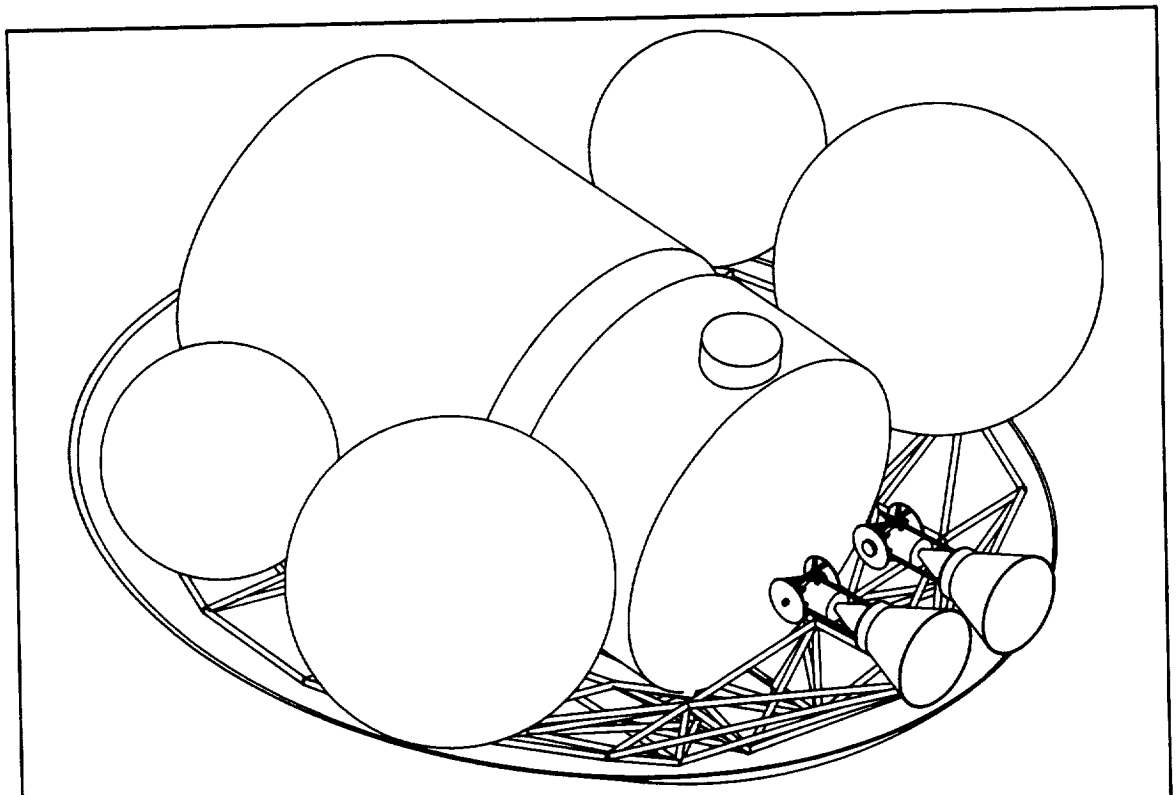

Figure 6. Disposable Tank Configuration - Isometric View

VEHICLE SPECIFICATIONS

ITEMS			
Crew size	Max. crew of 9 (3 per crew module)		
Cargo capacity trip LEO to GEO	6,000 lbm round		
	20,000 lbm to GEO and return empty		
	28,000 lbm to GEO and discard		
Transfer duration	Flight time only-14 hrs 39 min.		
Main propulsion:			
Number of engines	Two		
Engine type	Liquid oxygen/liquid hydrogen		
Isp	498 sec		
Design thrust	15,000 lbf per engine		
Mixture ratio	6:1 LO_2/LH_2		
Aerobrake:			
Geometry	Raked cone with a skirt		
Dimensions	37.0 ft x 30.2 ft x 5.3 ft deep (max)		
L/D	.230		
Thermal protection System	Multilayer insulation		
TPS material	Nextel Fibers, Stainless Steel foil radiation shielding		
Structural Material	HT graphite/epoxy composite material		
Reaction control System	Four main clusters: 34 60 lbf and 16 10 lbf thrust engines		
Power system	Three 4 kW LH_2/LO_2 fuel cells		
Masses:	Mission 1	Mission 2	Mission 3
Total dry mass (with RCS propellant)	17,860 lbm	31,860 lbm	39,860 lbm
Max total propellant	50,450 lbm	62,960 lbm	59,056 lbm
Max initial vehicle mass	68,310 lbm	94,820 lbm	98,916 lbm
CG locations (ft):	Mission 1	Mission2	Mission 3
Initial	x = 15.330	x = 15.130	x = 14.80
	z = 10.620	z = 9.800	z = 9.670
After 1st burn	x = 15.720	x = 15.300	x = 14.800
	z = 8.520	z = 7.680	z = 7.730
At GeoShack	x = 16.330	x = 17.060	x = 17.880
	z = 5.258	z = 5.308	z = 0.593
Prior to aeropass	x = 17.010	x = 18.630	—
	z = 1.640	z = -0.220	—

VEHICLE MASS BREAKDOWN

Components	Mass, lbm
Aerobrake System:	
-TPS	600
-Backing support (Al)	1,400
-Ribbing (Al)	1,250
Truss System:	1,866
-includes engine mounts, tank disposal mechanism	
Rails (crew/cargo supports)	1,132
Propellant Tanks and Insulation	1,352
-includes four disposable and ten reusable tanks	
Main Engines (two)	740
RCS System:	1,320
-includes thirty-four 60 lbf and sixteen 10 lbf thrusters	
Propellant Handling System:	700
-includes pumps and propellant lines	
Power Systems:	1,500
-includes batteries, guidance, communication, and computer hardwares	
Total Empty Weight	11,860

2. FLIGHT DYNAMICS

2.1 ORBITAL MECHANICS

2.1.1 MINIMIZING TOTAL ΔV REQUIREMENTS

Each mission requires the delivery of a payload to Geosynchronous Earth Orbit (GEO) from Low Earth Orbit (LEO). In a transfer from LEO to GEO, the vehicle must: (1) increase its altitude by applying impulses to increase its speed, and (2) change orbital planes from an inclination of 28.5° at LEO to 0.0° at GEO. A bi-elliptic transfer takes the vehicle from its initial orbit at LEO to some intermediate orbit at a distance R, and then on to GEO. This is shown in Figure 7. This type of transfer requires three impulses: the first impulse is applied at LEO, the second impulse is applied at the intermediate altitude, and the final impulse is applied at GEO to circularize the orbit at this altitude. By varying the value of R from LEO to GEO, the required change in velocity can be minimized. The orbital plane change, however, must also be accomplished. Three scenarios are compared to determine which requires the smallest ΔV.

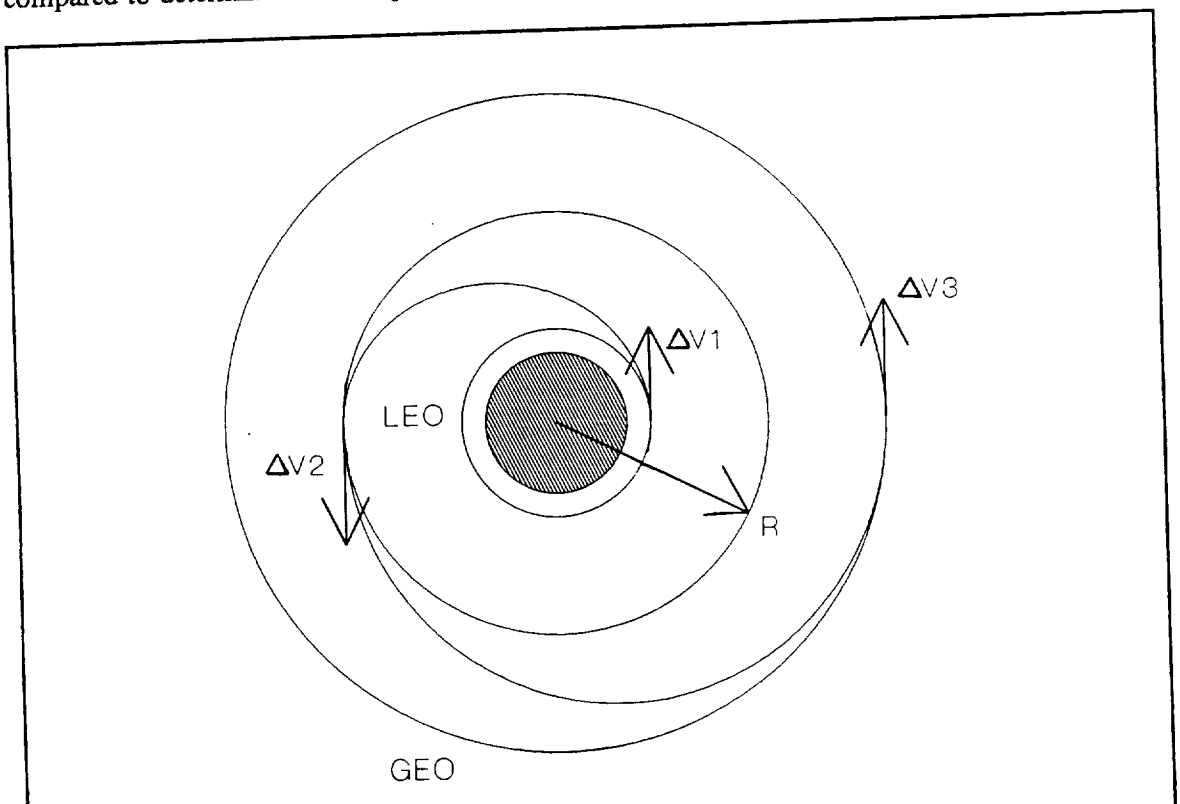

Figure 7. Bi-Elliptic Transfer

The first scenario involves a plane change at LEO, followed by a bi-elliptic transfer to GEO. The second scenario involves an initial burn at LEO to take the vehicle to its intermediate orbit altitude, then a burn at R which combines the plane change and the burn to reach GEO, and finally a burn at GEO to circularize. Figure 8 shows the burn which combines the plane change and the burn to reach GEO. The third scenario involves a bi-elliptic transfer to GEO, and then a plane change once the vehicle is at GEO. In each of these scenarios, the value of R (the intermediate orbit radius) is not fixed. Figure 9 shows how the required ΔV changes by varying R for each of the three scenarios.

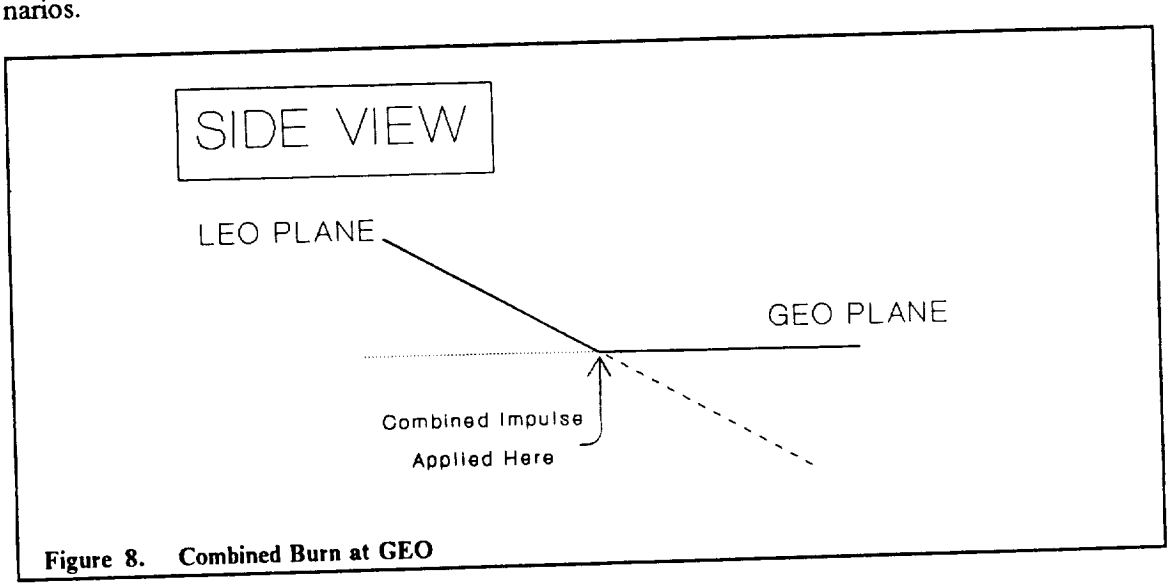

Figure 8. Combined Burn at GEO

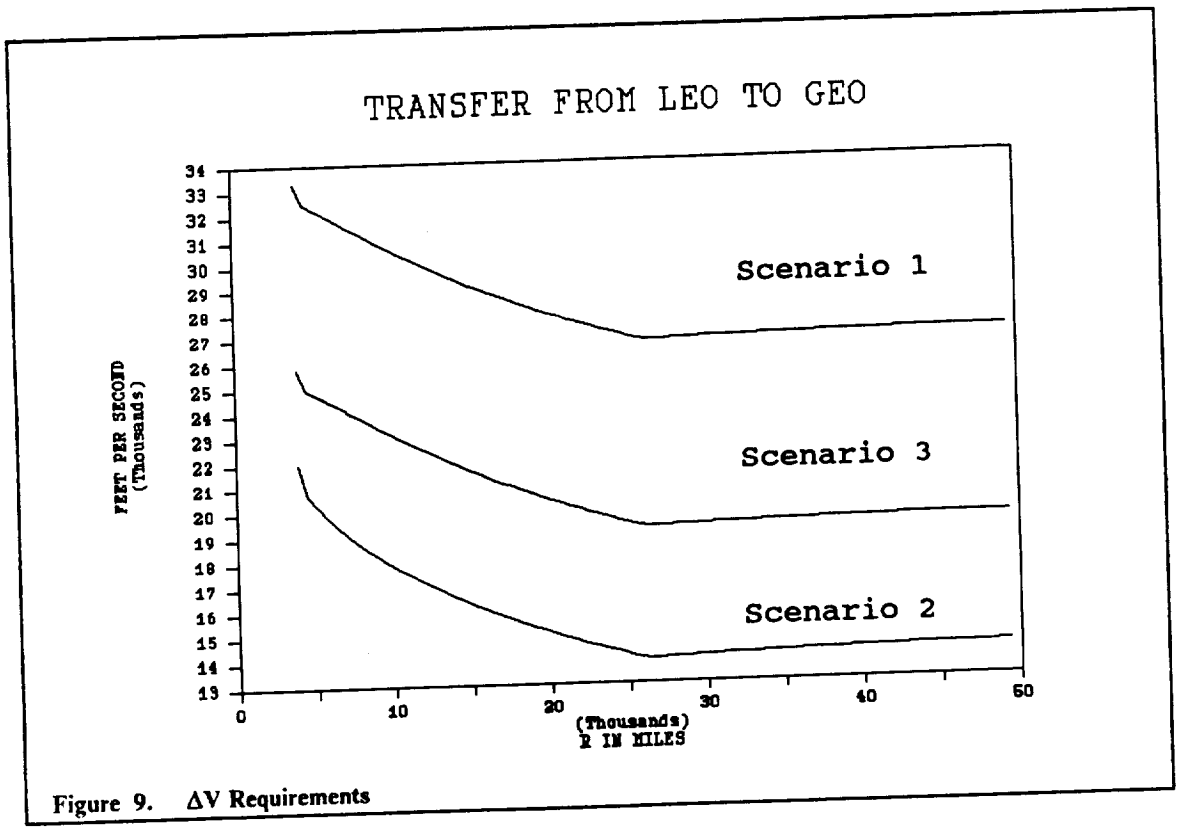

Figure 9. ΔV Requirements

From this diagram, the ΔV requirement is minimized when the second scenario is used and the value of R is made equal to the altitude at GEO. This two-impulse transfer is referred to as a Hohmann Transfer. The first impulse is applied at LEO and takes the vehicle to GEO altitude, where a single impulse is applied which changes the orbital plane and circularizes the orbit at GEO.

The ΔV required for the transfer from GEO to LEO is similarly minimized. Any necessary plane changes are made at GEO and are combined into a single burn which includes the de-orbiting boost to bring the vehicle within the Earth's atmosphere with the plane change. A low L/D aerobrake is unable to make large plane changes within the Earth's atmosphere. Therefore, much of the orbital plane change must be made before entering the atmosphere. Of the 28.5° plane change required, 2.2° will be made within the atmosphere, while 26.3° will be made at GEO as described above.

2.1.2 ΔV REQUIREMENTS

The transfer from LEO to GEO is accomplished by a Hohmann Transfer which includes an orbital plane change at GEO. The first impulse is applied at LEO and takes the vehicle along a Hohmann transfer ellipse to GEO. Figure 10 shows the first impulse, ΔV1, and the transfer ellipse.

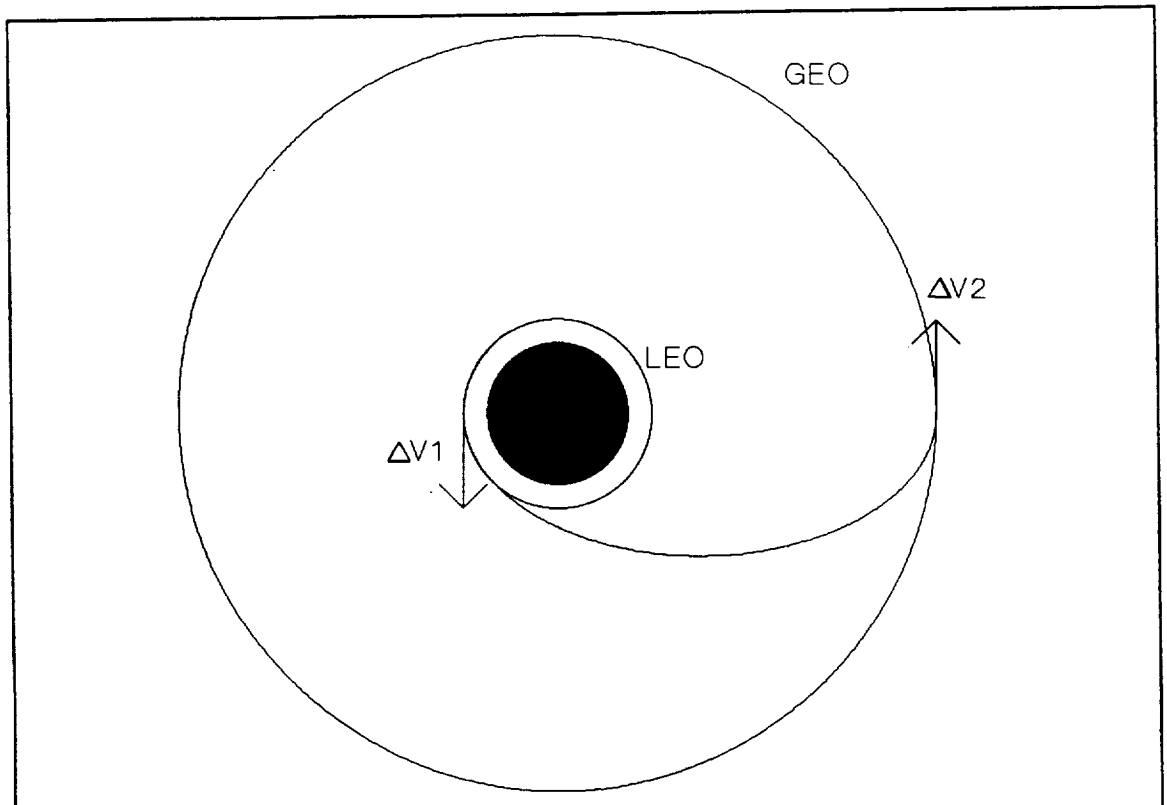

Figure 10. LEO to GEO Transfer

The magnitude of the first impulse is 7,938.0 ft/sec. The second impulse, ΔV2 on Figure 10, combines the plane change and GEO circularization burn. It has a magnitude of 6,000.2 ft/sec. Therefore, the transfer from LEO to GEO has a total ΔV requirement of 13,938.2 ft/sec.

Once the operations at GEO are completed, the vehicle will either be discarded (according to Mission 3) or return to LEO (according to Missions 1 & 2). The ΔV required to complete Mission 3 will be discussed first. The vehicle will be placed at an altitude 100.0 miles above the GEO orbit. This is done with a two-impulse transfer, shown in Figure 11 on page 20.

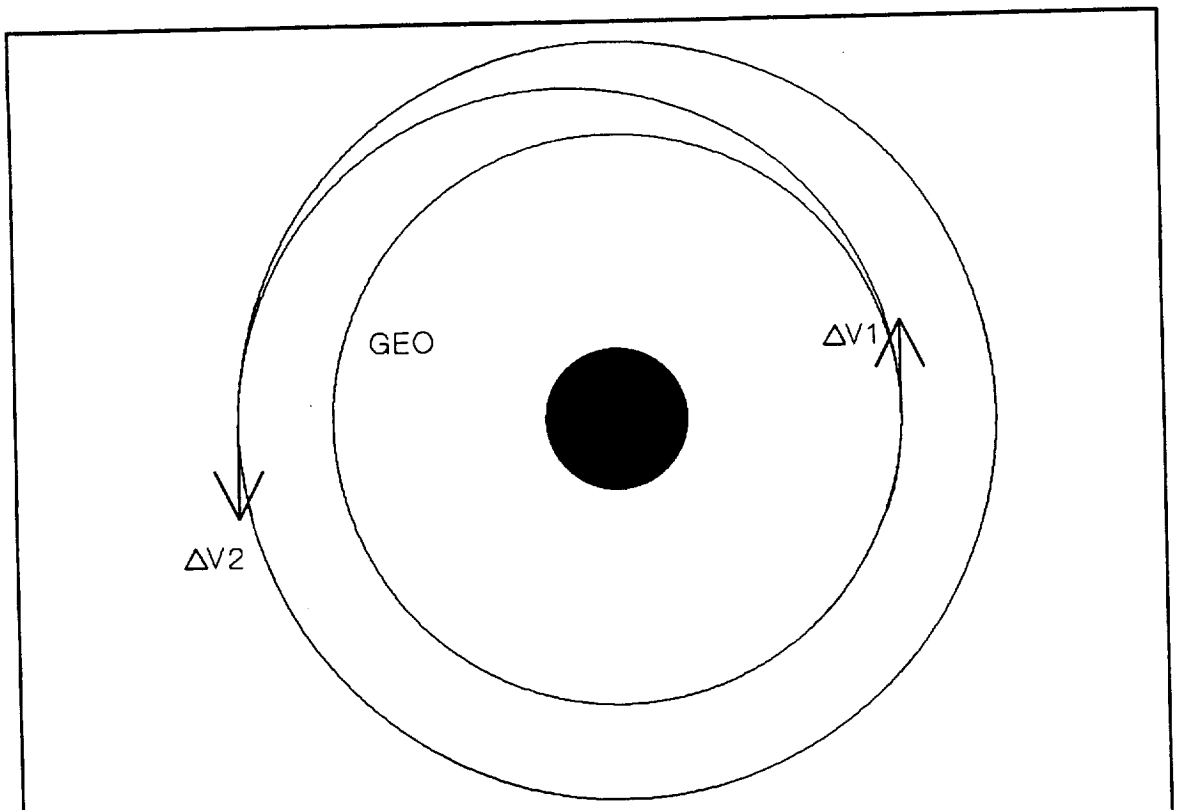

Figure 11. Ejection

The first impulse, ΔV1, takes the vehicle along a Hohmann transfer ellipse which arrives at an altitude 100.0 miles above GEO. The second impulse, ΔV2, circularizes the vehicle's orbit at this higher altitude. The total ΔV required to discard the vehicle is 19.2 ft/sec.

Missions 1 and 2 require that the vehicle return to LEO after making a pass through the atmosphere. For these missions, a deorbiting impulse is made at GEO which brings the vehicle within the Earth's atmosphere and changes orbital planes from 0.0° to 26.3°, the final 2.2° plane change is made within the atmosphere. To determine the magnitude of this deorbiting impulse, a target perigee must be chosen which will bring the vehicle within the Earth's atmosphere. Assuming that the Earth's atmospheric effects are observed up to 400,000 ft, a target perigee of 52.54 miles is found to give acceptable entry conditions. The magnitude of this deorbiting impulse, ΔV1 of Figure 12 on page 21, is 5,894.2 ft/sec. The target perigee of 52.54 miles gives an entry flight path angle of -4.00° and an entry velocity of 33,818.2 ft/sec. The atmospheric pass slows the vehicle to a speed of 26,127.6 ft/sec at atmospheric exit, with a flight path angle of 4.00° . While the vehicle is in the atmosphere a plane change of 2.2° is made. The vehicle enters the atmosphere with an inclination of 26.3° and exits with an inclination of 28.5°. Once the vehicle exits the atmosphere, it continues to coast until it reaches the phasing orbit altitude of 350.0 miles. At this altitude, a circularization burn of 448.0 ft/sec is made (ΔV2 of Figure 13 on page 21).

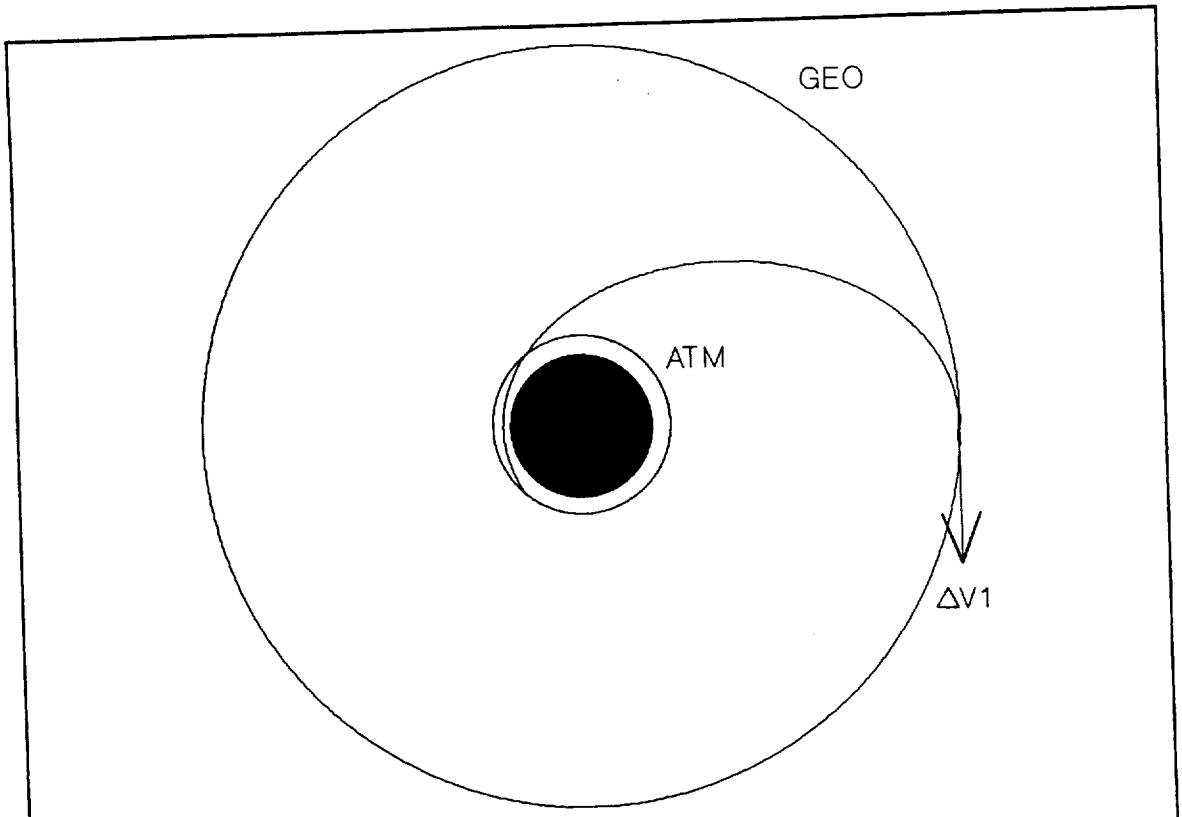

Figure 12. De-Orbiting Burn at GEO

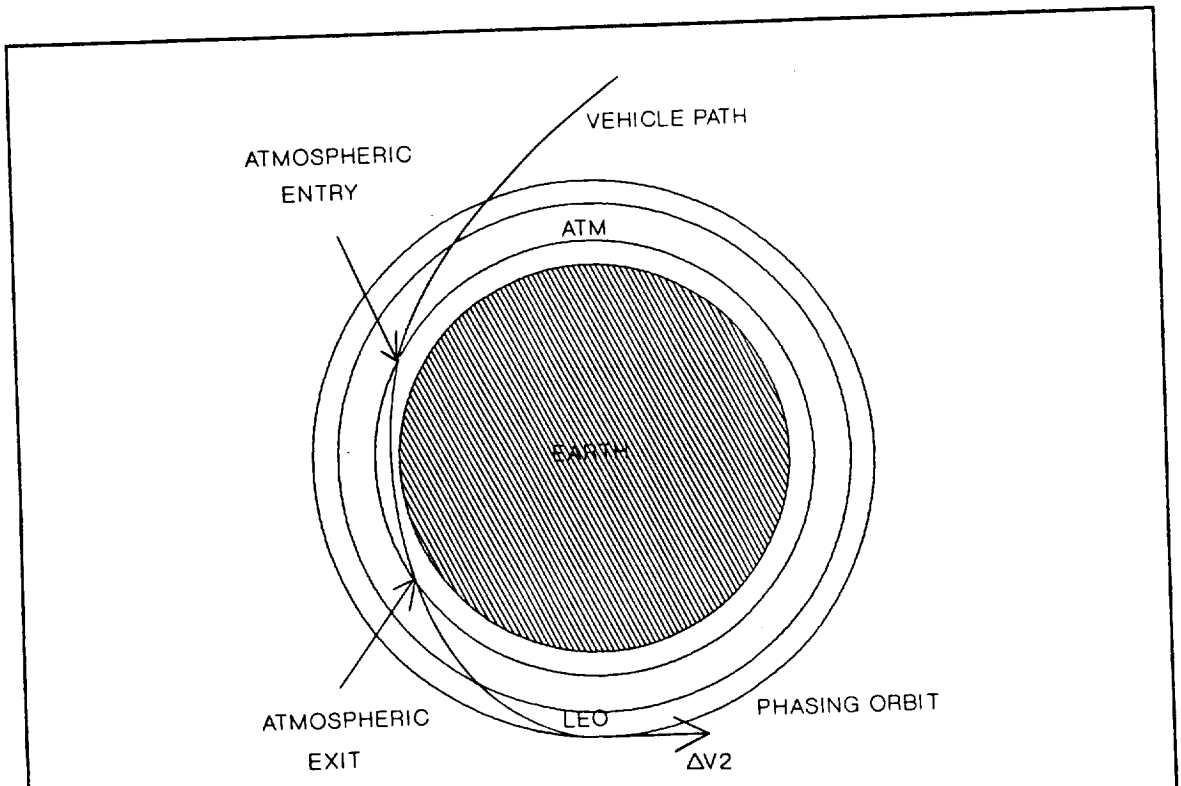

Figure 13. Burn to Circularize at Phasing Orbit

The phasing orbit allows the vehicle to make any necessary corrections and adjustments after the atmospheric pass, before arriving at the Space Station. Once corrections have been made, a burn is made which takes the vehicle along a Hohmann transfer ellipse to LEO. The first burn, ΔV1 of Figure 14, has a magnitude of 221.0 ft/sec. The burn to circularize at LEO, ΔV2 of Figure 14, has a magnitude of 222.9 ft/sec. The sum of the individual impulses required to take the vehicle from GEO to LEO is 6,786.1 ft/sec.

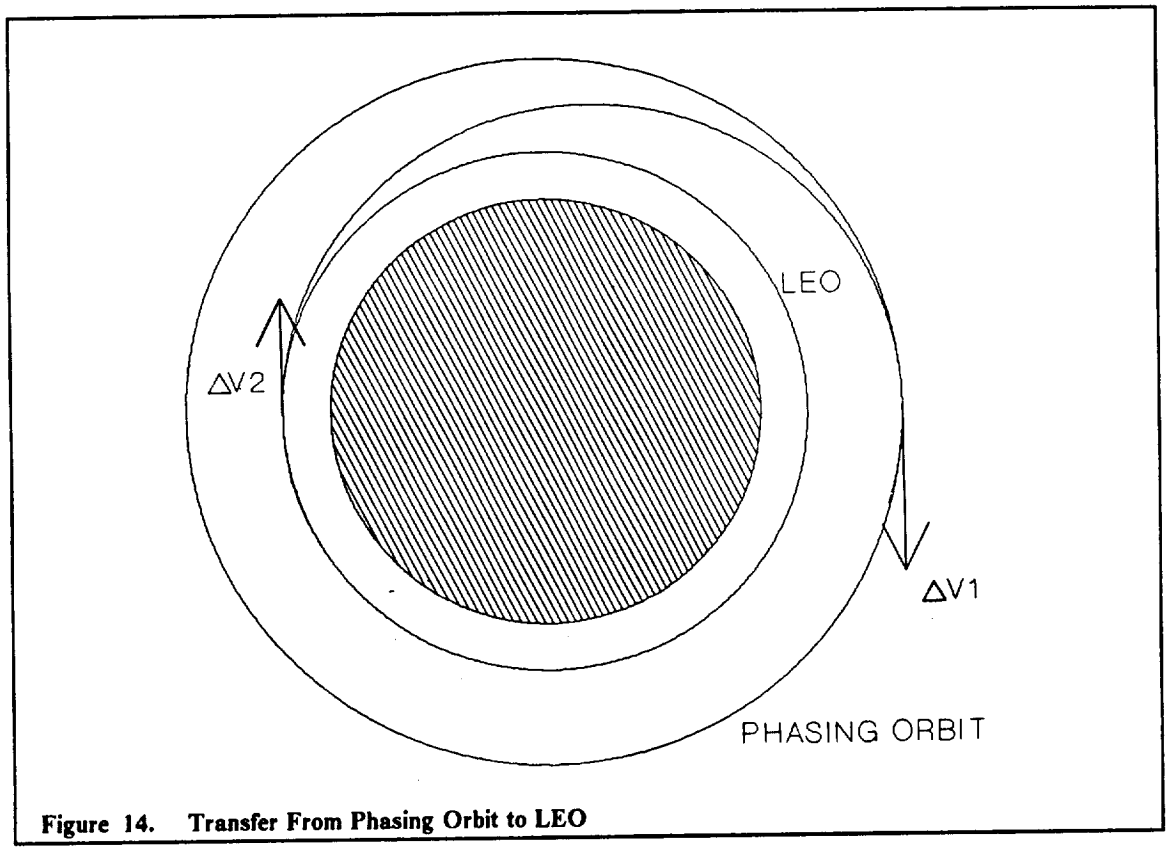

Figure 14. Transfer From Phasing Orbit to LEO

The total required ΔV for Missions 1 and 2 is found to be 20,724.3 ft/sec; for Mission 3, the total required ΔV is 13,957.4 ft/sec. An analysis of the time required to complete each portion of the transfer is supplied in Appendix A.

2.1.3 PROPELLANT REQUIREMENTS

PROPELLANT SELECTION

The propellant for both the main engines and the RCS engines will be liquid hydrogen/liquid oxygen. This fuel was chosen due to its proven performance in the space shuttle and its ability to attain high specific impulse. The propellant will be stored in a total of 14 tanks. Each component will utilize two large disposable-rated tanks and five small reusable-rated tanks. Section 4.5 describes the propellant tank characteristics in depth.

PROPELLANT REQUIREMENTS PER MISSION

The propellant requirements were calculated using an exponential relationship computing mass of propellant as a function of empty craft mass, Isp, and required ΔV.

In section 2.1.2, the individual missions were broken into key ΔV maneuvers. The ASTV main engine utilizes the bi-propellant fuel in a mass ratio of 6 to 1 (oxygen to hydrogen). This allows the engine to attain the desired specific impulse of 498 seconds. The empty craft mass of 11,860 lbm, also necessary for the calculation, includes:

1. Aerobrake
2. Supporting structures
3. Support systems
4. (Empty) propellant tanks
5. 2 main engines
6. RCS system (see Chapter 5.)
7. Plumbing and electronics
8. All guidance and navigation.

In addition, a reserve propellant supply was calculated. This includes sufficient propellant to perform the final two main engine burns in the event of either a main tank failure or the expenditure of additional propellant in an emergency return.

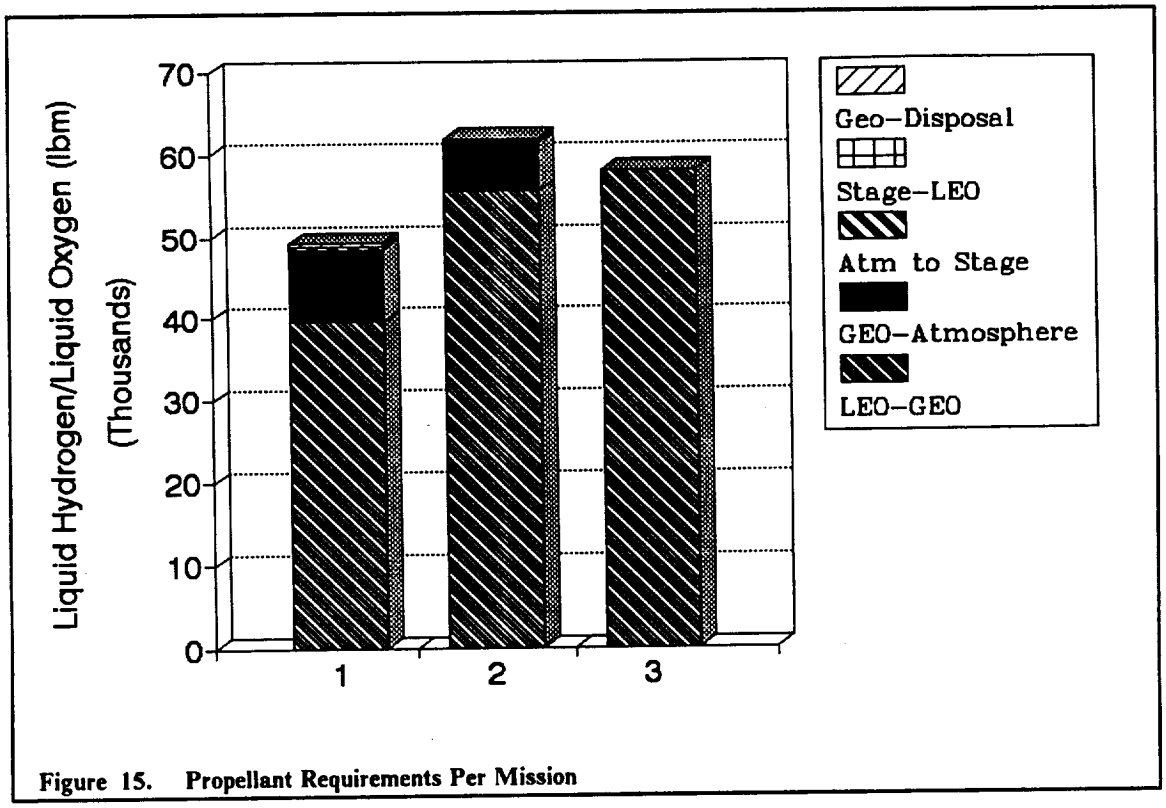

Figure 15. Propellant Requirements Per Mission

Table 3. Propellant Mass per Mission Phase

Mission	LEO-GEO	GEO-Atm	Atm-Stage	Stage-LEO	GEO-Disp	Reserve
1	39638	8798	530	502		983
2	55451	5843	357	357		983
3	58055				15	983

All amounts in lbm.

The results of the calculations are given in Figure 15 on page 23 and Table 3.

For the given Isp, empty craft mass, and velocity changes required to complete the individual missions, it was found that Mission 2 (20,000 lbm payload from LEO to GEO and an empty return) required the maximum amount of fuel, and would therefore be considered the design limit for propellant management.

Table 4. Oxygen and Hydrogen Breakdown per Mission

Mission	Total Fuel	Oxygen	Hydrogen
1	50449	43242	7207
2	62960	53965	8994
3	59056	50619	8437

All Amounts in lbm.

Table 4 lists the hydrogen and oxygen mass required for each mission. For Mission 2, 53,966 lbm of oxygen and 8,994 lbm of hydrogen are required. These fuel estimates do not include the RCS requirement. The RCS engines require approximately 581 lbm of fuel for the design scenario. This requirement is discussed in greater depth in the RCS section.

2.1.4 AEROBRAKING VS. ALL-PROPULSIVE TRANSFER

When designing a vehicle which uses an aerobrake to decrease its velocity, it is important that the mass of the aerobrake and supporting structure is less than the savings in propellant mass compared to an all-propulsive transfer. Table 5 on page 25 shows the results from the comparison between an aerobraking transfer and an all-propulsive transfer.

Table 5. Aerobraking vs. All-Propulsive Transfer

	Aerobraking Transfer	All-Propulsive Transfer
ΔV Required (ft/s)	20,724.3	27,876.5
Mass of Vehicle (lbm) (including 6,000 lbm cargo)	17,860.1	12,618.1
Propellant Mass (lbm)	49,872.1	62,752.3

Since 55,114.1 lbm, the total mass of the aerobrake and propellant for aerobraking transfer, is less than 62,752.3 lbm, the total mass of propellant for an all-propulsive transfer, the aerobraking vehicle is more efficient than the all-propulsive vehicle.

2.2 AEROBRAKING MANEUVERS

2.2.1 AEROBRAKING PHASE

Initial design uncertainties for the ASTV physical characteristics (i.e. weight, size, shape, etc...) led to the incorporation of Chapman's universal entry theory into planetary atmospheres. This particular entry analysis was not exact due to certain assumptions (mentioned later); however, solution of this theory (Runge-Kutta-Nystrom Numerical Method) did provide estimates for a wide range of pertinent parameters associated with the ASTV design process. These parameters were independent of vehicle characteristics. Thus, the generated values could be applied to any vehicle design, in particular, to any aerobrake design.

Using the values obtained from orbital mechanics for the entry conditions (speed, altitude, flight-path angle), the dimensionless method of Chapman was incorporated to provide the best lift-to-drag (L/D) ratio for these inputs, the "best" L/D being one that brought the peak atmospheric deceleration below the maximum load factor of 4 g's. This load factor results from a stress analysis of key vehicle components which focuses on eliminating unnecessary weight without detracting from component performance. Results indicate that a L/D = 0.23 yields a maximum horizontal deceleration of 3.72 g's in the atmosphere, well within the limits of human tolerance and the desired load factor. Care has also been taken to maintain an aeropass that does not involve skipping in order to avoid any detrimental effects that might occur, such as inducing undue stress and vibration on the ASTV structure and possible interference with maneuvering effectiveness.

Drawbacks to the Chapman entry analysis are inherent to its various assumptions, shown in the following list:

- Planar Entry
- Neither strictly isothermal nor exponential atmosphere used; assumed mean value of βr (scale height × radial distance) for Earth atmosphere model
- Velocity restricted to monotonically decreasing
- For a given time increment (dt), the change in radial distance (dr) is negligible compared to the corresponding change in the horizontal velocity component (dV): $|dV/V| >> |dr/r|$
- For a lifting vehicle, the horizontal component of lift is negligible compared to the drag component in the same direction, for small ϕ
- L/D is constant

- Flow in the region between the bow shock and vehicle surface is primarily laminar
- Total heat absorbed is predominantly a result of convective heating
- Sensible atmosphere begins at an altitude of 400,000 ft

The previously mentioned optimum L/D ratio therefore neglects variations due to banking and does not adequately represent free modulation of bank angle or lift coefficient. Chapman's planar theory provides good estimates for ASTV deceleration, heating, trajectory, dynamic pressures, and aerobraking time. Thus, initial studies of aerobrake design (materials, thermal protection, size, shape, structure) were carried through to narrow design considerations. The values determined for the total heat absorbed were based solely on the convective heat transferred to the aerobrake from the aft-shock region (this region assumed to be laminar flow). The values obtained included a 25% increase over the convective heat to account for radiative heat transfer during hypersonic reentry. This approximation was chosen based upon experimental results, rather than analytic results, due to the complexity of modeling nonequilibrium radiative heat transfer. Even though blunt bodies, i.e. the raked cone aerobrake, tend to minimize convective heating, the Chapman theory assumption that a primarily convective heating environment existed was in error. The radiative heat transfer could not be completely neglected at the speed at which the ASTV reenters the atmosphere. Negative lift was also required for parabolic entry speeds in order to remain within the earth's atmosphere until the desired exit velocity was attained (centrifugal force > gravity), see Figure 16 on page 27. This lift actually represents positive lift on the aerobrake, but due to the inverted position of the aerobrake the value changes sign. The other graphs and results were obtained in the same program solving Chapman's 2nd Order differential equation,with inputs being the entry conditions, L/D, and the ballistic coefficient (W/(Cd×A)) derived from the entry mass and aerobrake planform area. These values are as follows (for worst case - Mission 1):

$V(entry) = 33{,}818.2878$ ft/s
$h(entry) = 400{,}000$ ft
$\phi(entry) = -4.0°$

$V(exit) = 26{,}127.713$ ft/s
$L/D = 0.230$
$W/(Cd \times A) = 15.40$ psf

The results for these conditions are as follows:

- Maximum g's = 3.720
- Total heat absorbed = 2.60×10^{-6} Btu
- Maximum rate of heat transfer = 53.07 Btu/(sec-ft^2)
- Maximum dynamic pressure = 55.75 psf
- Total aerobraking time = 200 sec

A low ballistic coefficient is desired in order to lower the heating loads on the ASTV, and to yield corresponding decreases in maximum deceleration and maximum dynamic pressure. The heating rate, total heat absorbed, and dynamic pressure for both Mission 1 and Mission 2 are shown in Figure 17 on page 27, Figure 18 on page 28, and Figure 19 on page 28, respectively. All of these parameters are greater for Mission 1, primarily due to its higher ballistic coefficient. The methods and equations incorporated in the aerobraking solution to Chapman's theory are too lengthy to be included here (Ref. Chapman). It should also be noted that program values obtained were correct to the same degree of accuracy as those determined by Chapman (i.e. using Chapman's initial conditions, the results coincided with his analyses.) (Ref. Chapman and Kapphahn).

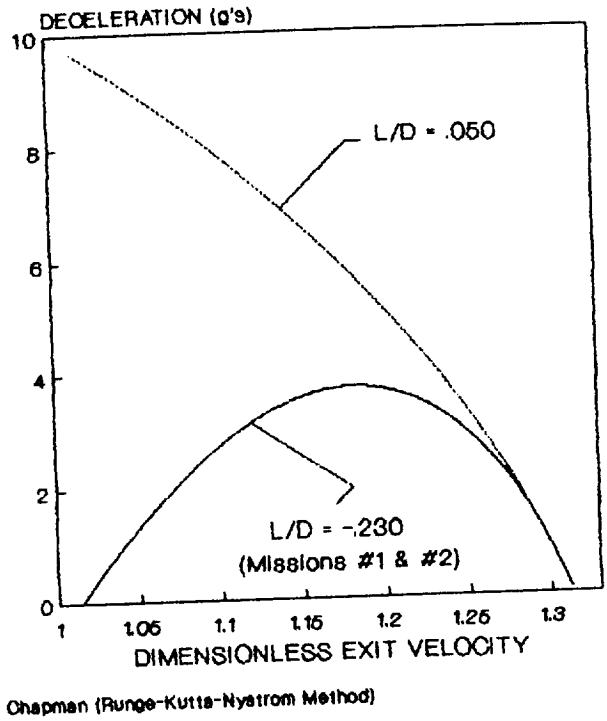

Figure 16. Atmospheric Deceleration

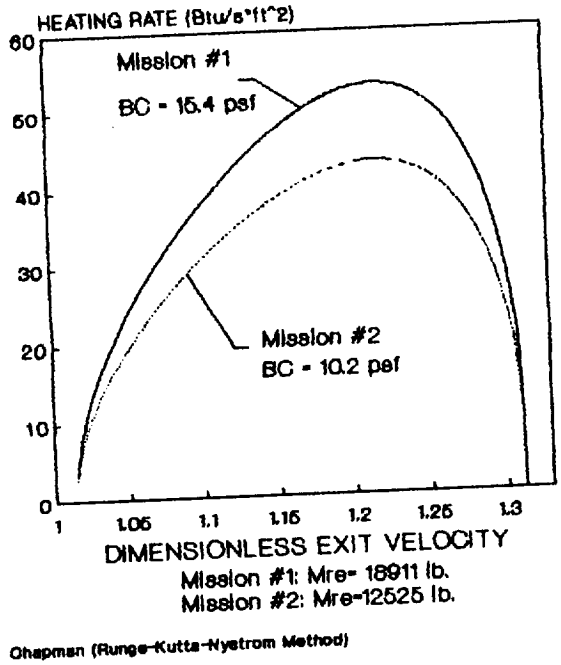

Figure 17. Heating Rate (Stagnation)

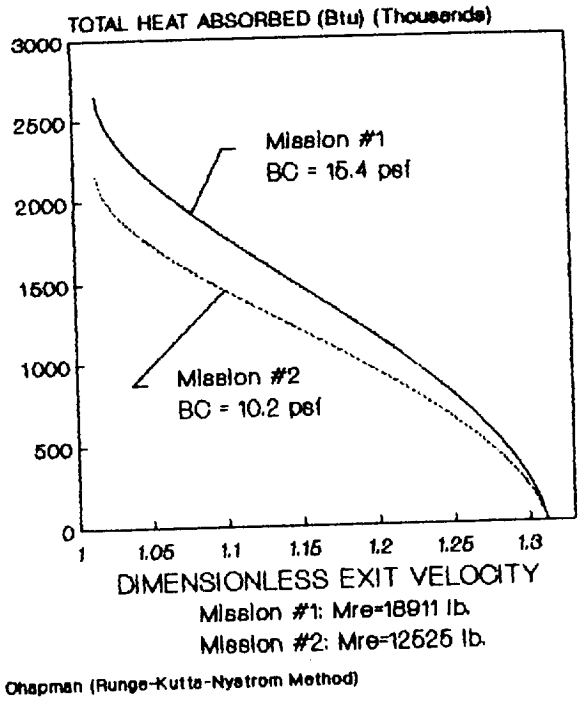

Figure 18. Total Heat Absorbed

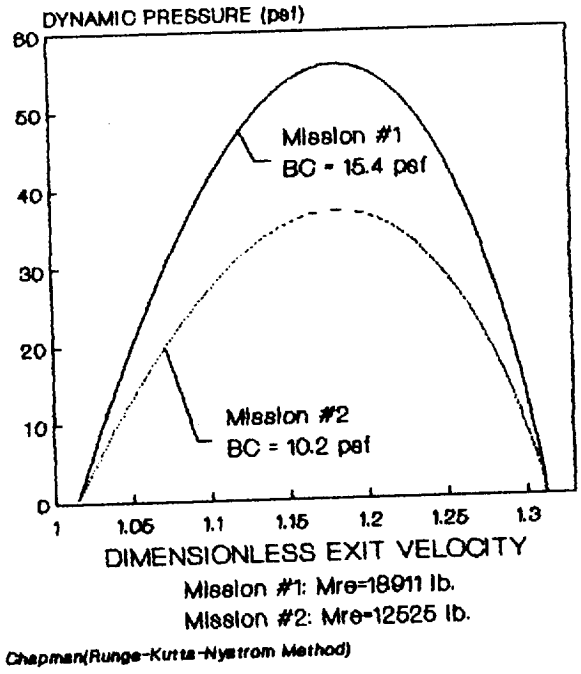

Figure 19. Dynamic Pressure

2.2.2 AEROBRAKE REQUIREMENTS

This section describes the desired characteristics for the final design of the aerobrake. Although many factors must be weighed in designing an aerobrake, the following list constitutes the primary requirements for the final brake design. Further discussion on the design choice of the raked cone, its geometry and benefits, will be expanded on later.

1. aerobrake shape minimizing surface temperatures and heating rates (which also allows for cheapest and lightest method for dissipation of heat absorbed--radiative cooling);
2. low ballistic coefficient;
3. comprised of separate parts (easy to replace, manufacture);
4. packageability (simple storage of primary divisions for transfer to space);
5. lifting shape (to provide maneuverability in atmosphere);
6. ease of assembly and disassembly - both of the aerobrake itself and of the aerobrake to the vehicle structure (aerobrake will be detached for disposable mission);
7. resistance to space environment: cosmic particle radiation, meteoroid impact, etc...

Because the aerobrake's value rests mainly on its ability to reduce fuel requirements, numerous studies have been made concerning the optimum mass for such a shield. Conservative results indicate that adequate fuel savings would occur with an aerobrake mass no greater than 40% of the ASTV entry mass (Ref. Schleinitz and Lo).

Thus, using previous results for total propellant mass, empty ship mass, and cargo mass for the worst case scenario:

$$\underset{\text{mass at reentry}}{\text{total propellant}} + \underset{\text{mass}}{\text{empty ship}} + \underset{\text{mass}}{\text{cargo}} = \underset{\text{mass}}{\text{reentry}} = 18{,}911 \text{ lb.}$$

max. allowable aerobrake mass = $.40 \times 18911 = 7{,}564.40$ lb.

Thus, the aerobrake should not exceed the above value in order to provide worthwhile savings in fuel.

2.2.3 AEROBRAKE ANALYSIS

For this analysis the aerobrake surface is decomposed into 1710 triangular shaped panels as shown in Figure 20 on page 30.

For each panel, the area and normal direction are found by taking the cross product of V1 and V2. The angle between the free stream velocity and the normal to each panel is found by taking the arctangent of the ratio of the cross product to the dot product of these vectors. Using this angle, the inclination of each panel with respect to the free stream direction is calculated. Since the ASTV enters the atmosphere at hypersonic speeds, Newtonian theory can be incorporated. The flow in the aft shock region may be assumed to be approximately parallel to the aerobrake surface due to the compression of the bow shock. This theory states that $Cp = Cpmax \times \sin^2\theta$, where θ is the panel inclination with respect to the free stream direction. Using Newtonian theory, Cp can be found for each panel, which in turn yields the Cp distribution for the entire aerobrake. From this distribution the lift and drag forces on each panel can be found. These forces are then summed for the entire aerobrake to give the total lift and drag. The lift and drag coefficients may be determined by incorporating the aerobrake planform area and maximum dynamic pressure, q (Chapman Results). This value of q gives lift and drag forces on the ASTV for the worst case scenario. Results from this analysis are as follows:

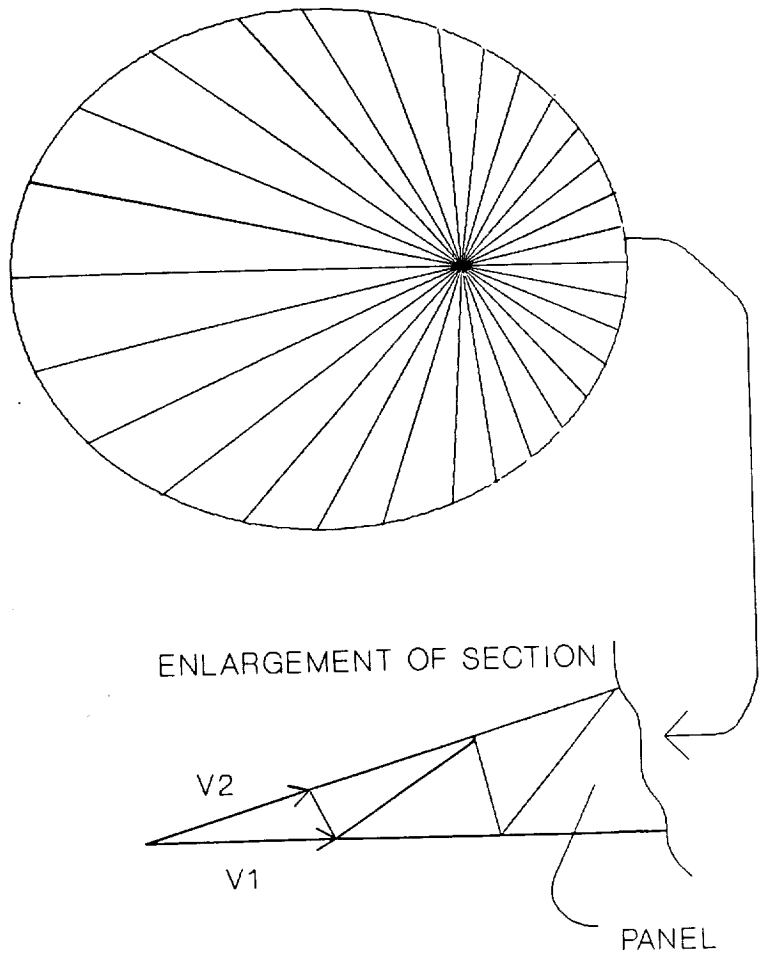

Figure 20. Aerobrake Analysis

CL = 0.344
CD = 1.495
L/D = 0.230

2.2.4 AERODYNAMIC FORCE CALCULATIONS

The beginning of any stability analysis involves calculating the aerodynamic forces acting on the vehicle. From these one can directly obtain lift, drag, and moment coefficients. Using the method of small perturbations one can also obtain stability derivatives.

METHOD

Modified Newtonian theory was selected to calculate aerodynamic forces acting on the ASTV. This theory gives reasonable results for the pressure distribution over an inclined surface at hypersonic Mach numbers. Freestream Mach numbers during the aerobraking pass range from 34.5 to 26.6.

Two assumptions were made in using this theory. The first was that the atmosphere behaves like an ideal gas at very high altitudes (where the aeropass occurs). At high altitudes the atmosphere

is rarefied and the ideal gas equation is less accurate. The second assumption was that atmospheric freestream pressure was insignificant in comparison to dynamic pressure. This assumption is valid for the high reentry velocities involved. Dynamic pressure is at least three orders of magnitude greater than freestream pressure.

Isentropic normal shock relations were initially used to determine the stagnation value of Cp (Cpmax). At high Mach numbers, however, these relations are invalid. An improved method for calculating properties behind a normal shock wave at high Mach numbers (Anderson, p.393) was therefore used to obtain more accurate values of Cpmax. This method assumes a calorically imperfect gas and takes into account disassociation effects. Additional help from a thermochemical equilibrium code (NOTS computer code) was required to implement this method.

The value of Cpmax was found to vary slightly throughout the aerobraking pass. Table 6 below lists calculated values for Cpmax at various points on the aerobraking pass.

Table 6. Variation of Cpmax during Aerobraking Pass

Altitude (ft)	Speed (ft/s)	Cpmax
250,000	32,800	1.975
232,500	29,900	1.967
245,000	27,400	1.982
261,100	26,700	1.944

A computer program was developed to implement the Modified Newtonian theory method for calculating aerodynamic forces. The program calculated the aerobrake pressure distribution and the resulting force distribution. For a given CG location and angle of attack, it also calculated the line of center of pressures and stability derivatives.

RESULTS

To achieve the desired L/D ratio of 0.23, it is necessary to fly the ASTV at an angle of attack of 13.25°. Although L/D is independent of Cpmax, lift and drag coefficients are not. For Cpmax = 1.967, the corresponding lift and drag coefficients were calculated to be:

$$CL = 0.344, \quad CD = 1.495$$

The required CG location needed to make 13.25° the trim angle of attack was calculated to be:

$$X = 18.67 \text{ ft}, \quad Y = 0.0 \text{ ft}, \quad Z = 1.38 \text{ ft}$$

By intersecting center of pressure lines for three angles of attack, the overall center of pressure for the vehicle was determined to be:

$$Xcp = 18.58 \text{ ft}, \quad Ycp = 0 \text{ ft}, \quad Zcp = 22.20 \text{ ft}$$

Figure 21 on page 32 shows the center of pressure lines and the overall vehicle center of pressure.

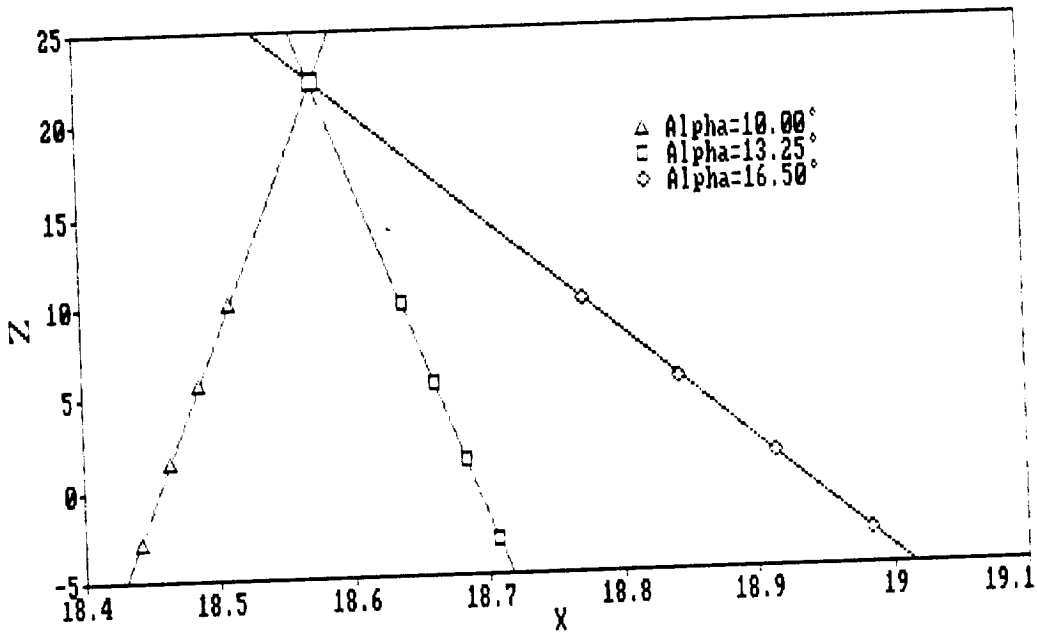

Figure 21. Determination of Overall Center of Pressure

The next table lists values for stability derivatives at the trim angle of attack of 13.25°. These were calculated using the method of small perturbations.

Table 7. Stability Derivatives at $\alpha = 13.25°$

Pitch:	$Cl\alpha = 0.000$	$Cm\alpha = -0.163$	$Cn\alpha = 0.000$
Roll :	$Cl\phi = -0.153$	$Cm\phi = 0.000$	$Cn\phi = 0.027$
Yaw :	$Cl\beta = -0.044$	$Cm\beta = 0.000$	$Cn\beta = 0.008$

2.2.5 AEROBRAKE STABILITY AND CONTROL

The aerobraking phase of each mission consists of a controlled pass through the upper atmosphere. In order to achieve this control at the orbital velocities involved, it is desirable to have a vehicle which possesses static stability in pitch, yaw, and roll. Technology does exist for the design of flight systems which can maintain vehicle control despite unstable flight characteristics; however, such systems are still in their infancy and their implementations are costly. To avoid having to use such a system, the ASTV was therefore required to be statically stable in pitch, yaw, and roll.

LONGITUDINAL STABILITY

The requirement for static pitch stability at a given trim angle of attack is that the numerical sign of Cmα be negative. The value of Cmα depends on both vehicle geometry and CG location.

The calculated value of Cmα was -0.163 for a CG location of (18.67, 0.0, 1.38) feet. The vehicle is therefore stable in pitch for this configuration. Figure 22 shows the corresponding graph of pitching moment versus angle of attack.

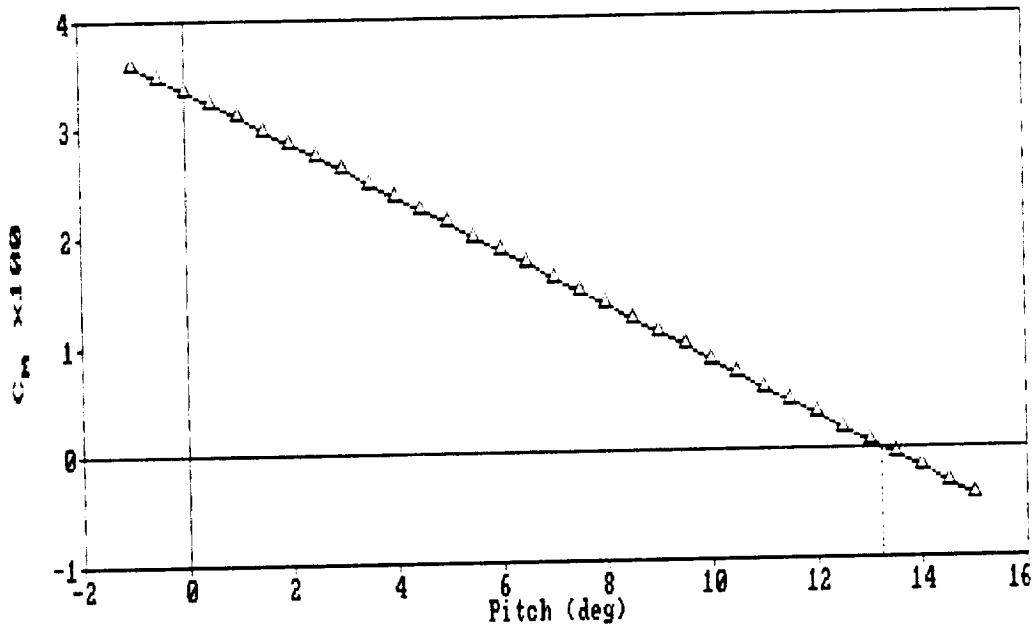

Figure 22. Effect of Pitch Angle on Pitching Moment Coefficient

The requirement for static pitch stability is also met if the center of gravity lies forward of the center of pressure. By "forward" we mean the velocity direction. Figure 23 on page 34 shows the aerobrake at a 13.25° angle of attack along with the corresponding center of pressure. It is clear from the figure that the center of gravity will always lie forward of the center of pressure, hence the vehicle is stable in pitch.

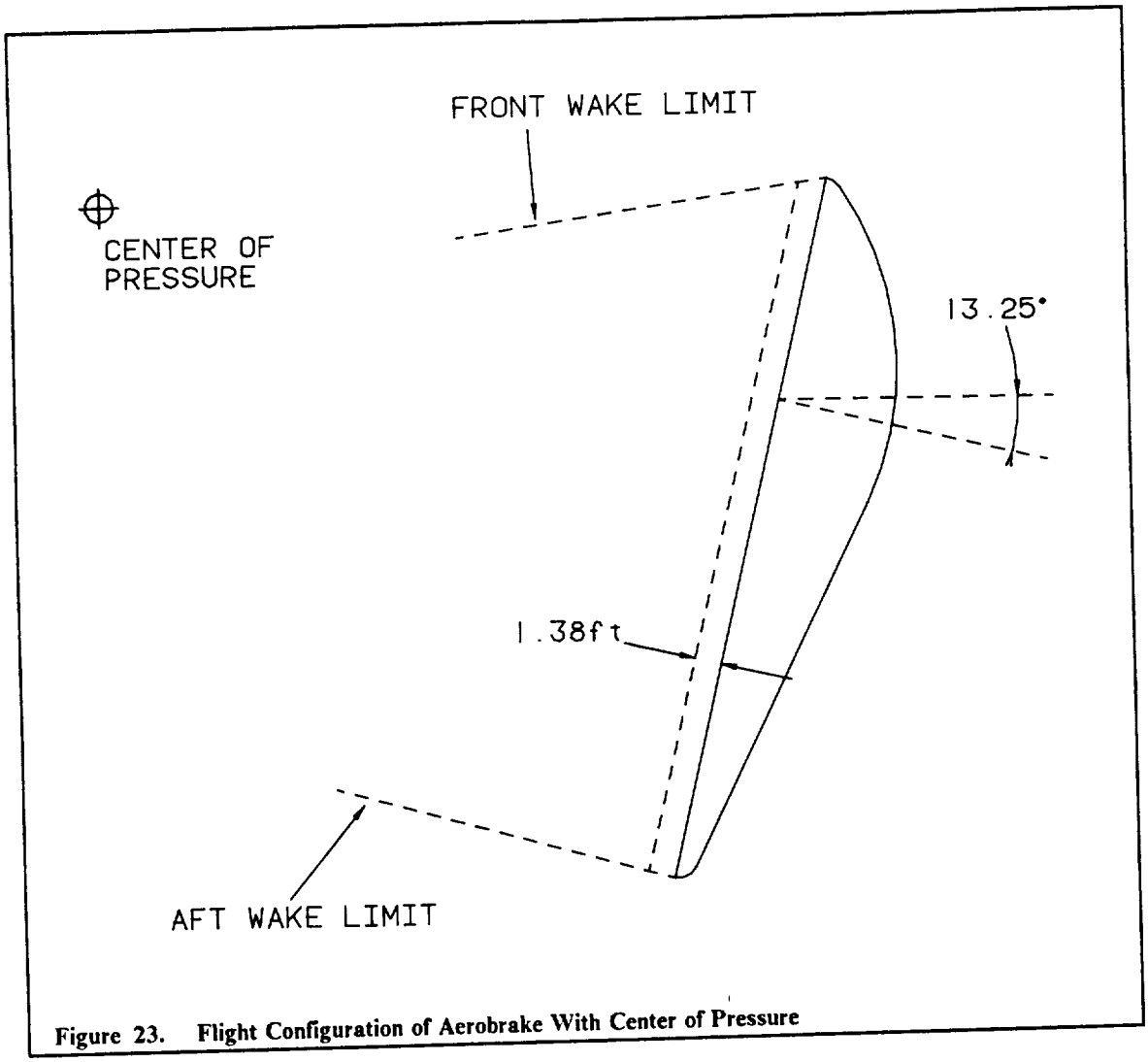

Figure 23. Flight Configuration of Aerobrake With Center of Pressure

ROLL STABILITY

The requirement for static roll stability is that the sign of $Cl\phi$ be negative. Since the CG will always be located in the vehicle plane of symmetry, CG location will not be a factor influencing the roll stability of the aerobrake.

A value of -0.153 for $Cl\phi$ indicates static roll stability. Figure 24 on page 35 shows a graph of roll moment moment coefficient versus roll angle.

LATERAL STABILITY

The requirement for static lateral stability is that the sign of $Cn\beta$ be positive. The sign requirement is positive because yaw is measured in the antisense direction (contrary to pitch and roll). CG location does affect the value of $Cn\beta$; however, the degree of this effect is small.

The aerobrake demonstrates static lateral stability at the trim angle of attack since $Cn\beta$ is equal to 0.008. The small magnitude of $Cn\beta$ implies a weak tendency for lateral stability though. Only small moments are needed to overcome the restoring moment due to a deviation in yaw. Figure 25 on page 36 shows a graph of yaw moment coefficient plotted versus yaw angle.

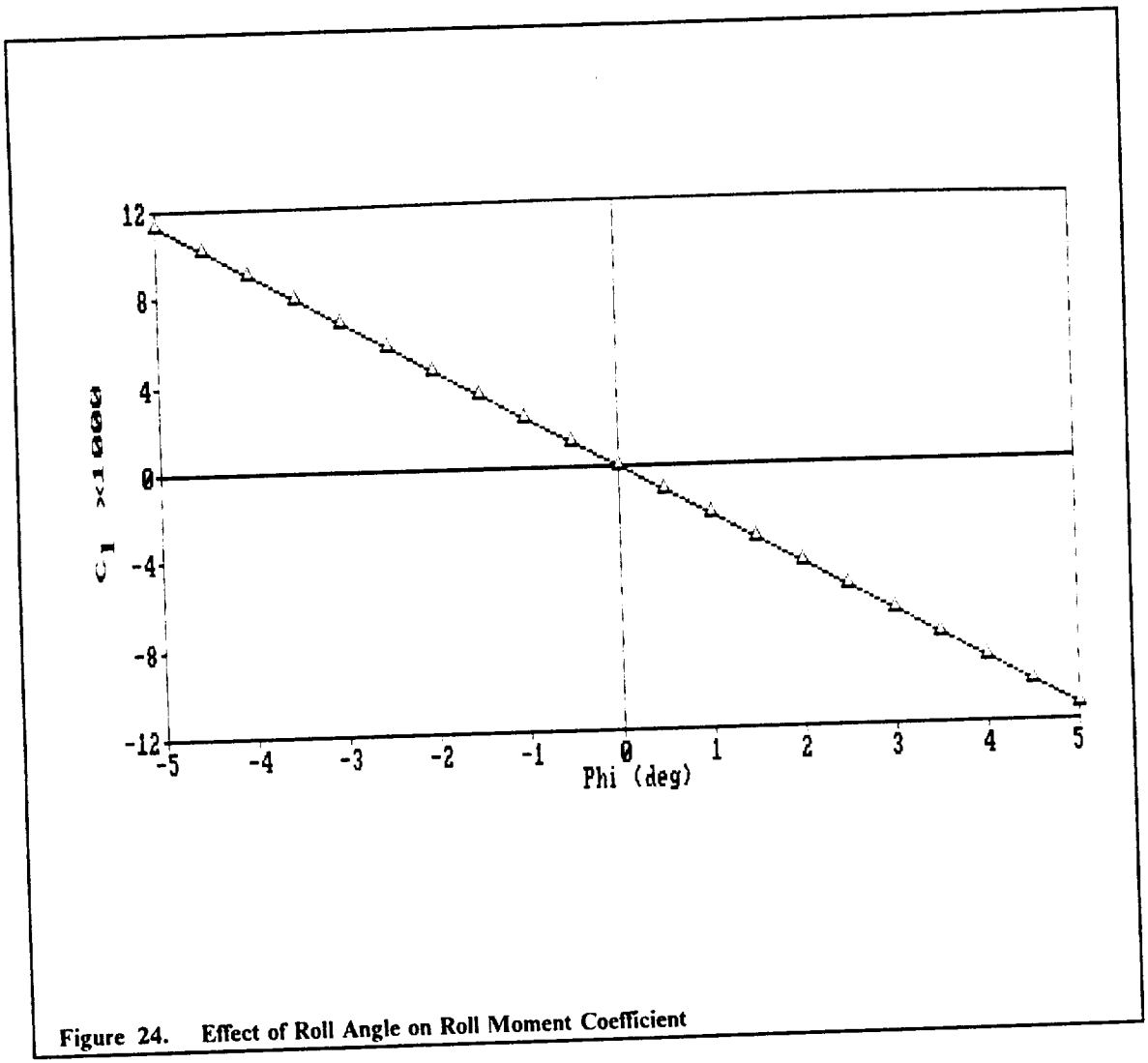

Figure 24. Effect of Roll Angle on Roll Moment Coefficient

CONTROL

Control is necessary for the vehicle to maintain the planned trajectory. Deviation from this trajectory can result from initial errors at reentry and from fluctuations in atmospheric properties (such as density) during the aeropass. Control allows these deviations to be corrected.

Modifications to the trajectory are achieved by offsetting pitch, roll, and yaw angles from their trim values. This will be done through use of the Reaction Control System (RCS). The RCS thrusters will create moments along the appropriate axes to yield an offset in pitch, roll, or yaw. This applied moment will be equal but opposite to the restoring moment created by the vehicle's stable tendency. The deviations will be small to avoid placing large loads on the vehicle structure.

Using the previously mentioned computer program, it was possible to determine the magnitudes of the moments needed to create rotation offsets of 1° along each of the three flight axes. Deviating pitch by 1° from αtrim (13.25°) would require a moment of 4,508 ft-lbf about the CG and parallel to the y-axis. A 1° deviation in roll would require a moment of 4,237 ft-lbf about the x-axis. Finally, a 1° deviation in yaw would require a moment of 170 ft-lbf about the z-axis.

Control is necessary to carry out the atmospheric plane change maneuver. The plane change is achieved by adjusting roll angle. This causes the drag force to be slightly offset from the velocity direction, thereby changing the vehicle's trajectory.

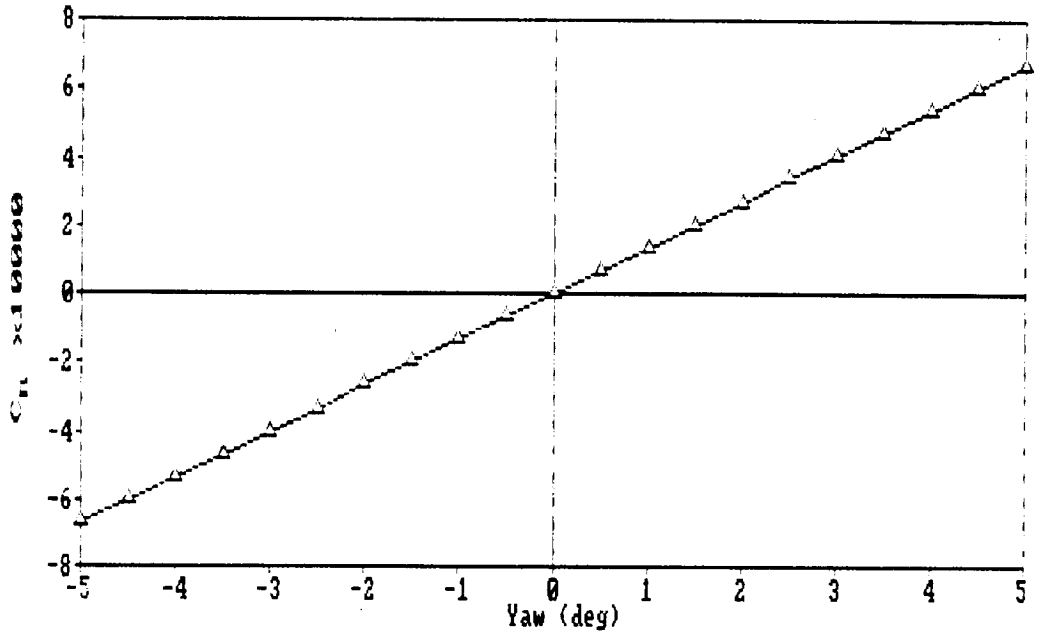

Figure 25. Effect of Yaw Angle on Yaw Moment Coefficient

2.2.6 LIMITATIONS ON CG POSITION DUE TO WAKE EFFECTS

The purpose of the aerobrake is to protect the ASTV from the heat encountered during the pass through the atmosphere. All vulnerable vehicle components are positioned in the protective zone provided by the aerobrake. This protective zone has boundaries determined by both aerobrake geometry and the angular orientation of the aerobrake relative to the flight path.

One factor affecting the angular orientation of the ASTV is the CG location. As the CG location changes so does trim angle of attack. Hence, CG position affects the boundaries of the aerobrake's protective zone. It was therefore necessary to determine the range of allowable CG positions which keep all vulnerable vehicle components within the protective zone behind the aerobrake.

A computer program was used to calculate the protective zone provided by the aerobrake. Inputs to this program included aerobrake geometry, wake angle, and estimated minimum and maximum roll and pitch angles. The protective zone was then output and used to place the vulnerable vehicle components. components. Figure 26 on page 37 graphically depicts the region protected by the aerobrake.

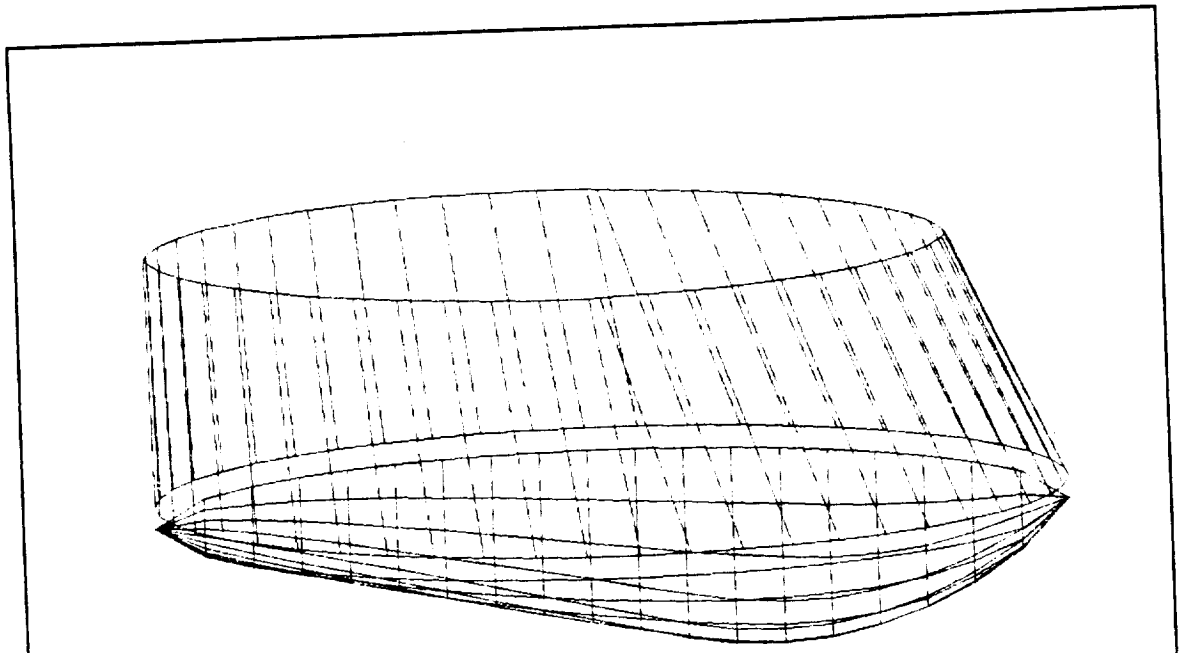

Figure 26. Aerobrake Protection Zone

During the aerobrake sizing process, the minimum and maximum angles of attack were limited to ±5° from the optimum trim angle of attack. A 1° control margin was also included to give an overall range of trim angles of attack from 9.25° to 17.25°. These angles subsequently give a range of allowable horizontal CG positions. The minimum and maximum αtrim values correspond to horizontal CG positions of 18.43 feet and 18.92 feet respectively. The CG location must therefore remain within this 0.49 foot margin during the aerobraking phase. The CG will only shift minutely due to propellant use by the RCS thrusters. It is essential though that the payload be positioned correctly so as to provide this CG location.

REFERENCES

1. Anderson, John D. Jr., *Modern Compressible Flow with Historical Perspective*, New York, McGraw Hill, 1982.

2. Bate, R.R., Mueller, D.D., and White, J.E., *Fundamentals of Astrodynamics*, New York, Dover, 1971.

3. Chapman, D.R., "An Approximate Analytical Method for Studying Entry into Planetary Atmospheres," *NASA TR-R-11*, 1959.

4. Chapman, D.R., and Kapphahn, A.K., "Tables of Z Functions for Atmospheric Entry Analyses," *NASA TR-R-106*, 1961.

5. Hill, P.G. and Peterson, C.R., *Mechanics and Thermodynamics of Propulsion*, Addison Wesley Publishing Co., Reading, Mass. 1970.

6. Loh, W.H.T., *Dynamics and Thermodynamics of Planetary Entry*, Prentice Hall, Englewood Cliffs, New Jersey, 1963.

7. Schleinitz, J.P., and Lo, R.E., "Solar-Thermal OTVS in Comparison with Electrical and Chemical Propulsion Systems," *IAF-87-199*, October 1987.

8. Vinh, N.X., Busemann, A., and Culp, R.D., *Hypersonic and Planetary Entry Flight Mechanics*, University of Michigan Press, Ann Arbor, Michigan, 1980.

9. *NOTS computer code.* Naval Ordinance Test Center, China Lake, CA. 1986.

3. PROPULSION

INTRODUCTION

ASTV propulsion is provided by two engines in a side-by-side configuration. These engines have been designed to yield high performance and reliability while also being compact. Main features of these engines include a bell nozzle optimized for minimum length, a nozzle retraction mechanism, and gimballing about two rotational degrees of freedom. Liquid hydrogen/liquid oxygen propellant is fed to the engines via settling, pressurized tanks, and boost pumps.

3.1 ASTV ENGINE DESIGN

3.1.1 DESIGN CONSIDERATIONS

Two main factors influenced the design selection of the ASTV main engine. The first factor was performance. Engine performance determines, to a large extent, the propellant requirements for a mission. The focus was on achieving a specific impulse goal of 500 seconds without threatening engine reliability. The second factor influencing engine design was compactness. The engine must fit in a space limited by the aerobrake's size and protection zone. Keeping engine size to a minimum reduces aerobrake size requirements. It also increases the range of allowable engine positions to give greater configuration flexibility. The extendible nozzle concept was an important ingredient in this design consideration.

3.1.2 ENGINE SPECIFICATIONS

ENGINE OPERATING/DESIGN PARAMETERS

The Space Shuttle Main Engine (SSME) was used as a starting point for determining the ASTV engine design parameters. The SSME was selected because it has shown excellent performance and reliability during shuttle flights, and because it is consistent with the ASTV engine design considerations.

A thermochemical equilibrium code developed at the Naval Ordinance Test Station in China Lake, California (NOTS computer code) was also used to assist in the determination of the operating parameters. This program calculates the equilibrium combustion reaction in a chamber for a set of reactants chosen by the user. The user may specify two thermodynamic properties in the chamber and the list of combustion products to be considered. The program then expands the combustion products isentropically through a nozzle, and calculates flow properties at the throat and at any desired station in the nozzle.

The design oxidizer/fuel (O/F) ratio was set at 6:1. This is the predominantly used value for LO_2/LH_2 engines. Using a hydrogen rich mixture lowers the average exhaust molecular weight, thus yielding higher nozzle exit velocities and improved engine efficiency. Valves allow this ratio to be modified to suit current engine operating conditions, as well as available propellant.

Oxygen was assumed to enter the combustion chamber at its boiling temperature of 162 R. Hydrogen inlet temperature was taken to be 325 R, the same as that for the Pratt & Whitney RL-10A-3 engine which has a similar hydrogen flow schematic (Ref. Hill and Peterson, p.441).

Chamber pressure was assumed to be 3,000 psi. The initial estimate of 3,260 psi (used in the SSME) was reduced to compensate for lower turbopump outlet pressures.

Based on O/F ratio, propellant inlet temperatures, and chamber pressure, an equilibrium chamber temperature of 6,760 R was calculated using the NOTS program. Input also included a list of combustion products to be considered. The selected products were water vapor, monatomic and diatomic hydrogen, and monatomic and diatomic oxygen. Combustion chambers already exist which operate at these high temperatures. A prime example is the SSME, which has a chamber temperature of 6,819 R.

The engine's nozzle area ratio was set to 650. Large nozzle area ratios improve engine performance in a vacuum environment. Engine size restrictions pose an upper limit to this ratio though. The extendible nozzle concept allows this area ratio to be achieved while still keeping engine size to within constraints.

Table 8 summarizes the engine operating/design parameters.

Table 8. ASTV Main Engine Parameters

Parameter	Value
Oxidizer/Fuel Ratio	6:1
Chamber Temperature (R)	6,660
Chamber Pressure (psi)	3,000
Propellant Inlet Temp.	
Hydrogen/Oxygen (R)	325/162
Nozzle Area Ratio	650

ENGINE PERFORMANCE CHARACTERISTICS

Using the dual-engine configuration (to be discussed), required vacuum thrust was set at 15,000 lbf per engine. Preliminary thrust estimates were on the order of 30,000 lbf, but these were reduced to decrease engine size and weight and reduce loadings on engine components. Required mission burn times were also considered. Lower thrust yields longer burn times and also increases propellant requirements slightly. Assuming an initial vehicle mass of 94,275 lbm, a total thrust of 30,000 lbf yields a reasonable 10 min. 12 sec. worst-case burn time for the initial burn from LEO to GEO.

A specific impulse goal of 500 seconds was set for the ASTV main engine. This assumed a modest performance improvement over existing LO_2/LH_2 engines which typically have Isp values in the range of 450 to 475 seconds. This goal, however, was not fully achieved. Based on the previously listed engine operating parameters, results from the NOTS program showed the engine to have a vacuum Isp of 511 seconds. The final Isp after efficiency losses is 498 seconds.

ENGINE OPERATION

The ASTV engine will be capable of starting with the turbopump inlets at boost pump pressures. The boost pump will initiate flow through the turbopump. Turbopump outlet pressure will then increase as engine temperature increases. Engine cutoff will be controlled by gradually decreasing the fuel flow rate. This extends engine life by allowing a gradual cool down of the combustion chamber, throat, and nozzle.

Turbomachinery for the ASTV engine will be modeled after the Rocketdyne advanced OTV engine concept, with the exception that both turbines will be driven by hydrogen. A two-stage axial flow hydrogen turbine will drive the hydrogen pump, while a single-stage hydrogen turbine will drive the

oxygen pump. An additional modification is that oxygen and hydrogen pumps are synchronized using a gear train. The four-stage centrifugal hydrogen pump will yield an outlet pressure of 8,000 psi at its operating speed of 178,000 rpm, while the single-stage centrifugal oxygen pump will yield 3,400 psi of outlet pressure at its operating speed of 56,200 rpm. Both turbopumps will incorporate hydrostatic bearings to increase their life and reliability.

The propellant flow diagram is given in Figure 27 below. The oxygen flow rate is 26.6 lbm/s, while the hydrogen flow rate is 4.4 lbm/s. Oxygen enters the combustion chamber immediately after passing through its pump, while hydrogen follows a more complex route. After passing through its pump, the hydrogen cools the combustion chamber and throat regions. It then drives the first turbine before flowing back to cool the nozzle. Finally, it returns to drive the second turbine before entering the combustion chamber.

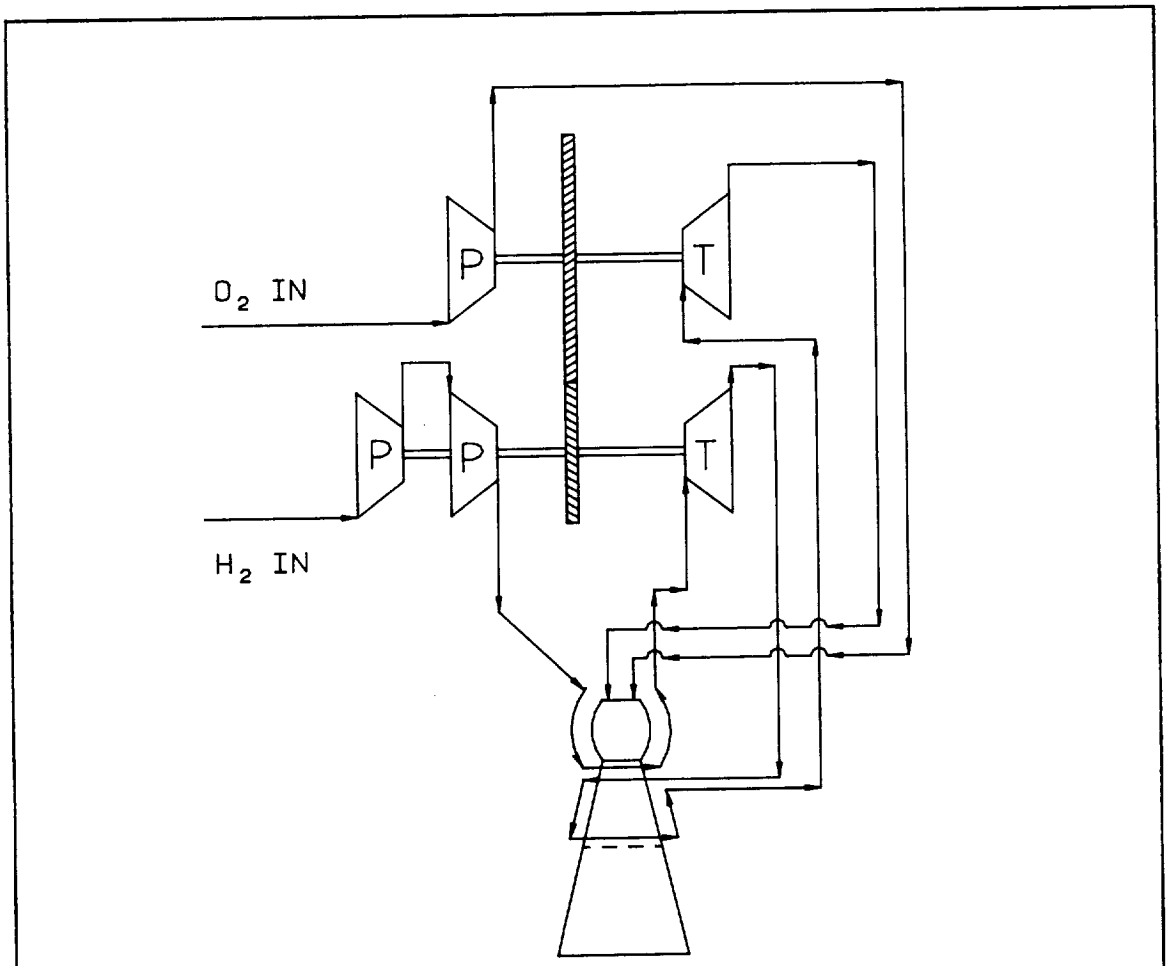

Figure 27. ASTV Engine Propellant Flow Diagram

The ASTV engine uses a regenerative cooling system. Critical areas requiring cooling are the combustion chamber, the throat region, and the first nozzle segment.

Cooling is achieved in two passes, both using hydrogen. The first pass cools the throat and combustion chamber. The NOTS program calculates gas temperatures of 6,760 R in the combustion chamber and 6,235 R at the throat. Cooling in these high temperature regions is achieved by series of channels through which the hydrogen flows, as shown in Figure 28 on page 42.

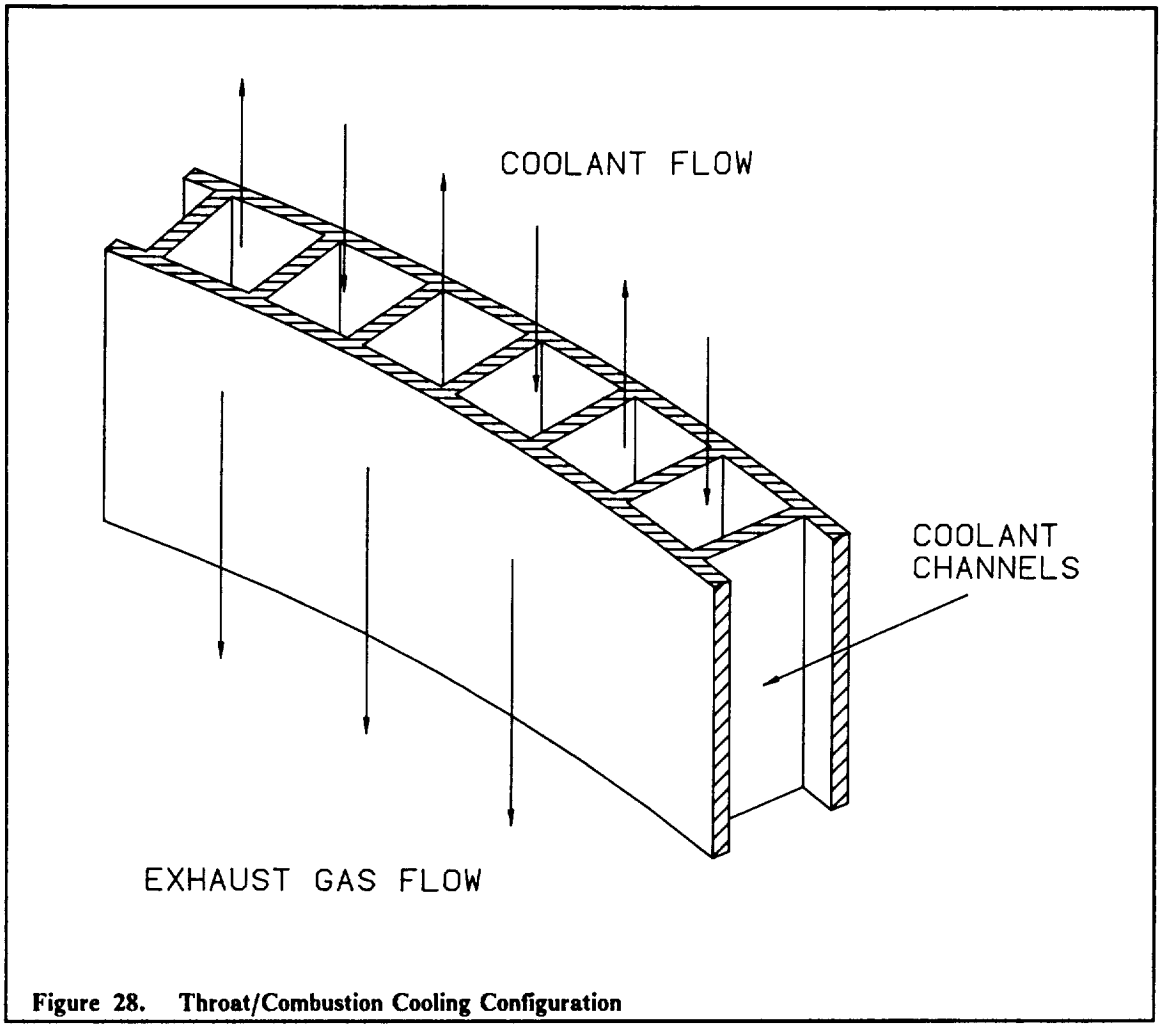

Figure 28. Throat/Combustion Cooling Configuration

In the second pass, the hydrogen cools the first nozzle segment. The extendible nozzle segment is not cooled, for the maximum gas temperature in this extendible segment is only 1,350 R. Instead, the extendible segment is made from a temperature resistant carbon composite.

The extendible nozzle section is retracted to reduce engine length when the engine is inoperative. A drive mechanism will pull the second nozzle section towards the combustion chamber past the first section. To extend the nozzle, the drive slides the extendible section back into place. O-rings between both sections insure no no leakage of exhaust gases.

3.1.3 ENGINE DIMENSIONS AND MASS

The maximum width of the ASTV engine is 47.0 inches at the nozzle exit diameter. The maximum length is 76.7 inches in the extended (operating) position and 44.0 inches in the retracted (stowed) position. Figure 29 on page 43 shows the engine in both its extended and retracted positions. The nozzle throat and exit diameters were calculated from thrust considerations and operating parameters.

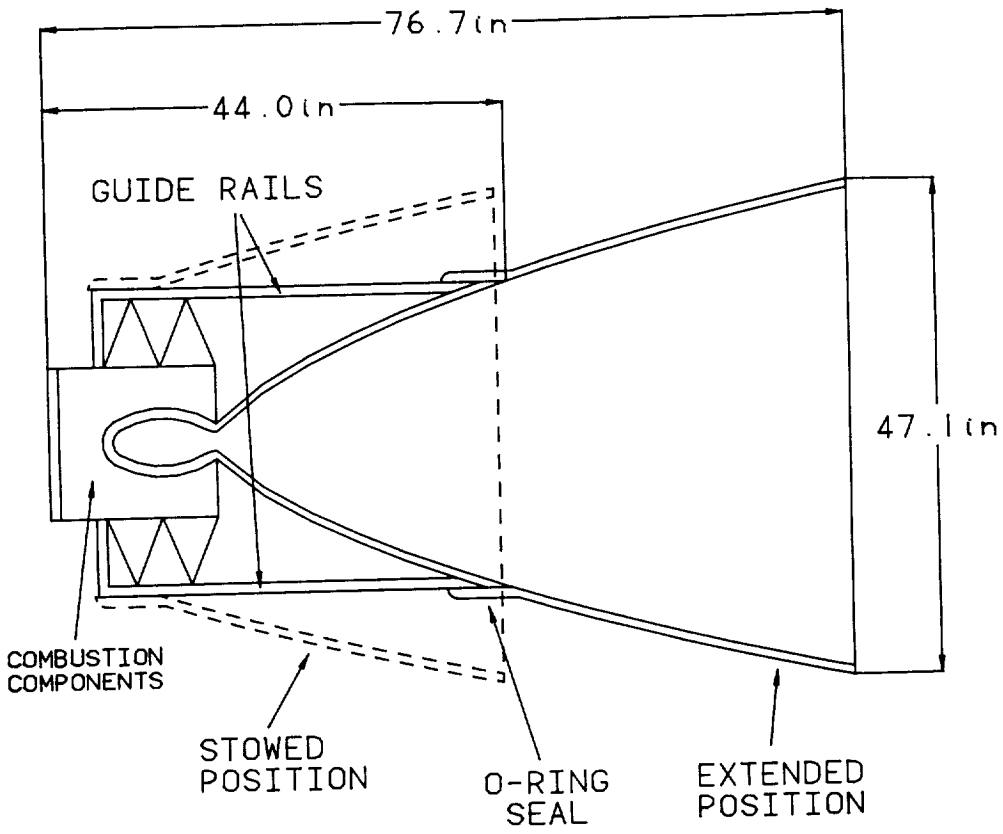

Figure 29. ASTV Engine Dimensions

Figure 29 also shows the nozzle cross-section. The engine uses a bell nozzle optimized with respect to length (Ref. Tuttle and Blount). The nozzle has a corner expansion at the throat, and a design area ratio of 1,680. Truncation reduces the area ratio to 650 and gives a nozzle contour slope of 10.5° at the exit. Length of the nozzle is just over 5 feet when fully extended. The predicted nozzle efficiency is 0.97 including losses due to both friction and nonaxial exhaust velocity at the exit.

Figure 29 also shows the nozzle retraction mechanism. Guide rails go from the first nozzle section to the combustion components. During retraction the extendible nozzle moves along these guides and actually passes over the combustion components.

Engine length was determined by combining the calculated nozzle length with an estimated combustion chamber length. The estimated combustion chamber length was obtained through comparisons with other similarly sized engines.

The engine mass was also obtained through comparisons with other engines. Mass was assumed to be proportional to thrust. This estimate was then increased by 25% to get a final estimated ASTV engine mass of 370 lbm.

The compact design of the ASTV engine allows it to easily fit in the space shuttle bay for delivery into space.

3.1.4 CONFIGURATION

A number of options had to be weighed before the final ASTV propulsion configuration could be realized. These options included choosing the type of propellant, selecting the number of engines, determining if an extendible nozzle would be required, and deciding whether to use one of the advanced OTV engine concepts under development.

The first option was choosing the type of propellant to be used. Candidates included liquid oxygen/liquid hydrogen (LO_2/LH_2) and liquid fluorine/liquid hydrogen (LF_2/LH_2). Each combination has its advantages and disadvantages. Table 9 lists advantages and disadvantages of each combination.

Table 9. Factors Influencing Propellant Selection

Propellants	Advantages	Disadvantages
LO_2/LH_2	• Relatively high Isp • Proven past performance	• More propellant required • Less handling risk
LF_2/LH_2	• High Isp • Reduced propellant	• Storage difficulties

The LO_2/LH_2 combination was selected based on its proven past performance and its lower handling risks.

The second option involved the number of engines. The two choices included a single-engine configuration or a dual-engine configuration. Table 10 lists advantages and disadvantages of each.

Table 10. Comparisons of Single and Dual Engine Configurations

Configuration	Advantages	Disadvantages
Single	•Simpler layout	•Larger engine required
Dual	•Engine redundancy •Better thrust control	•More complex engine mount

Despite the increase in design complexity, the dual-engine configuration was preferred over the single-engine configuration. The deciding factor was engine redundancy. Since the ASTV will support manned missions, it is important that it have component redundancy in case of failure. If one engine fails to operate, the other engine will provide sufficient thrust to return the crew to safety.

The extendible nozzle concept was determined to be appropriate for the ASTV engine. It improves engine performance and increases compactness, thus agreeing with both design considerations. During engine operation the nozzle is fully extended to create a high expansion ratio suited to a vacuum environment. During inoperative periods the extendible portion is retracted to reduce overall engine length. This feature allows the engines to be placed closer to the aerobrake lip without the danger of wake exposure during the atmospheric pass.

The final configuration option involved the possible use of an existing engine. Three other engines are currently under development for use with orbital transfer vehicles. The contractors include

Aerojet Tech Systems, Rocketdyne, and Pratt & Whitney. These engines were evaluated for possible use in the ASTV.

Primary characteristics of the both the Aerojet and Rocketdyne engines include 7,500 lbf of thrust, specific impulse of 480 seconds, an extendible nozzle section, and a dual propellant expander cycle. The Pratt & Whitney engine shares the same thrust and specific impulse ratings, but differs in that it only has a hydrogen expander cycle.

All three engines were rejected on the basis of their thrust and specific impulse ratings. The ASTV thrust requirement was set at 15,000 lbf per engine, twice that of these engines. Each engine also fell short of the ASTV engine specific impulse goal of 500 seconds.

ENGINE LAYOUT

Both engines will be mounted at the front of the ASTV (the positive X direction). The aerobrake protection zone analysis required positioning the mission module closer to the aft end of the vehicle. It was then natural to assume a forward engine position. Figure 30 on page 46 shows side and top views of this layout. The dashed lines near the front and back of the aerobrake show the extent of the protection zone along the axis of symmetry.

The engine pivot points are located 66 inches from the front of the aerobrake and 42 inches above the surface of the aerobrake. Separation between the engine pivots is 54 inches. These distances are indicated in the top view of the engine configuration.

In positioning the ASTV engine, the following four factors were taken into account:

1) clearance between engines
2) protection from wake during atmospheric pass
3) no main exhaust impingement on vehicle components
4) thrust vectoring through all CG locations

In order for the engines to have clearance, total separation between the two adjacent engine pivot points must be greater than the maximum engine width of 47.0 inches. Actual separation between the pivots is 54 inches, hence giving a clearance of 7.0 inches between the engines.

The engine position must also insure that all components remain contained in the aerobrake protection zone during the aerobraking phase of the mission. With the position shown in Figure 30 on page 46, the only engine component which ever enters this zone is the extendible nozzle section. This section, however, will be retracted and rotated down during aerobraking since the main engines do not operate during this phase. Figure 31 on page 47 shows the engines in their stowed position.

Another factor which governs engine position is the possible impingement of main engine exhaust gases on either the aerobrake lip or an adjacent engine. From Figure 30 on page 46 it is clear that main engine exhaust will not impinge on the aerobrake lip. It is also clear that exhaust will not impinge on either engine when they are undeflected in yaw as shown. During yawing maneuvers, however, it will be necessary to limit engine yaw deflection angles so that main exhaust impingement on the engines does not occur. This will be more fully discussed in the section describing the engine mount.

A final factor which affects engine layout is the requirement that the thrust vector pass through all possible vehicle CG locations. Figure 32 on page 47 shows the engines rotated to extreme angles, along with the extreme vehicle CG locations. In both cases the thrust vector is aligned through the CG.

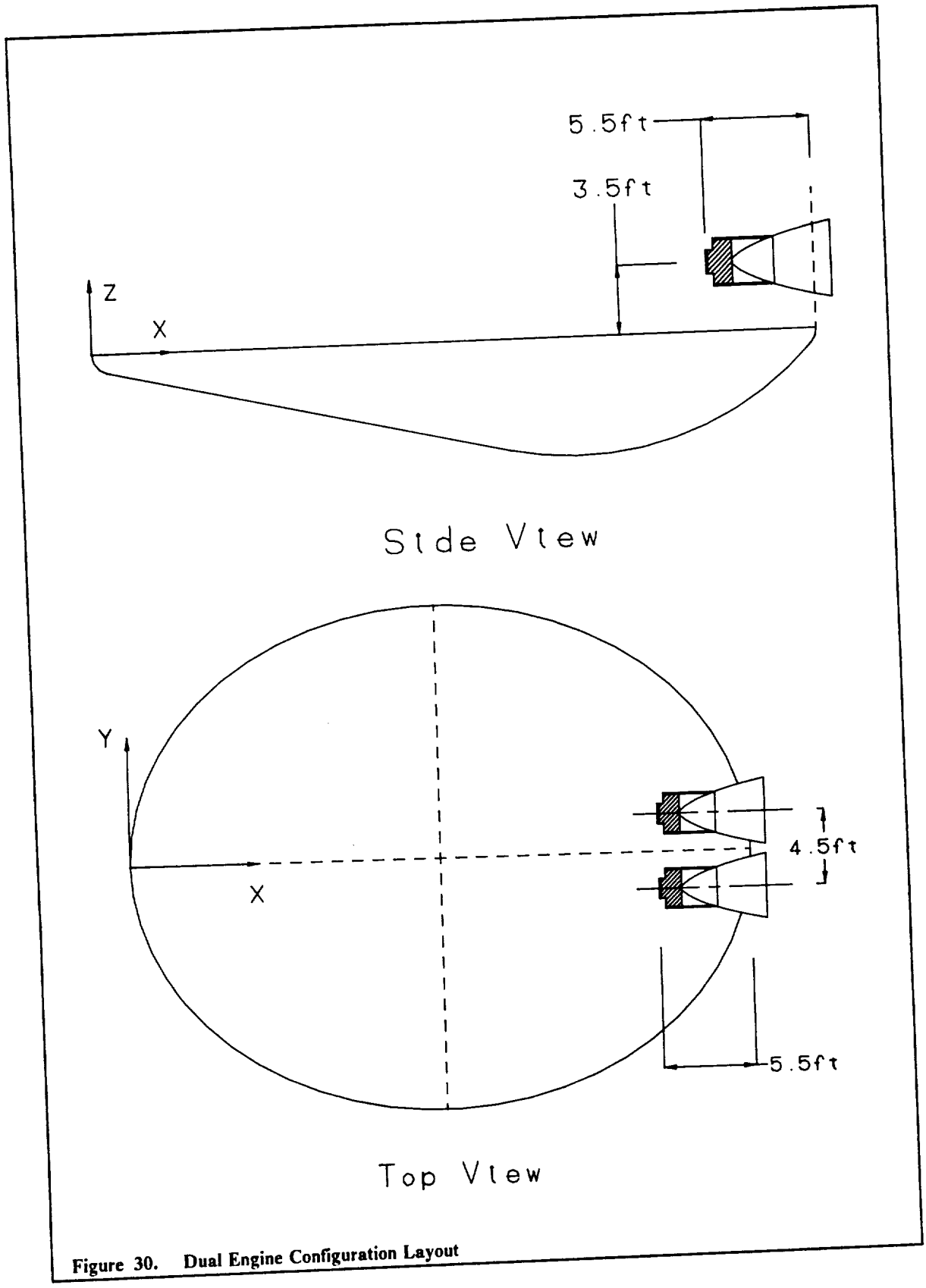

Figure 30. Dual Engine Configuration Layout

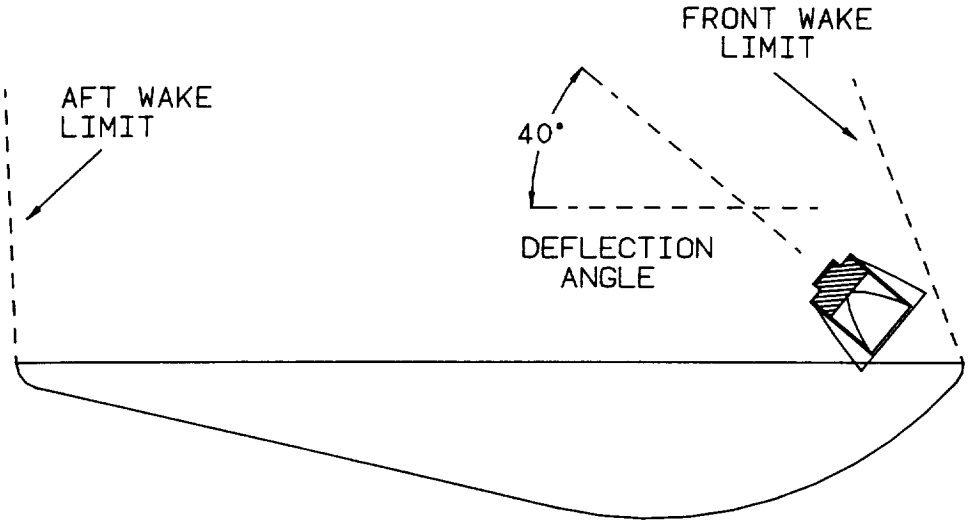

Figure 31. Engines in Stowed Position

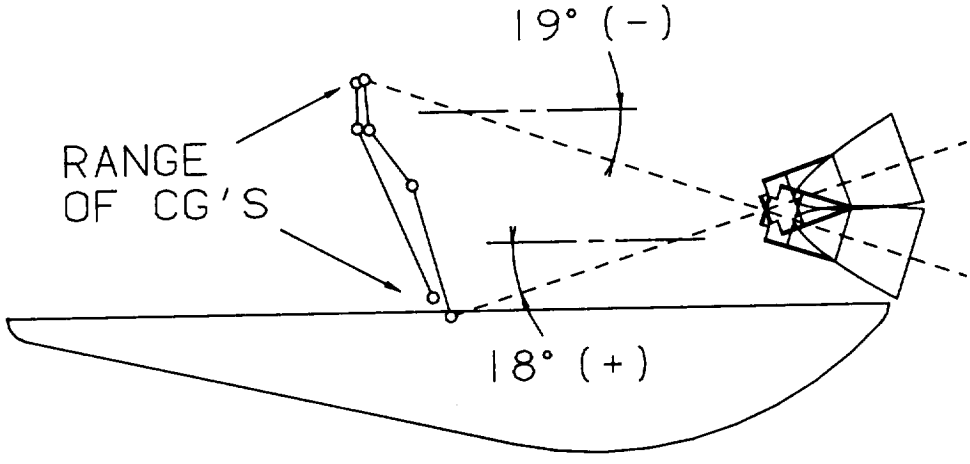

Figure 32. Thrust Vectoring through Extreme CG Locations

ENGINE MOUNT

The purpose of the engine mount is to provide the engine with two rotational degrees-of-freedom for purposes of thrust vectoring. Thrust vectoring is needed both for keeping thrust aimed through changing CG locations and for maneuvering. The entire thrust chamber pivots about the engine mount. Figure 33 shows the engine mount.

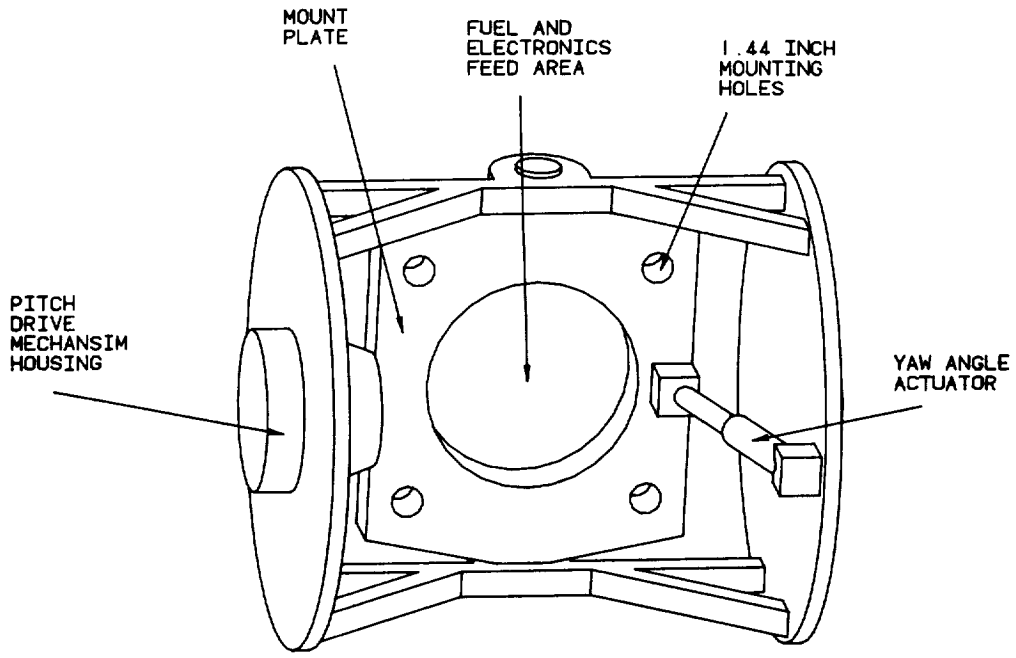

Figure 33. ASTV Engine Mount

The engine mount allows both pitch and yaw gimballing. Pitch gimballing would be visible in the side view, and yaw gimballing would be visible in the top view. The minimum and maximum required pitch angles are -40° and 18° respectively. The minimum pitch angle is used during stowage of the engine, while the the maximum pitch angle is used when the CG is deepest and farthest forward, as shown in Figure 32 on page 47. The minimum and maximum yaw angles are $\pm 7.5°$. Each engine, however, will only be allowed to gimbal so that the thrust vector points away from the center. This is illustrated in Figure 34 on page 49.

If both engines were gimballed in yaw at the same time, there would a danger of main exhaust impingement on an engine. Figure 35 on page 49 illustrates this problem. The angle made by the exhaust with respect to the nozzle is the Mach angle corresponding to the exit Mach number. The design exit Mach number is 6.51, thus giving an 8.8° exhaust expansion angle.

An electric drive mechanism will pivot the engine in pitch. Actuators would not be suitable in this case because of the large range of required pitch angles, and because pitch gimballing will occur with the engine inoperative. The power requirement for each drive is 180 W. Yaw gimballing will be done with actuators. Each engine mount will have one actuator. The actuators will be operated using propellant at pump-outlet pressure. The drive mechanism and actuator for one engine mount are included in Figure 33.

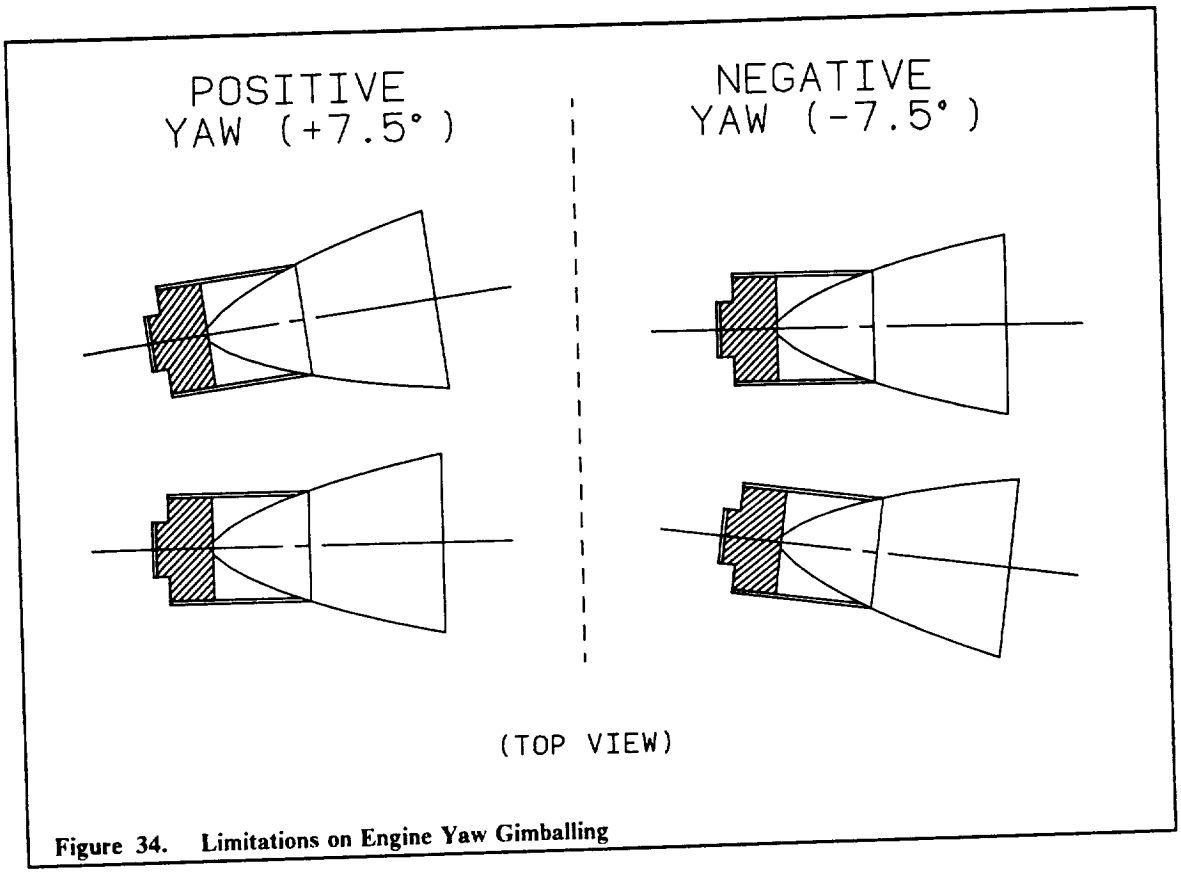

Figure 34. Limitations on Engine Yaw Gimballing

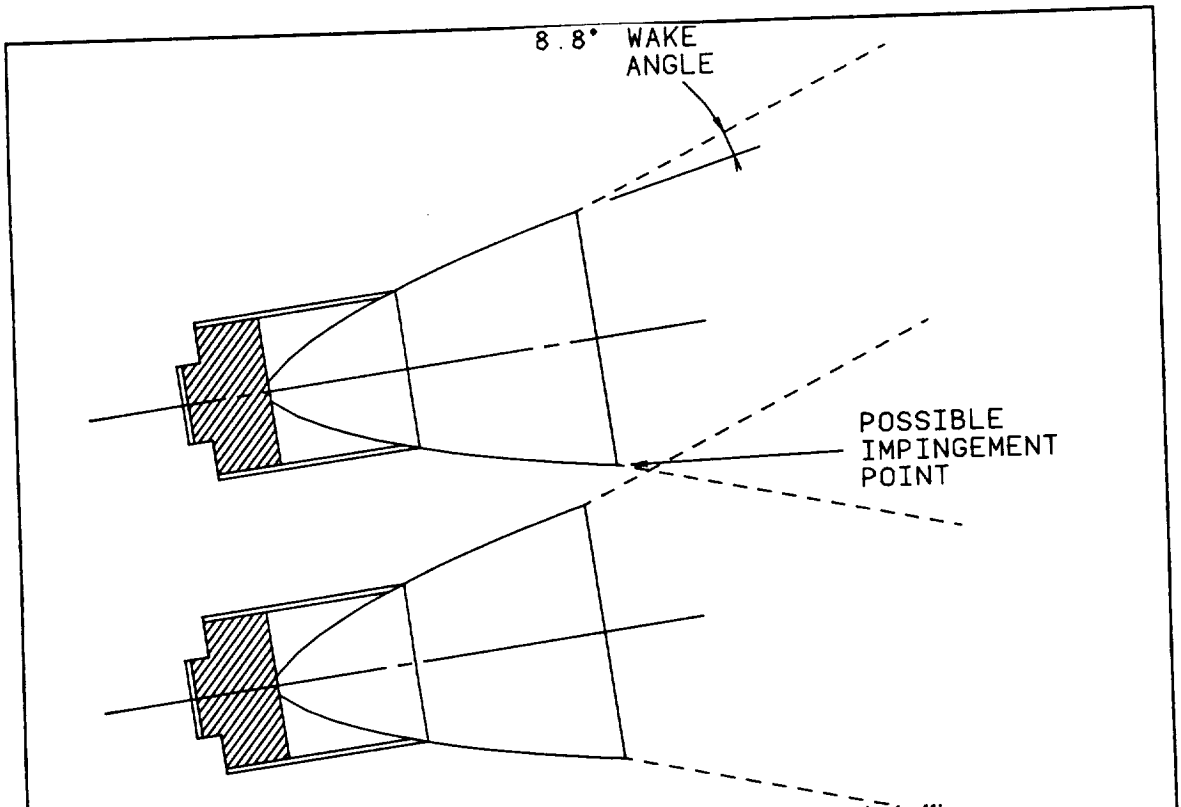

Figure 35. Exhaust Impingement Problem Arising During Parallel Yaw Gimballing

In the case of engine failure, it will be necessary for an astronaut to install a new engine while in space. The engine mount simplifies this task. The entire engine can be quickly removed by unbolting it from its mount. Low pressure propellant lines are removed via quick release valves.

3.2 PROPELLANT HANDLING

Propellant handling is the process of extracting the fuel from the tanks and transporting it to the engines or RCS. The fuel and oxidizer, liquid hydrogen and liquid oxygen respectively, are stored in a system of fourteen tanks.

3.2.1 PROPELLANT ACQUISITION

There are several ways to make the propellants available for pumping. These include capillary acquisition devices, propellant settling with pressurized tanks and boost pumps, and propellant settling with subcoolers and boost pumps.

Capillary acquisition devices work by using wetted screens to obtain a reserve of propellant. The system consists of the capillary acquisition device, thermal subcoolers, and a pumping system that pumps the propellant from the cold side of the subcooler back to the tanks. The reserve of propellant, stored in a start basket, is used to start the engines. Once the engines have been started and are thrusting, the acceleration causes the propellants to settle in the tanks providing a constant supply.

The next system of propellant acquisition utilizes propellant settling along with subcoolers and boost pumps. Before the engines can be fired, a supply of propellant is needed. The RCS system is utilized to initially accelerate the vehicle to cause the propellants to settle in the tanks. The subcoolers are then used to provide the net positive suction pressure (NPSP) required by the boost pumps. The boost pumps then pump the propellants through the ducts to the engines.

The third and final scheme studied for the acquisition of the propellants also utilizes propellant settling. However, the tanks will be pressurized to provide the NPSP required for the boost pumps.

There were three criteria used in choosing an appropriate propellant handling system: weight penalty, technology, and reliability. The capillary acquisition device has the most costly weight penalty, the lowest reliability, and requires the most as far as technological advancement is concerned. Therefore a settling scheme has been chosen. Due to the size of the subcoolers and the propellant residual volume created, the subcooler scheme was eliminated. The pressurized tank scheme was the most reliable and also the lightest. Also, this method requires the least amount of new technology, and thus is the recommended system.

This method of settling and pressurizing is integrated into the tanking system. The tanking system consists of four main disposable tanks and ten small permanent tanks. Each of the main tanks is pressurized to 20 psi. Each main tank is also equipped with an axial inducer type boost pump to push the propellant to the main engine's turbopumps (Ref. Cooper and Sheer). The smaller permanent tanks are pressurized to 500 psi. These smaller tanks are pressurized to the operation pressure of the RCS thrusters, thereby eliminating the need for pumps on these tanks. Pressure is maintained by helium.

3.2.2 PROPELLANT LINES

Propellant ducts are responsible for carrying the propellants from the tanks to the main engines, RCS thrusters, and fuel cells. The RCS thrusters will be fed from the smaller permanent tanks due to pressure requirements. The fuel cells will also be fed from the small tanks because of their compatible pressure requirements. The main engines draw propellant from the main tanks until the tanks are ejected before reentry. The small tanks subsequently provide the propellant necessary to circularize at LEO. All tanks will be interconnected via a valve control system. By operating the valve system correctly, a damaged or clogged tank can be shut down and propellant can be routed from another tank. All connections to tanks and engines are quick connect/disconnect type connectors. These are used for safety and ease of maintenance reasons.

The ducts will be made of an aluminum alloy. This will save weight compared to stainless steel ducts. To accommodate thermal and structural deflections, aluminum bellows joints will be utilized. Engine gimballing will be accounted for with flexible supply lines. All ducts are wrapped with insulation to protect them from radiation and debris. A propellant flow flow schematic follows in Figure 36.

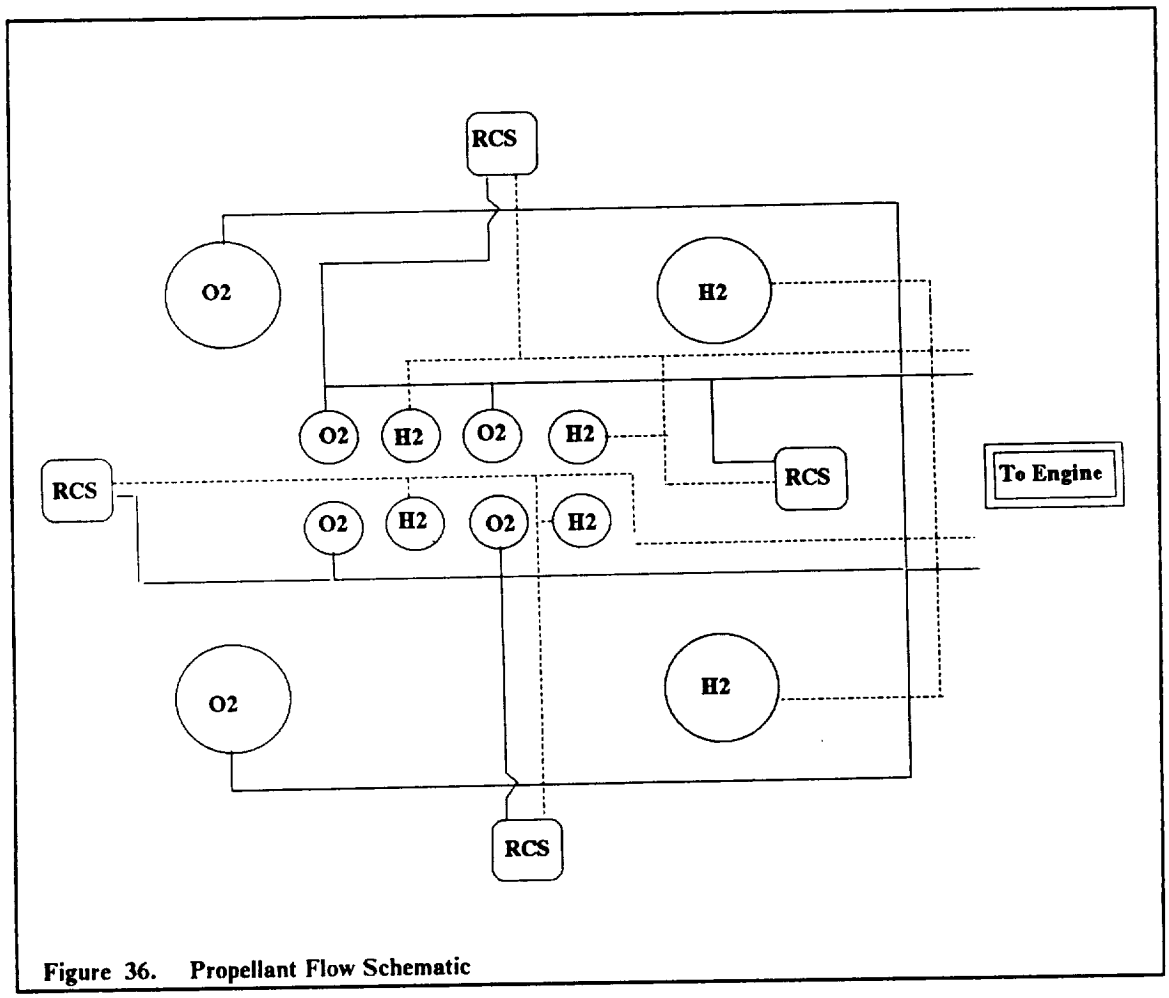

Figure 36. Propellant Flow Schematic

REFERENCES

1. Blatt, M.H., Bradshaw, R.D. and Risberg, J.A., Capillary Acquisition Devices for High Performance Vehicles - Executive Summary, General Dynamics Convair Division, NASA-CR-159658 (1980).

2. Cooper, L.P. and Scheer, D.D., "Status of Advanced Propulsion for Space-Based Orbital Transfer Vehicle," *Acta Astronautica*, Vol 17, No 5, 1988.

3. Tuttle, J.L. and Blount, D.H., *Perfect Bell Nozzle Parametric and Optimization Curves,* NASA Reference Publication 1104, Marshall Space Flight Center, 1983.

4. *NOTS computer code,* Naval Ordinance Test Center, China Lake, CA. 1986.

4. STRUCTURES

INTRODUCTION

The ASTV consists of four major structural components: a frame, mission modules, propellant tanks, and the aerobrake supporting structure. The frame is made of 181 tubular members of an advanced composite material and is the superstructure connecting the aerobrake to the various vehicle components. The cylindrical modules store the mission payload and provide crew life support. Up to three interconnected modules may be carried by the vehicle. The ASTV propellant tank layout consists of four disposable and ten reusable tanks. The disposable tanks are ejected prior to entry into the atmosphere. The aerobrake is made rigid by seven longitudinal and five lateral supporting stringers. The aerobrake attaches to the frame via these stringers. These elements are made such that they can be integrated in orbit at the space station.

4.1 FRAME

A frame composed of tubular members serves a dual role in the vehicle design. It provides a scheme to integrate ASTV components and it provides support for the aerobrake. Although the aeroshell itself is rigid, it requires additional support during mission phases which impose severe aerodynamic, thermal, an inertial stresses to the vehicle. Figure 37 on page 54 shows an isometric view of the structural components. The two phases of main concern are the aerobraking phase and the thrusting phase. The frame consists of tubular members rigidly connected at all joints. It provides 37 connection points to the aerobrake, a cradle for the mission module, and a mounting support for the propulsion system. The frame members are fabricated from an advanced graphite epoxy composite and are connected by structural aluminum elements. In addition, this frame has provisions for a payload configuration for orbital delivery of the frame and aerobrake. The frame design was analyzed using a PC supported computer structural analysis program called PC-STRAN. Using this program, the internal stresses and deflections of the frame during the aerobraking and thrusting phases were calculated.

4.1.1 MATERIALS

The two structural materials required for the ASTV aerobrake frame are an advanced graphite/epoxy composite and aluminum. The former is used for the tubular members of the frame while the latter is used for the endfittings required to join these members.

The composite material which was selected is an HT graphite fiber/epoxy matrix. This material was chosen as a baseline due to its exceptional material properties. In selecting a material there were three major factors that were considered: strength, mass, and thermal characteristics. Several structural materials were compared based on modulus, ultimate strength, and density. Table 11 on page 54 lists and compares the material candidates in these categories. Figure 38 on page 55 shows that HT graphite/epoxy has an exceptional combination of ultimate strength-to-density and

modulus-to-density ratios. Table 11 on page 54 lists the characteristics of this material. The coefficient of thermal expansion for this composite material does not exceed 5.0×10^{-6} in/in/°F.

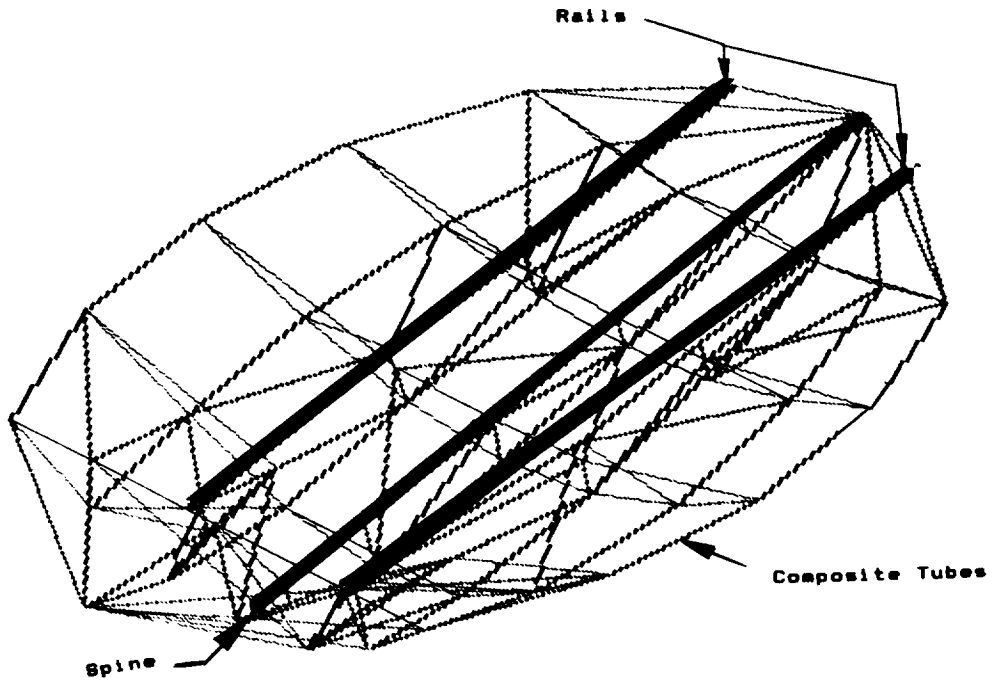

Figure 37. ASTV Frame

Table 11. Frame Material Candidates

Material	Young's Modulus psi E+6	Ultimate Strength psi E+3	Density lb/cu.in	Specific Modulus in. E+8	Specific Strength in. E+6	Modulus to Density Ratio	Strength to Density Ratio
Aramid/Epoxy	12	280	0.055	5.9	5.09	218.18	5090.91
S-Glass/Epoxy	7.5	300	0.070	1.1	4.29	107.14	4285.71
T300/Epoxy	17	230	0.056	4.1	4.10	303.57	4107.14
HT graphite/Epoxy	22	205	0.054	4.1	3.80	407.41	3796.30
Boron/Epoxy	31	220	0.075	4.1	2.90	413.33	2933.33
E-glass/Epoxy	7.5	200	0.070	1.1	2.86	107.14	2857.14
HM graphite/Epox	30	135	0.058	5.2	2.30	517.24	2327.59
Beryllium	35	90	0.066	5.3	1.40	530.30	1363.64
Titanium 6Al-4V	15	155	0.155	1.0	1.00	96.77	1000.00
Aluminum 7075	10	82	0.100	1.0	0.80	100.00	820.00

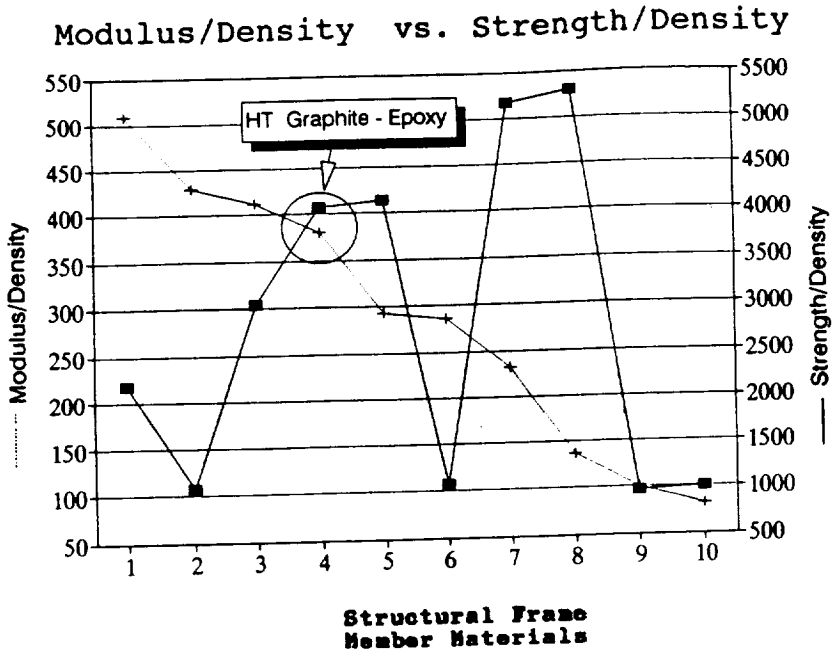

Figure 38. Material Characteristic Comparison

Due to the material's unidirectional properties, it is necessary to design endfittings that can be used to attach the tubular members to one another. These endfittings are be made of Aluminum 7075. The mission module mounting rails are also made of aluminum. Aluminum was chosen because of its proven effectiveness in space applications and its low density. Properties of Aluminum 7075 are listed in Table 11 on page 54.

4.1.2 FRAME COMPONENTS

The frame consists of 181 tubular members. These members have a 5.00 inch inner diameter and an 0.125 inch thickness to give a total cross sectional area of 2.013 in^2. This area allows the member to withstand a 412,000 lbf axial load. Each tubular member is constructed of HT Graphite fibers in an epoxy matrix laid in a (-5/0/5) pattern. Figure 39 on page 56 shows the fiber directions. The off-axis layers serve as a safety factor against unexpected transverse loads, and also help to dampen vibrations.

The simplest manufacturing method for the frame members utilizes a preimpregnated composite tape laid up on a cylindrical tool and cured in an autoclave under an approved cure cycle. The autoclave must be large enough to cure the longest members (13.5 feet).

A special member is centered along the length of the mission module cradle. Figure 40 on page 56 shows this member. It is a square graphite/epoxy tube having inner dimensions of 8.0 inches by 8.0 inches and a 0.125 inch wall thickness. This beam greatly enhances the overall structural rigidity of the frame. It is made in two 13.5 foot sections and manufactured similarly to the standard frame members.

Each node of the frame is joined by an aluminum endfitting such as the one shown in Figure 41 on page 57. These endfittings form a 7.5 inch long sleeve over each joining composite member. The sleeve has a thickness of 0.1875 inch. Individual tubes are bonded to these endfittings with a

high temperature adhesive capable of withstanding the 800°F temperature shifts occurring during the aerobraking phase. These endfittings also use reinforcing ribs where necessary.

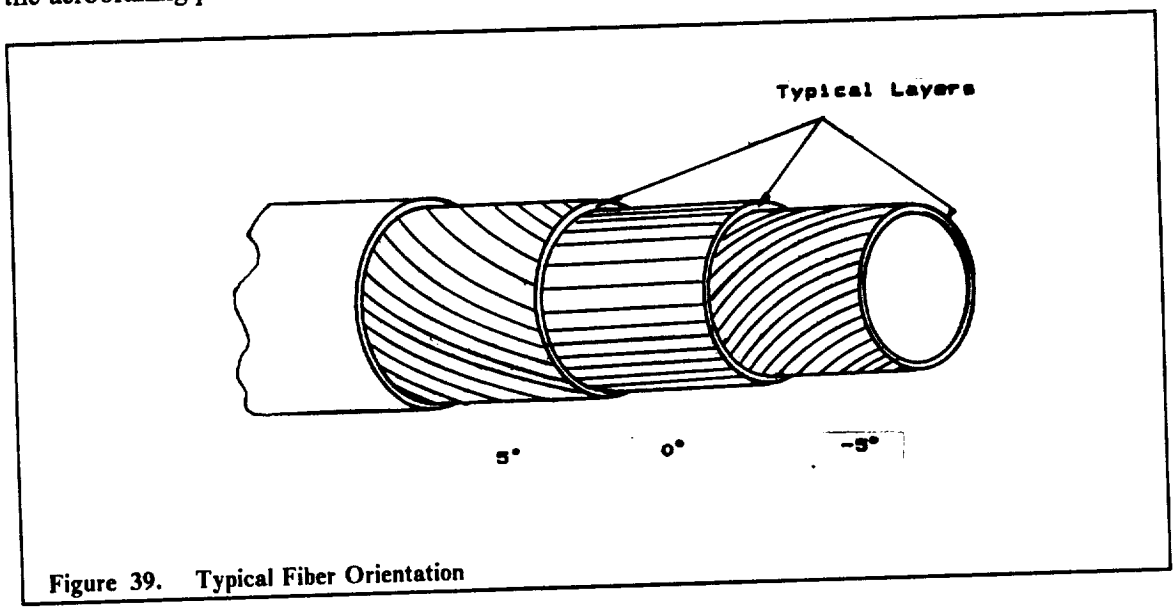

Figure 39. Typical Fiber Orientation

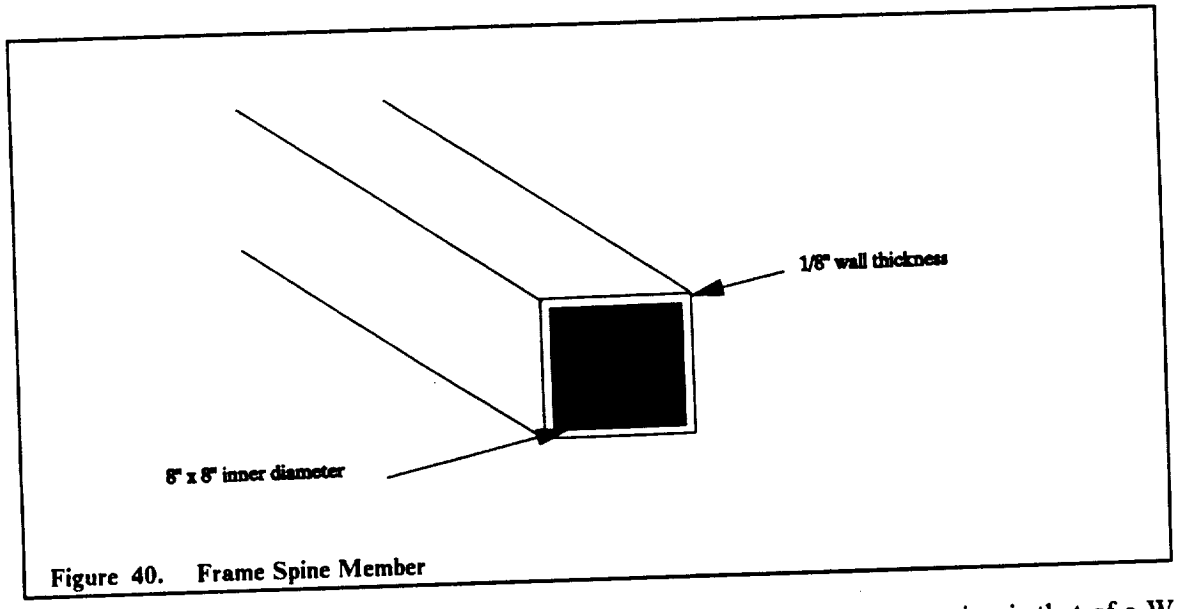

Figure 40. Frame Spine Member

The mission module mounting rails are made of aluminum. The rail cross section is that of a W 12x96 Steel I-beam. The flange is 12.2 inches wide, the web 12.7 inches deep, and the beam 27 feet long. The total cross sectional area is 28.2 in^2. An aluminum I-beam was chosen because of the complex loads that accelerating and decelerating a 28,000 lbm payload would have on an nonisotropic material. These rails are placed 9.4 feet apart and angled 8° to the plane of the aerobrake. Each is tilted 42° to lie tangent to the mission module surface. These raiis also aid in docking (Chapter 8) for they provide the basis of the frame's rigidity. Chapter 4.3 discusses the mounting of the modules in depth.

Figure 41 on page 57 also shows the aerobrake attachment accessory. Mating plates 0.75 inches thick are joined as shown using 0.5 inch diameter aluminum bolts. These bolts can be either regular or explosive. An explosive bolt allows quick removal of the aerobrake. One section of the mating assembly contains a mounting plate which is connected to the aerobrake stringers. This lower half is considered part of the aerobrake and not the frame.

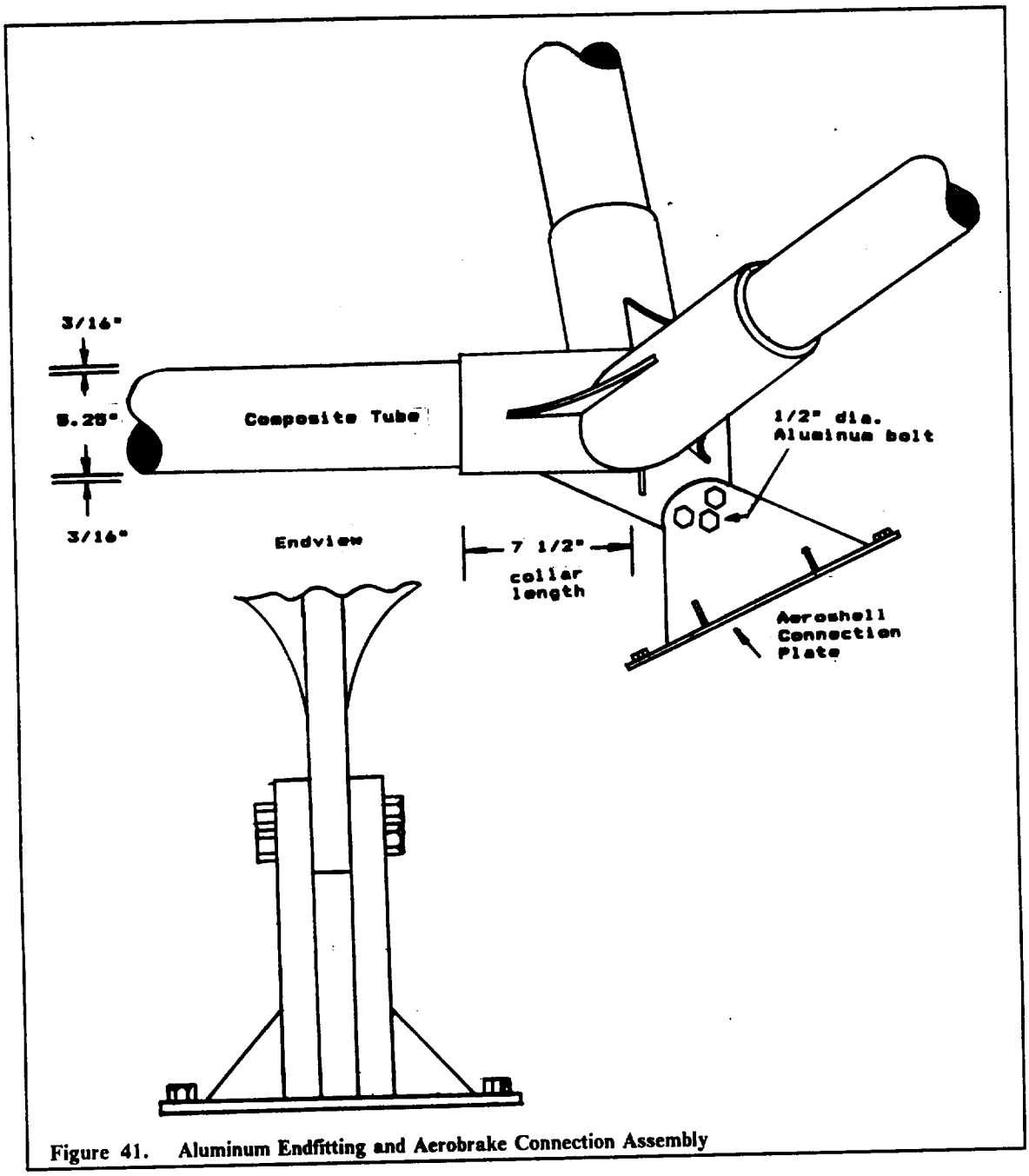

Figure 41. Aluminum Endfitting and Aerobrake Connection Assembly

4.1.3 STRUCTURAL ANALYSIS

The frame structure was designed to carry the loads that the craft receives during the entire flight regime. These include thrusting loads, aerodynamic loads, inertial loads, and thermal loads. Additional rigidity from the aerobrake and mission module components provides a factor of safety. The structure was modeled on a PC program, called PC-STRAN (Ref. Murphy), which uses a direct stiffness method to predict stresses and deflections on three-dimensional structures.

For the aerobraking maneuver, the aerodynamic analysis (Chapter 2.2) showed a maximum deceleration of less than 4 g's. This was used to determine a preliminary load requirement on each of the 181 members of the truss. An input load file for PC-STRAN was created which included the aerodynamic, thermal, and inertial loadings. The program was then implemented. The final frame

structure was determined after some member manipulation. The dimensions of the members are described in section 4.1.2.

Figure 42 and Figure 43 show the original and deformed structures due to loadings during the aerobraking phase. The program's in-depth output shows that all internal stresses remain within a safety factor of 1.5 of the ultimate material strength, and that the node deflections are kept at low levels (2 inches maximum).

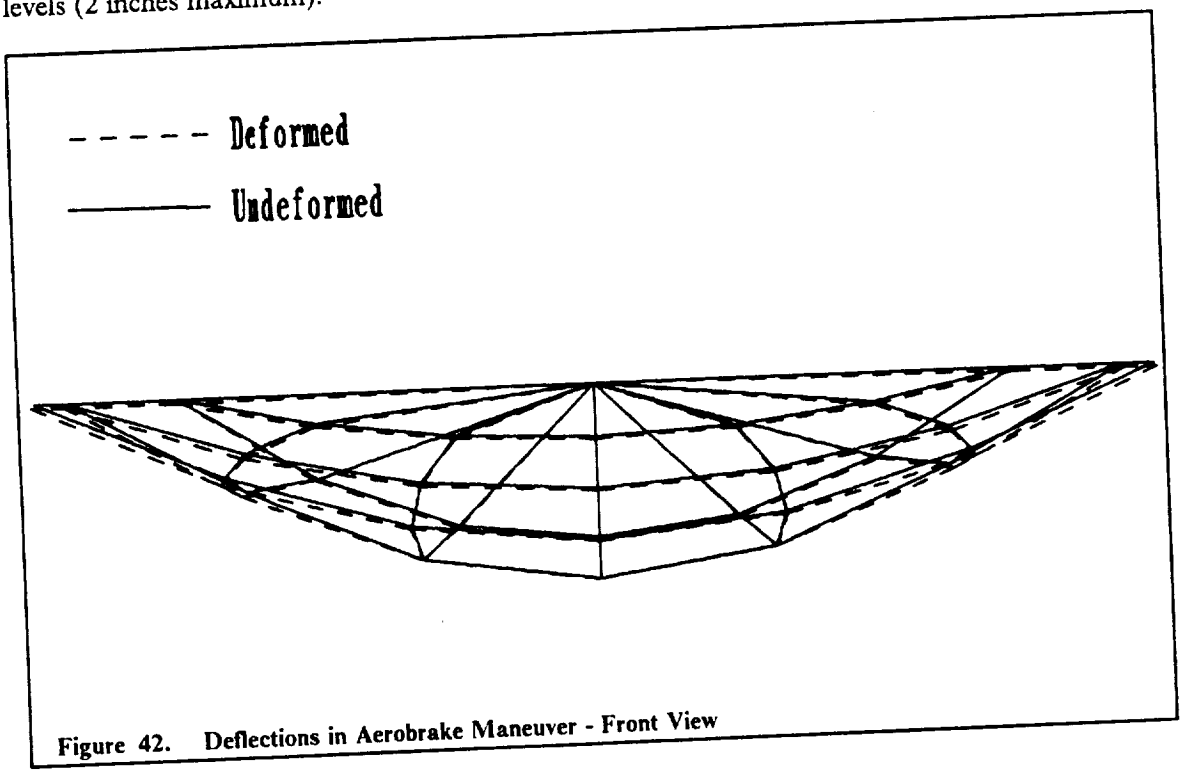

Figure 42. Deflections in Aerobrake Maneuver - Front View

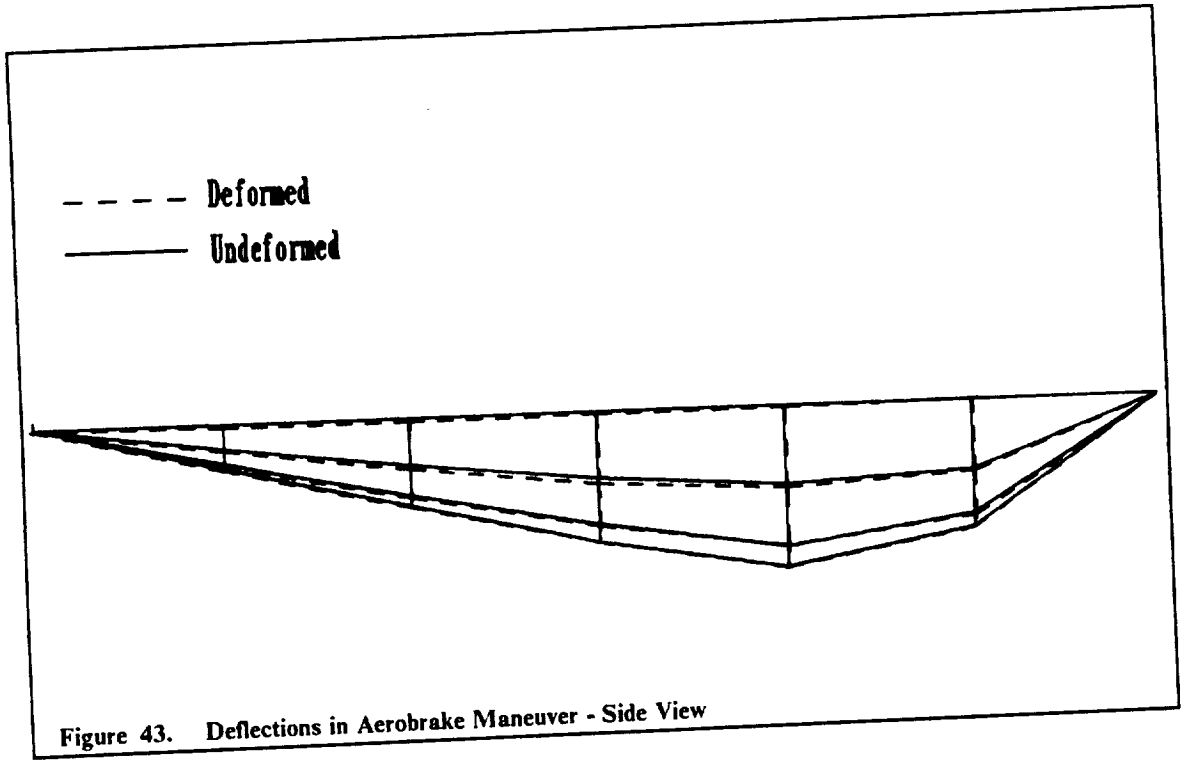

Figure 43. Deflections in Aerobrake Maneuver - Side View

This frame was then tested in the thrusting phase using two 15,000 lbf engines (Chapter 3.1). This phase is less demanding than the aerobraking phase, and PC-STRAN results supported this. Figure 43 on page 58 shows the deflections for the thrusting phase.

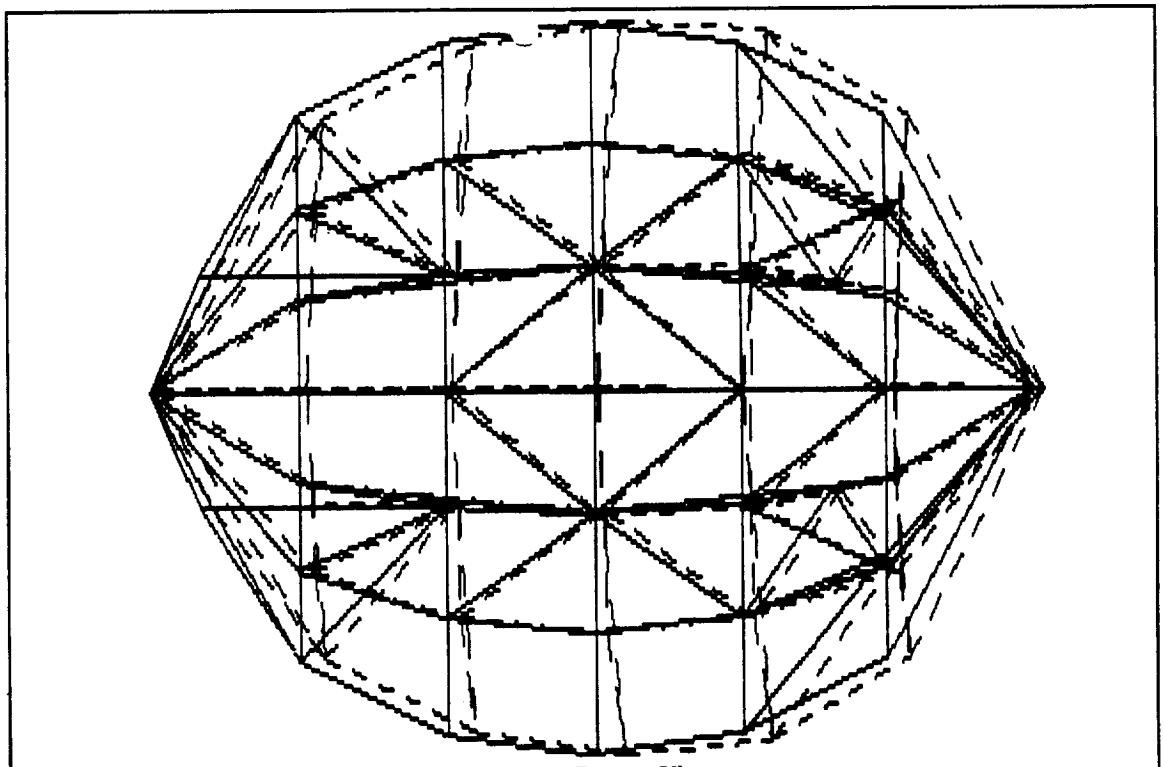

Figure 44. Deflections in Thrusting Maneuver - Bottom View

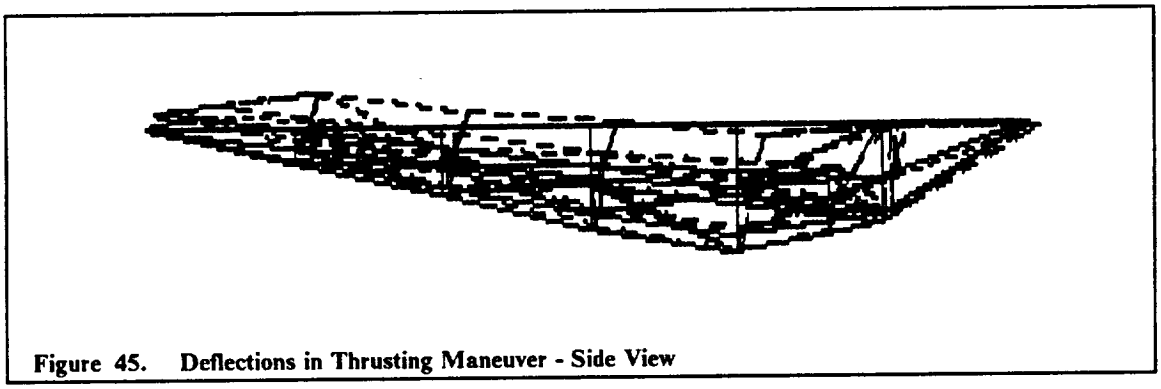

Figure 45. Deflections in Thrusting Maneuver - Side View

4.1.4 FRAME SPECIFICATIONS

All characteristics of the frame are listed in Table 12 on page 60. The frame mass (including endfittings) is 1,866 lbm. This is approximately 1/6 of the empty craft weight (Chapter 2.1.3).

Table 12. Frame Specifications

TUBE CHARACTERISTICS			
HT Graphite/Epoxy			
Density		0.054	lbm/in^3
Total Length		1,068.570	ft
Total Mass		1,393.870	lbm
ENDFITTINGS			
Total Number		65	
Average Mass Each		3.000	lbm
Total Mass		195.000	lbm
Mass of Spine		277.000	lbm
Mass of Rails (2)		1,132.000	lbm
Total Mass		2,997.870	lbm
Center of Gravity Position:			
	X	18.15	ft
	Y	0.00	ft
	Z	-1.67	ft
Moments of Inertia:			
	Ixx	64,700	$lbm\text{-}ft^2$
	Iyy	124,600	$lbm\text{-}ft^2$
	Izz	184,080	$lbm\text{-}ft^2$
	Ixy	0	$lbm\text{-}ft^2$
	Iyz	0	$lbm\text{-}ft^2$
	Izx	4,00	$lbm\text{-}ft^2$

4.1.5 EARTH-TO-ORBIT DELIVERY

For delivery into orbit the aerobrake components are packaged so as to fit into a 60 foot long by 15 foot diameter cargo area. The frame with the aerobrake attached can be split into three sections and packaged as in Figure 46 through Figure 50 on page 62.

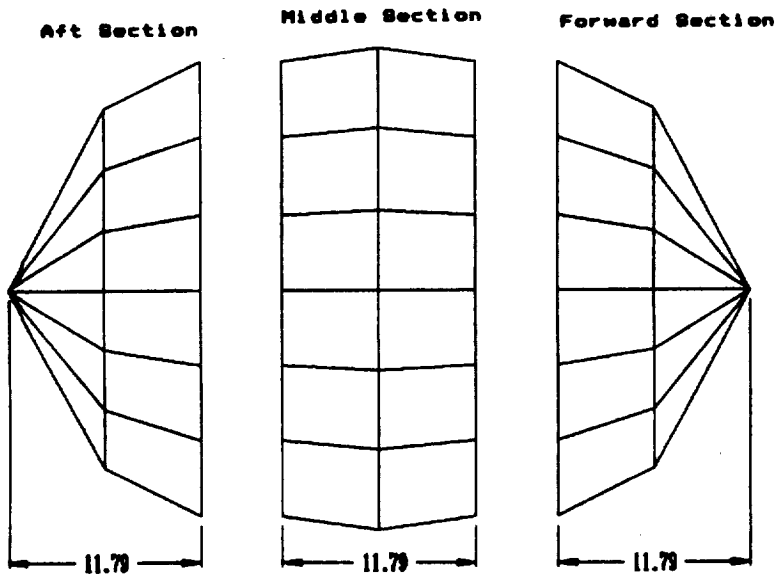

Figure 46. Frame Partitioning For Delivery

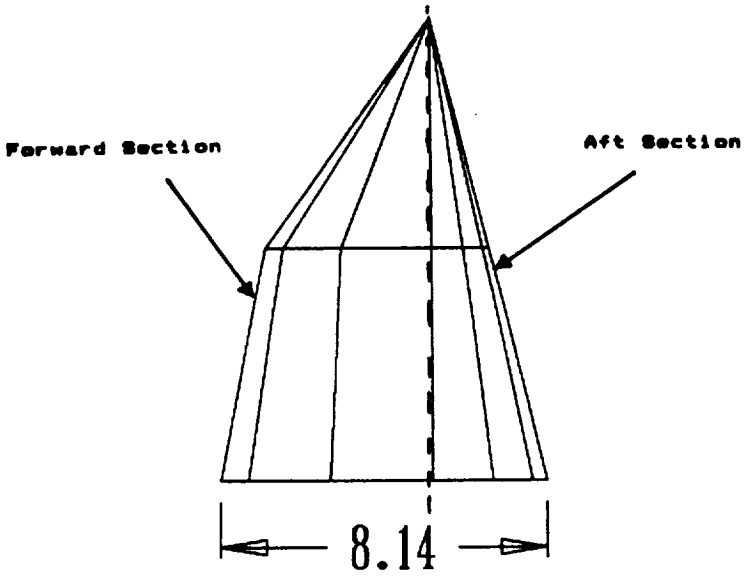

Figure 47. Frame Fore and Aft Section Joining

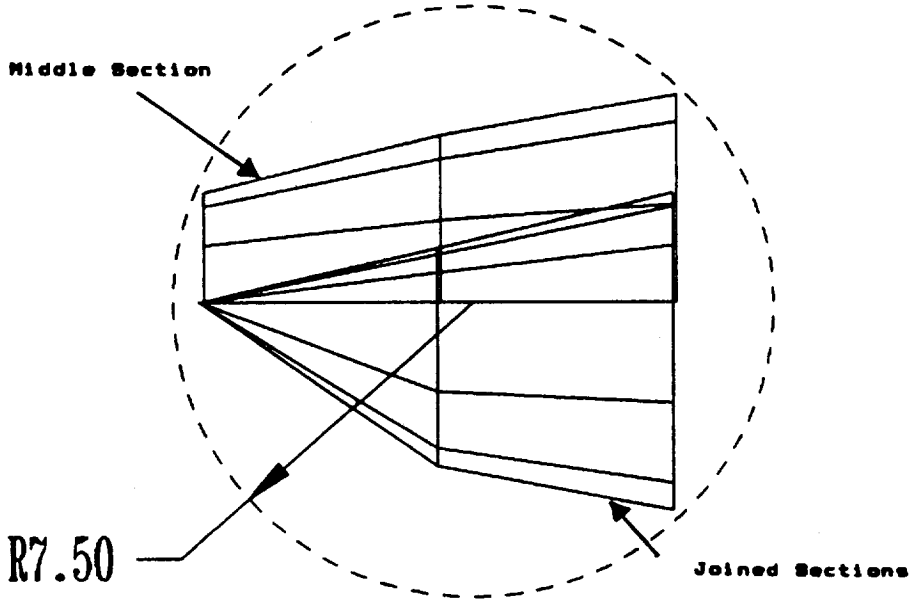

Figure 48. Frame Final Payload Configuration - Side View

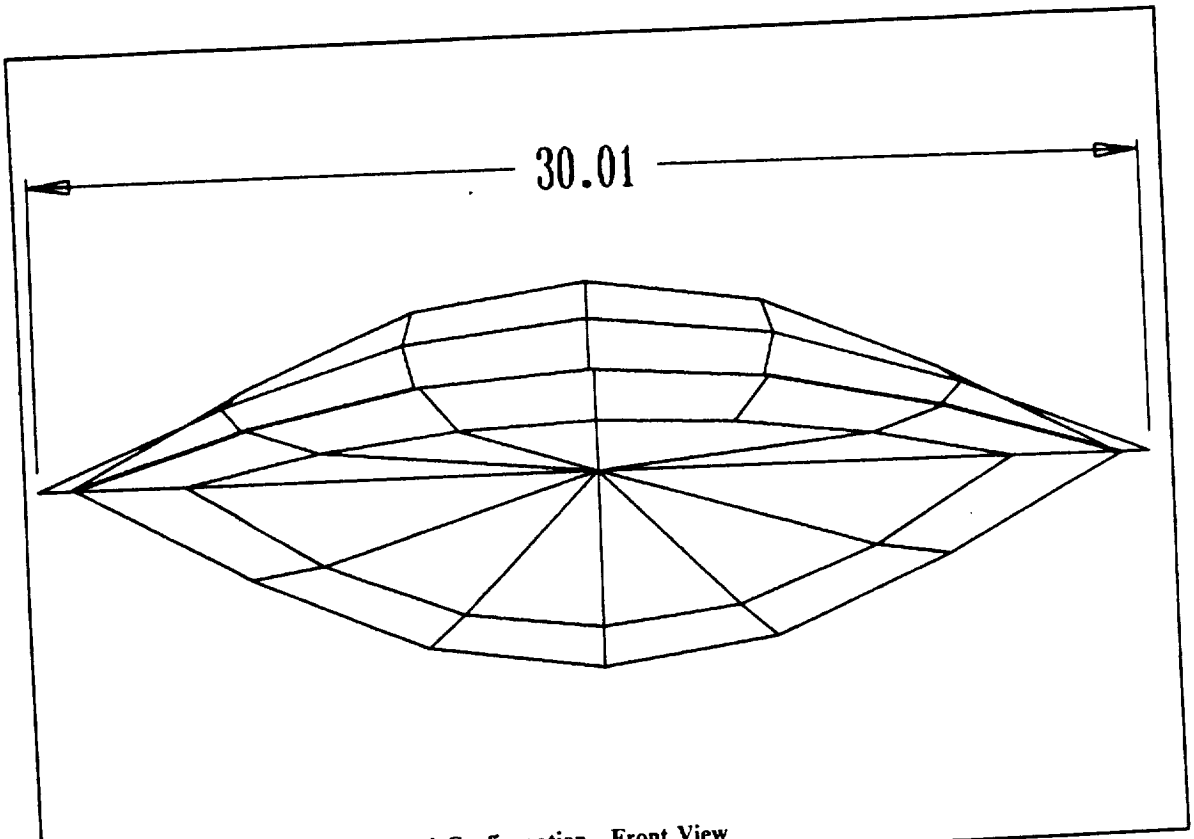

Figure 49. Frame Final Payload Configuration - Front View

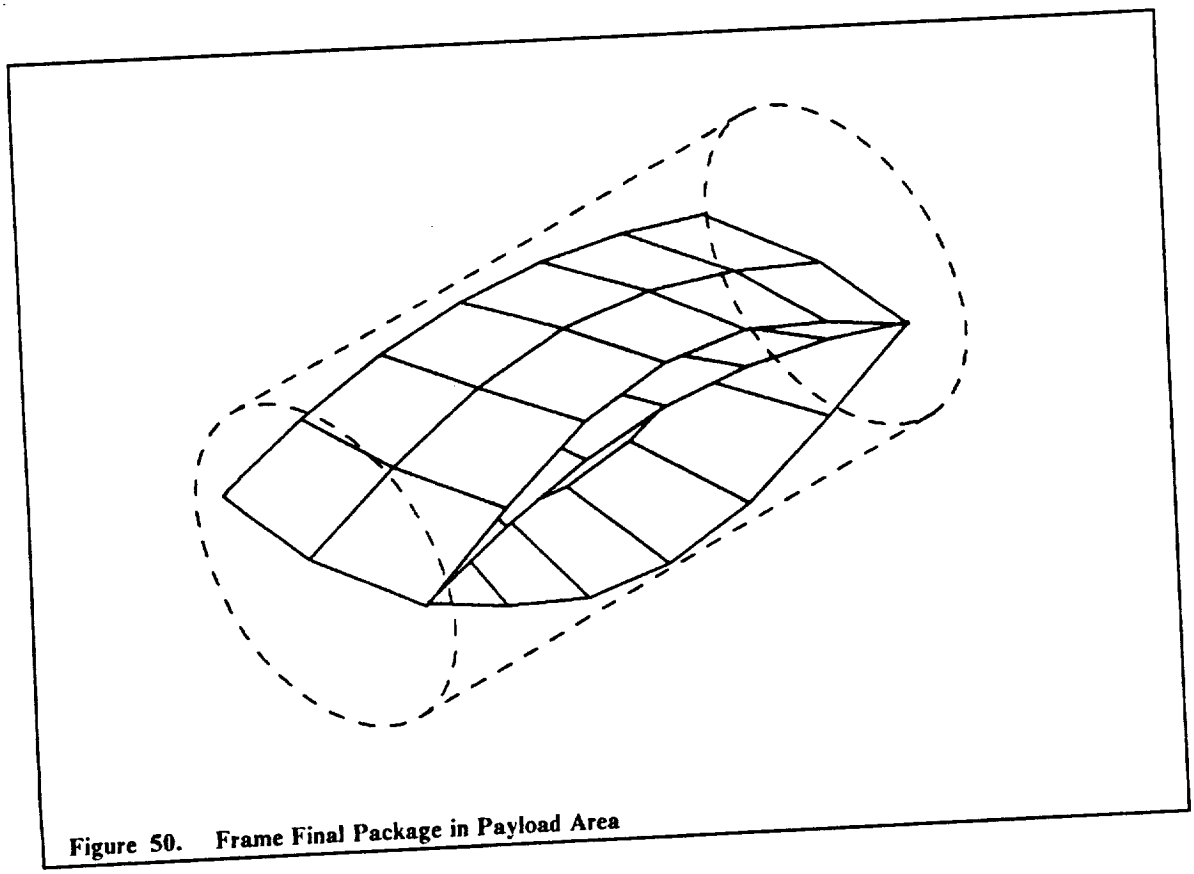

Figure 50. Frame Final Package in Payload Area

Packaging consists of three steps. First, the aerobrake and frame are split into three sections as shown in Figure 46 on page 60. Second, the forward and the aft thirds are joined together by their similar nodes as seen in Figure 47 on page 61. Finally, the middle third is placed over the aft third as shown in Figure 48 on page 61 and Figure 49. This final packaging scheme is pictured in Figure 50 and fits into a 15 foot diameter by 30 foot long cargo bay.

4.2 AEROBRAKE

4.2.1 DIMENSIONS

The raked-cone aerobrake derives its name from the geometry upon which it is based. The aerobrake surface is formed by clipping upper and lower edges off of a right circular cone, and then covering the lower edge with a circular cap.

Figure 51 on page 64 shows side and top views of the aerobrake. The 37 foot length shown is the inner length. The actual length of the aerobrake is 37.06 feet after addition of the thermal protection layers. The aerobrake inner width, shown in the top view, is 30.2 feet. Overall width including the thermal protection layers is 30.26 feet.

4.2.2 GEOMETRICAL PROPERTIES

A computer program was written to create a set of data points representing the raked-cone aerobrake surface. An additional program was written to calculate the geometrical properties of the aerobrake. After generating the surface points (using the algorithm from the first program), the program divided the surface up into a finite number of triangular elements. Next, the program made use of formulas which give the area, first moments of inertia, and area moments of inertia for a triangle having a general orientation in 3-D space. Summing these values over all triangles then gave approximate values for the geometrical properties of the entire aerobrake.

Table 13 shows the results of the second program. The data are based on a 110 x 110 grid of points and an aerobrake length of 37 feet.

Table 13. Aerobrake Geometrical Properties

Length =	37.0	ft	
Width =	30.2	ft	
Area =	1,009.4	ft^2	
Center of Gravity Position:			
X =	18.94	ft	(measured from tip)
Y =	0.00	ft	
Z =	-1.81	ft	
Ixx =	64,831	ft^4	
Iyy =	95,072	ft^4	
Izz =	154,843	ft^4	(about centroid)
Ixy =	0	ft^4	
Iyz =	0	ft^4	
Izx =	-4,678	ft^4	

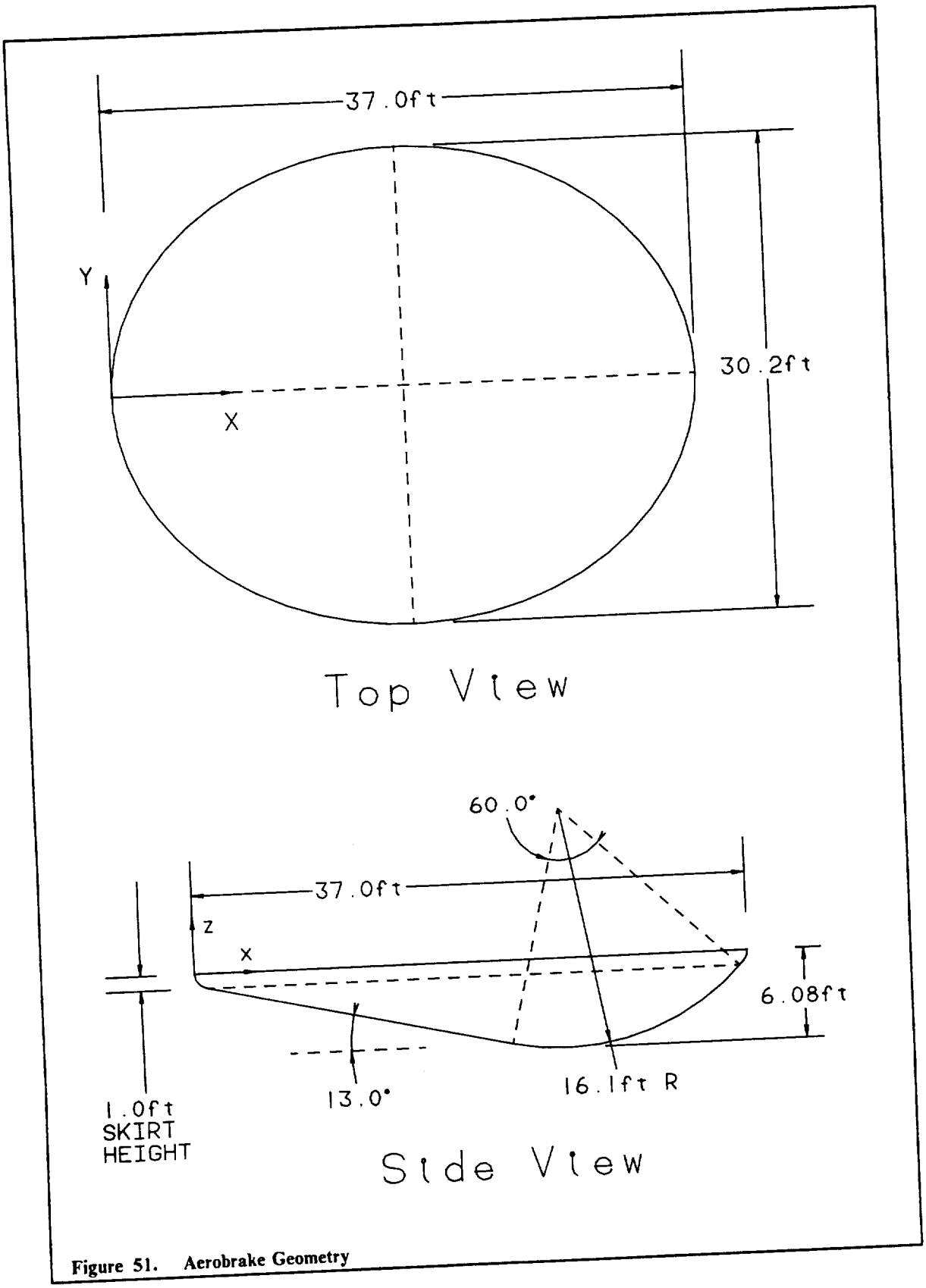

Figure 51. Aerobrake Geometry

4.2.3 STRINGERS

A series of stringers attached to the aluminum skin of the aerobrake add support and allow for connections between the aerobrake and the main structure. The stringers are made of aluminum-lithium alloy and are riveted to the aluminum skin. Six stringers run down the length of the aerobrake and five stringers run along the width of the aerobrake as shown in Figure 52 on page 65. The cross section of the stringers is of the "Z" type as shown in section A-A with the noted dimensions. The stringers attach to the structure at 37 node points. These occur where the lines cross on the top view in Figure 52.

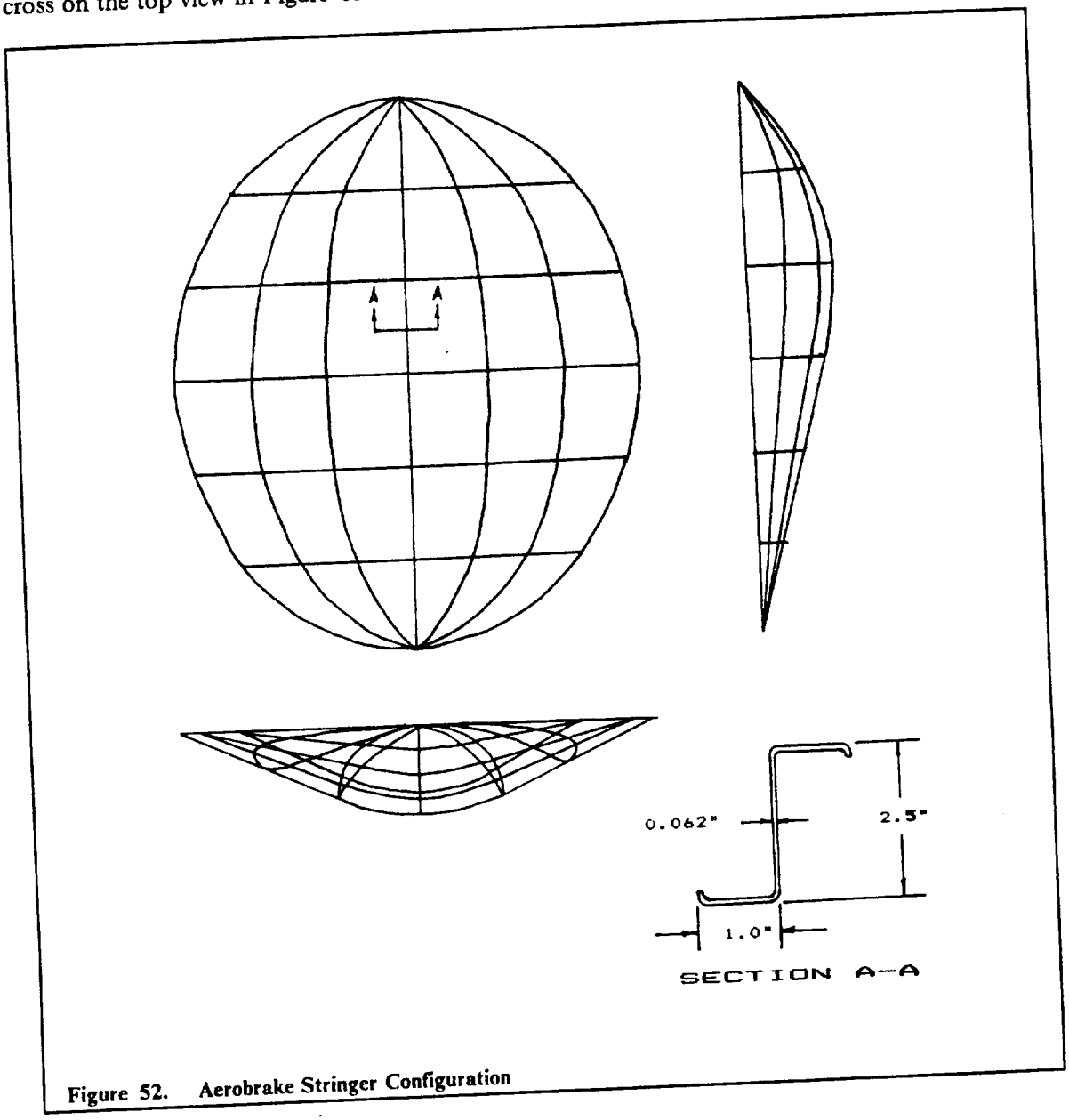

Figure 52. Aerobrake Stringer Configuration

4.2.4 THERMAL PROTECTION SYSTEM

One of the most important considerations in the thermal protection system (TPS) of the ASTV is the requirement for highly efficient lightweight insulation. A significant advance in thermal insu-

lation was the development of multilayer insulation technology. The ASTV thermal protection system is based on this technology.

The TPS chosen consists of a top surface of Aluminoborosilicate cloth followed by insulation, and then layers of stainless steel foil radiation shields, each 0.002 in thick, separated by ABS scrim cloth. The scrim cloth is used to maintain an efficient separation between the foils without adding a significant conductive heat path to the system. The stainless steel foil is used as the radiation shield material because of its relatively low emittance and high reflectance at high temperatures.

Heat transfer in multilayer insulations (MLI) in general occurs through conduction, convection, and radiation. For space applications, the convection process may be neglected since the gas is at such low pressures. The heat transport processes which must therefore be considered include conduction through the solid phase of the insulation and radiation.

A one dimensional heat transfer analysis was performed to determine the TPS thickness and mass. The total thickness was found to be 0.337 in and the mass of the TPS was calculated to be 593 lbm. This amount of protection resulted in a back face temperature of 350°F which is tolerable for the aluminum structural support of the aerobrake.

The skirt of the aerobrake extends 1 ft above the edge of the aerobrake. Its purpose is to decrease wake impingement. It uses the same TPS scheme as the aerobrake, and has the same back face material of aluminum but has no stringers.

4.3 CARGO MODULE

A cargo module was developed to accommodate mission payloads on the ASTV. This cargo module serves three purposes. First, it will provide the base mounting platform for the payload. Payloads will be joined to the cargo module, which in turn will be joined to the ASTV. Second, the cargo module will protect sensitive payloads from impact and radiation hazards. Payloads will not require "inbuilt" protection and will therefore be less massive. Finally, the cargo module will allow selective positioning of the payload on the ASTV. This essential feature aids in positioning the overall center of gravity of the ASTV.

The cargo module design was based around three additional criteria. It had to have low weight, it had to be compatible with a wide range of payload sizes, and it had to be easily installable and removable.

4.3.1 DIMENSIONS

Figure 53 on page 67 and Figure 54 on page 67 show side and transverse views respectively of the cargo module. The module is cylindrical in shape, having a diameter of 14 feet and a length of 8 feet. Its total internal volume is 1,230 ft^3. A mass breakdown (included at the end of this chapter) yields an estimated mass of 556 lbm per cargo module.

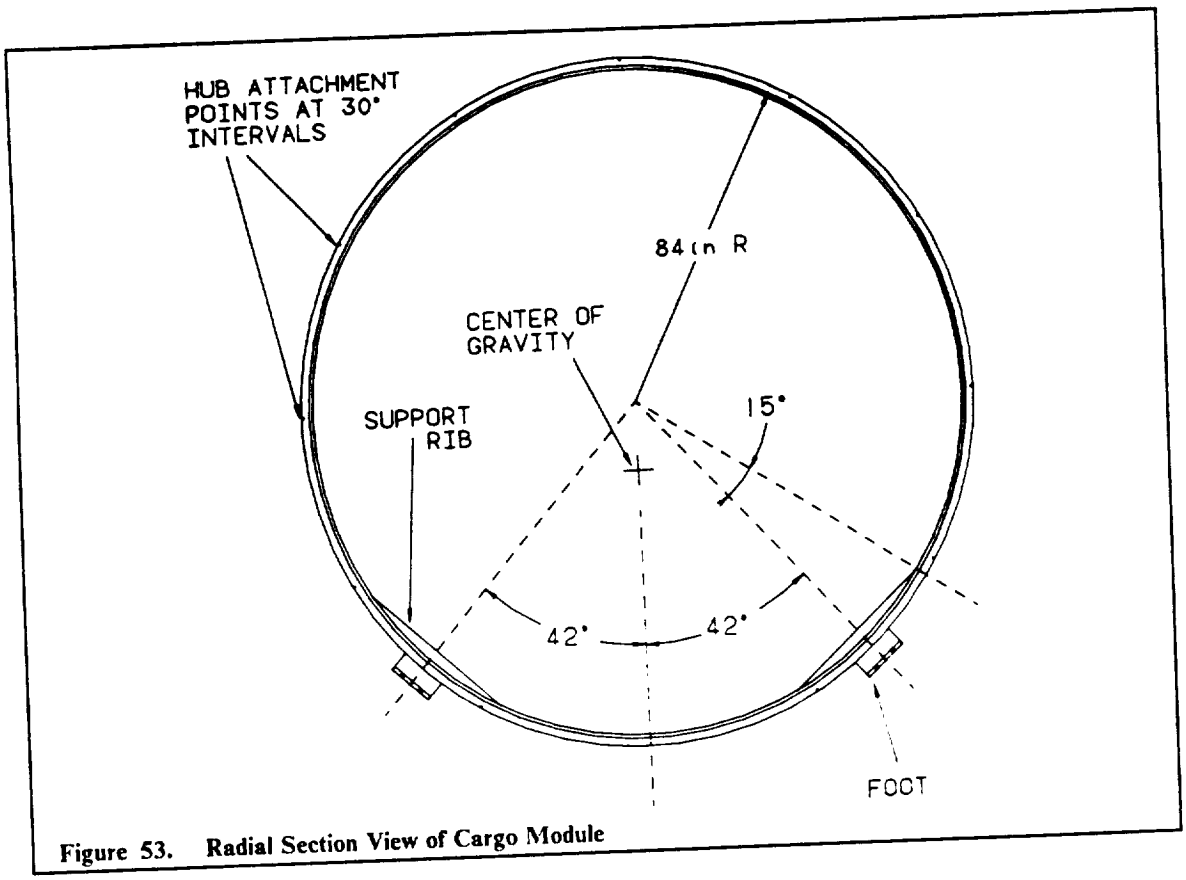

Figure 53. Radial Section View of Cargo Module

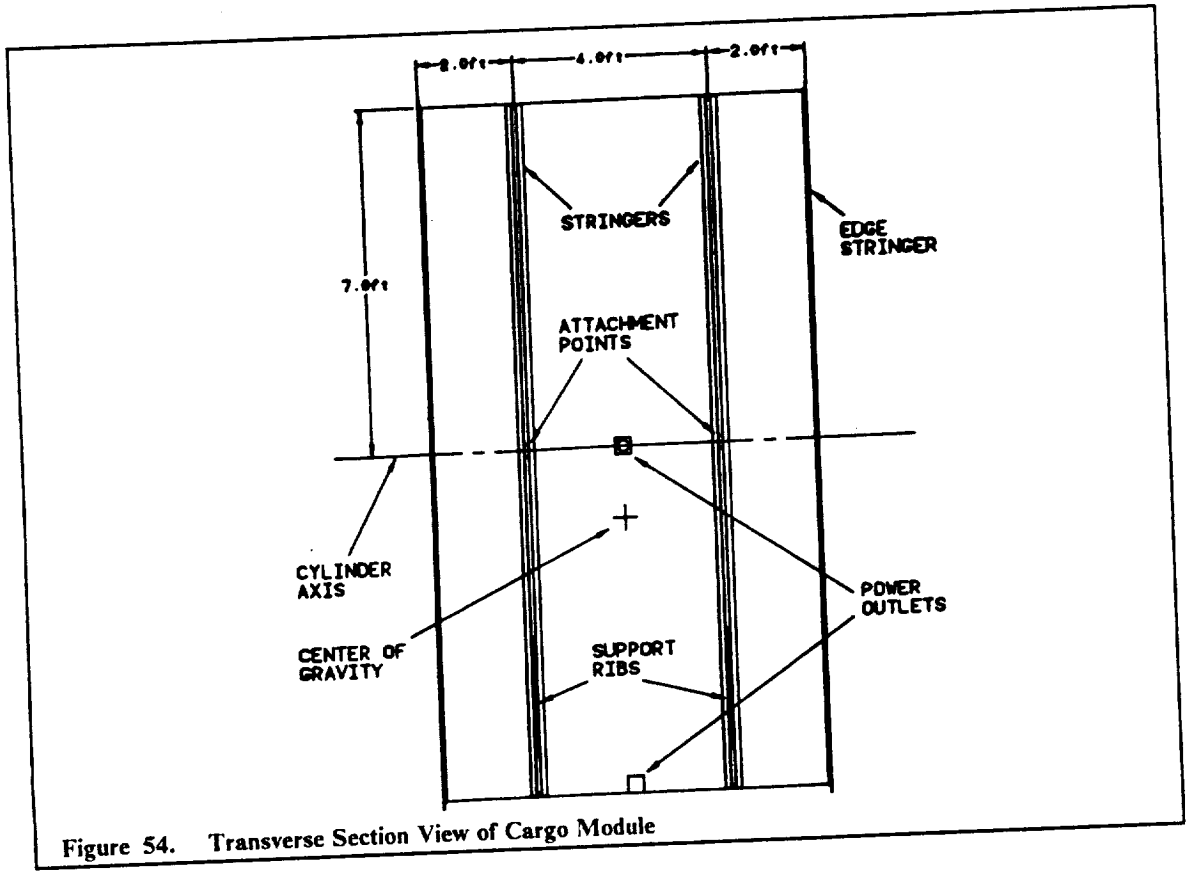

Figure 54. Transverse Section View of Cargo Module

The centroidal mass moments of inertia for the cargo module were calculated to be

$$Mxx = 15{,}808 \text{ lbm-ft}^2$$
$$Myy = 9{,}810 \text{ lbm-ft}^2$$
$$Mzz = 10{,}020 \text{ lbm-ft}^2$$

with the centroid at

$$X = -0.01 \text{ ft}, \quad Y = 0.00 \text{ ft}, \quad Z = -1.45 \text{ ft}$$

4.3.2 CARGO MODULE DESIGN

STRUCTURAL COMPONENTS

Structural components of the cargo module include the skin, internal stringers, support ribs, hubs, and feet. All structural components are fabricated from aluminum-lithium alloy #2090.

The primary structural component of the cargo module is the cylinder skin. Its thickness was determined by considering the maximum shearing stresses it would have to withstand. These occur during the aerobraking phase of the mission with 6,000 lbm payload. The maximum deceleration during this phase is 3.72 g's. From this a minimum thickness of 0.01 inches was calculated. To include a safety factor of 2 the final skin thickness was made 0.02 inches. The skin is constructed by wrapping the sheet of metal around internal stringers and welding the seam.

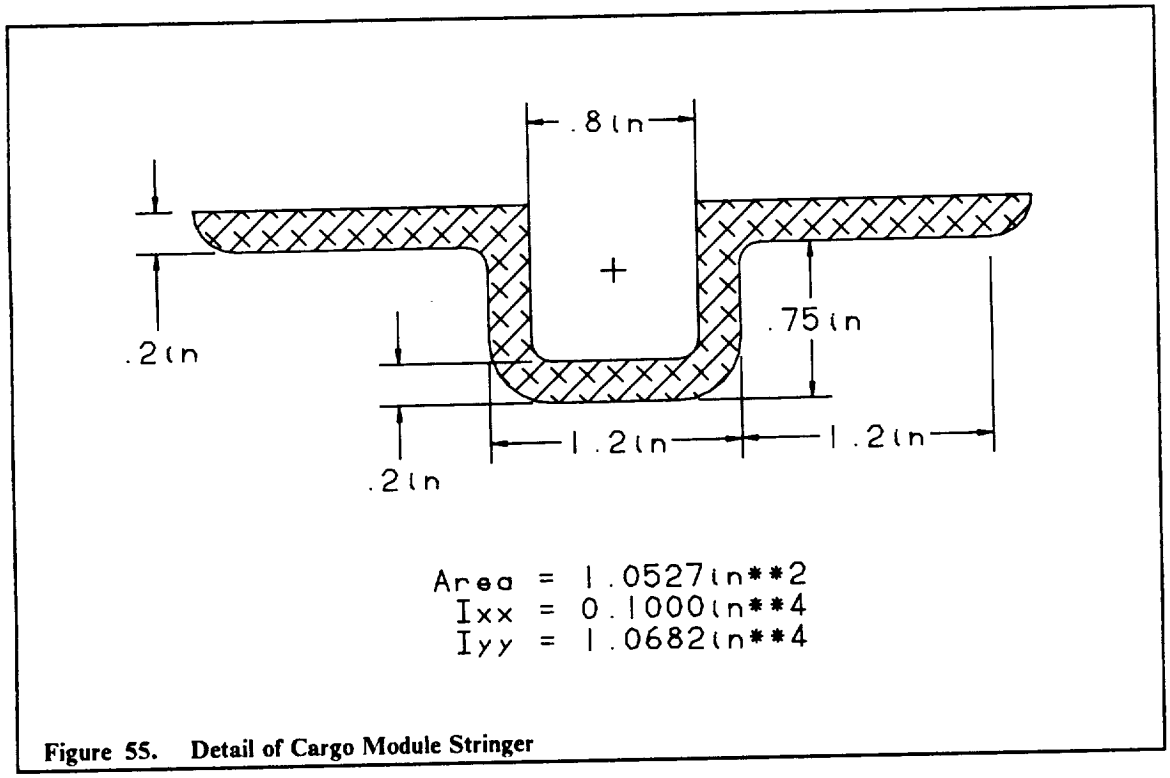

Figure 55. Detail of Cargo Module Stringer

Stringers are incorporated into the cargo module design to provide rigidity. Figure 53 on page 67 shows the location of the two stringers which lie along the inside perimeter of the cylinder. Figure 55 gives a detailed cross-section of this stringer and lists its inertial properties. Two additional stringers at each edge connect the skin to the hub. These are shown in Figure 56 on page 69. A support rib is placed behind each foot on the other side of the skin. The rib, shown in detail

in Figure 57 on page 69 and Figure 58 on page 70, distributes the loads from the foot over a larger area and eliminates high stress points.

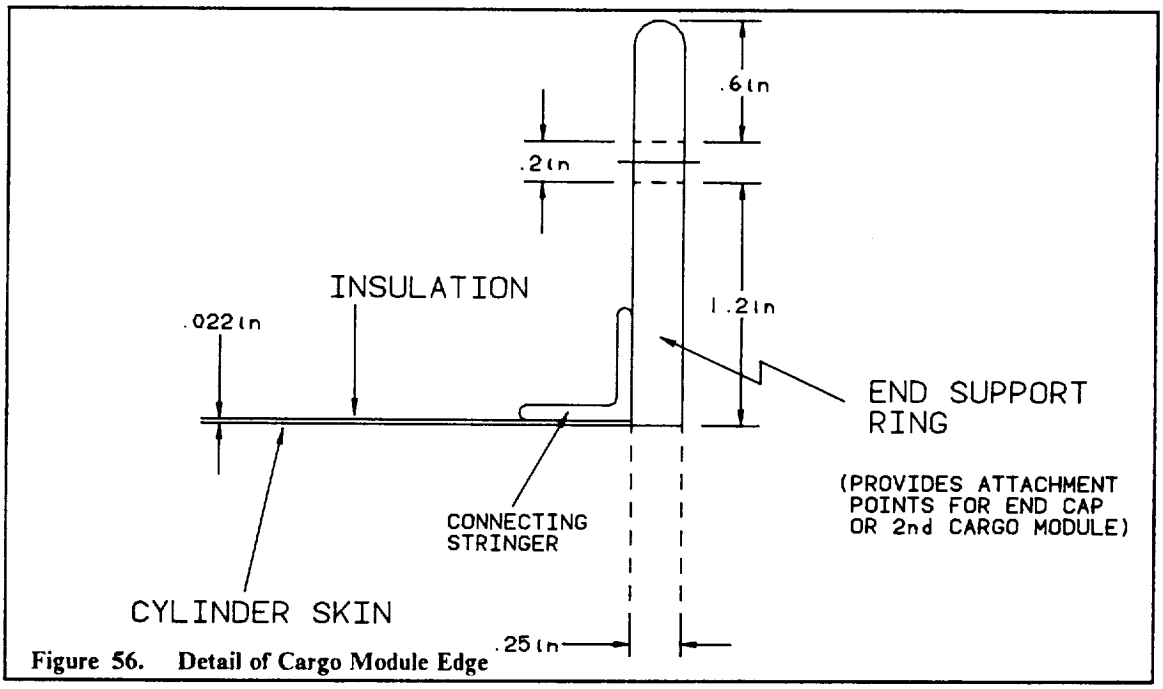

Figure 56. Detail of Cargo Module Edge

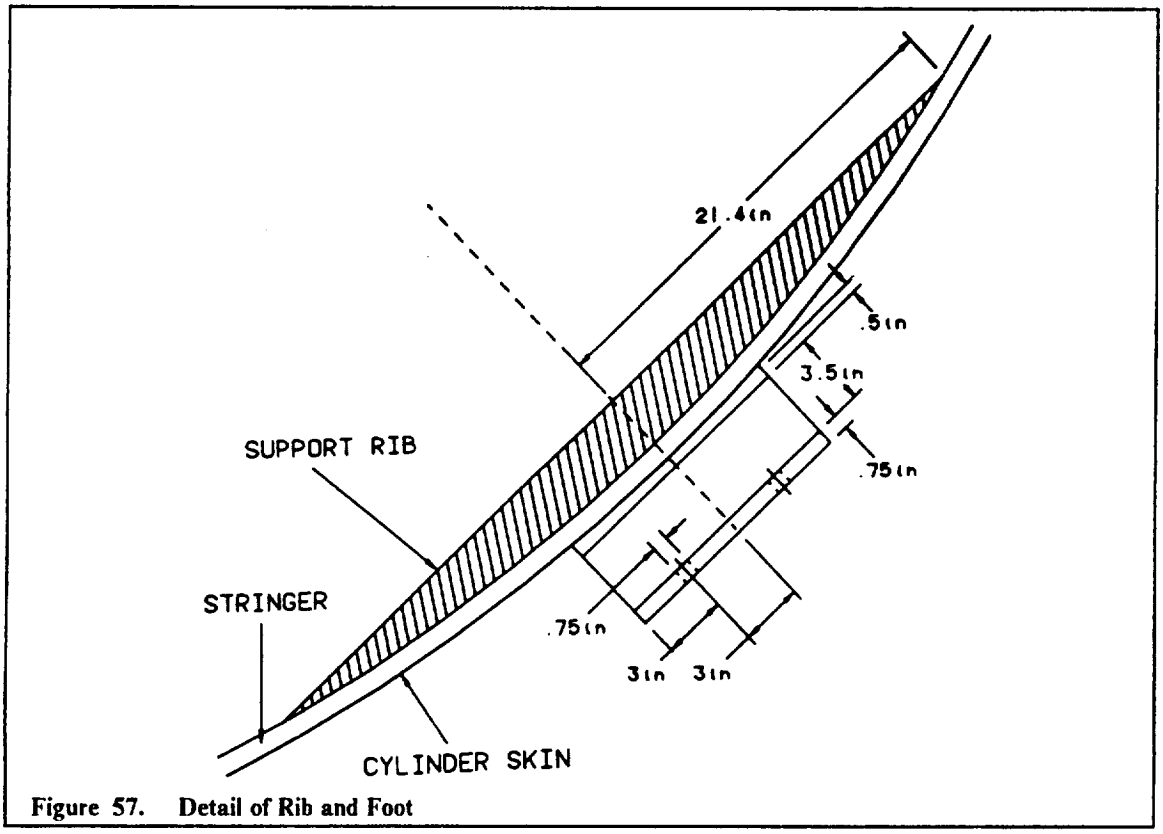

Figure 57. Detail of Rib and Foot

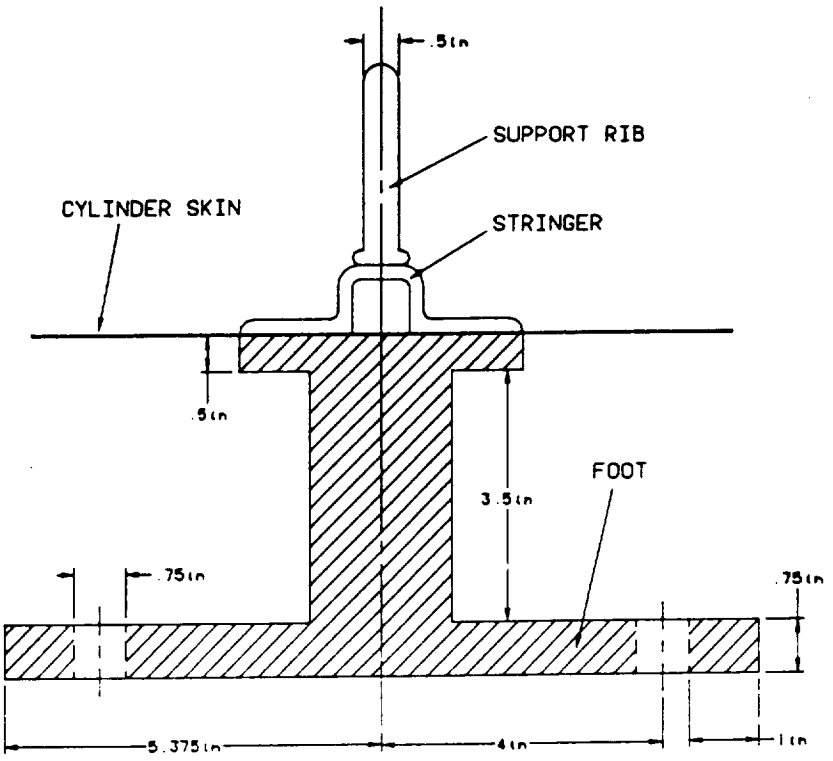

Figure 58. Cross Section of Rib and Foot

Circular hubs provide stiffness at each end of the cargo module. They also serve as the joining platforms when modules are stacked (to be discussed). Each hub has 12 evenly spaced attachment holes. Figure 53 on page 67 and Figure 56 on page 69 show the hub and attachment points. Covers can be attached to the hub. These covers are 0.02 inches thick, the same as the skin.

Extending from each module are two pairs of feet which connect to the rails. Figure 54 on page 67, Figure 57 on page 69, and Figure 58 show the feet in detail. The feet are sized to withstand the shearing stresses associated with propulsive maneuvers. Projecting the feet at an angle with respect to the cargo module simplifies installation and removal of the mission module. As the module is lowered it will automatically slide into the correct position. Figure 59 on page 71 shows this automatic positioning feature.

STACKING FEATURE

To reduce the overall structural mass of the ASTV, a stacking feature was incorporated into the cargo module design. This feature allows a cargo module to be joined (mated) with other cargo modules. The size of the containment structure can be optimized for the current payload, thus eliminating excess structural weight. In addition, cargo modules may be joined to the crew module since it also incorporates this feature. Not only does this allow all modules to be installed and removed as a single unit (the mission module), it also increases the overall structural rigidity of the ASTV. Another important advantage of this feature is that the payload mass distribution can be set so as to aid in positioning of the overall ASTV center of gravity.

Modules are joined together along the circular hub located at each end. Up to three modules can be mated together to form a complete mission module of 24 foot length. The joining process is simple and therefore suitable for the space environment. The process entails two steps. First, the two modules to be joined are positioned next to each other. This may be done by either an astronaut (the modules are relatively light) or by a robot arm (modules are provided with grasping hooks). Finally, fasteners are inserted through the adjoining hubs at the attachment points and tightened.

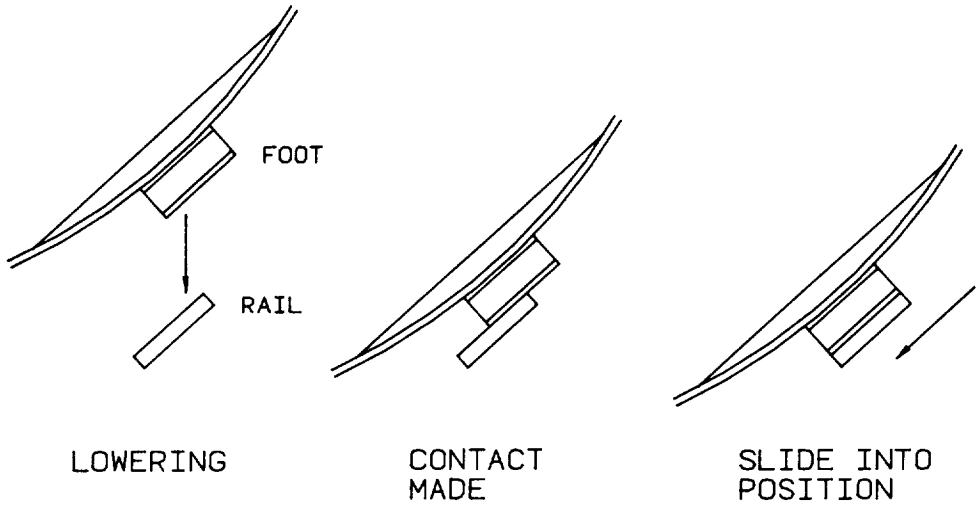

Figure 59. Automatic Positioning During Cargo Module Installation

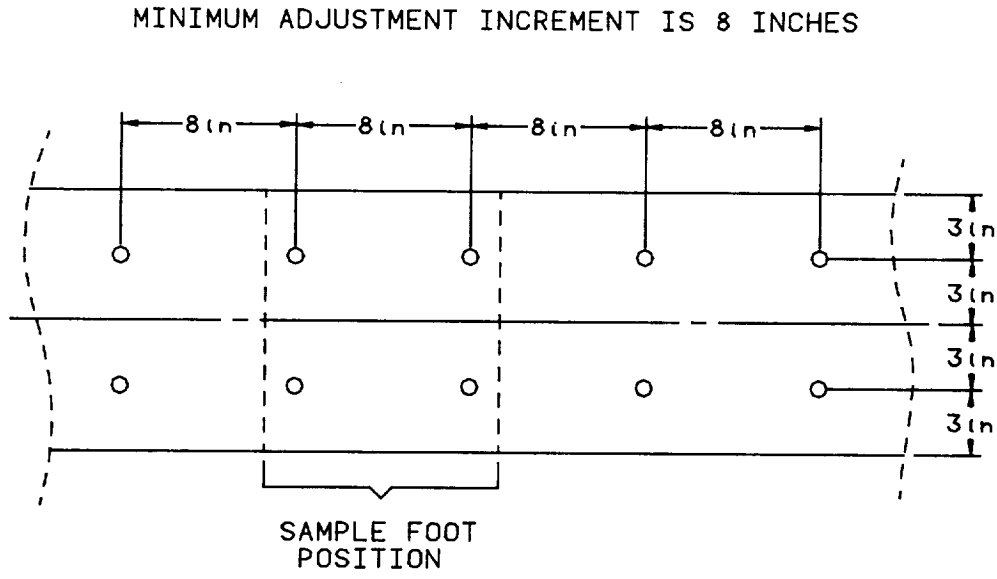

Figure 60. Detail of Mounting Rail

IMPACT/RADIATION PROTECTION

Each cargo module is covered by 10 alternating layers of Nextel cloth and steel foil to give both orbital debris impact protection and radiation protection. Each layer of Nextel cloth is 0.002 inches thick, while each layer of foil is 0.0002 inches thick. The total insulation thickness is therefore 0.022 inches, and the insulation mass was calculated to be 48.2 lbm.

RAIL SYSTEM

The purpose of the rail system is to provide evenly spaced mounting points for the mission module. Figure 60 on page 71 shows a top view of one rail. Holes are placed at 8 inch intervals. A mission module can therefore be positioned to within 8 inches. The actual placement of the mission module will be dictated by both the number of cargo and/or crew modules and the required overall CG position for the ASTV. Since the mission module is only part of the entire vehicle mass, the overall CG position can be adjusted to much smaller increments than 8 inches.

POWER SUPPORT

Besides being just a mounting platform, each cargo module will be capable of routing 200 W of electrical support power to its payload. This power will come from the ASTV's main power system. Figure 61 shows the location of the power supply outlets.

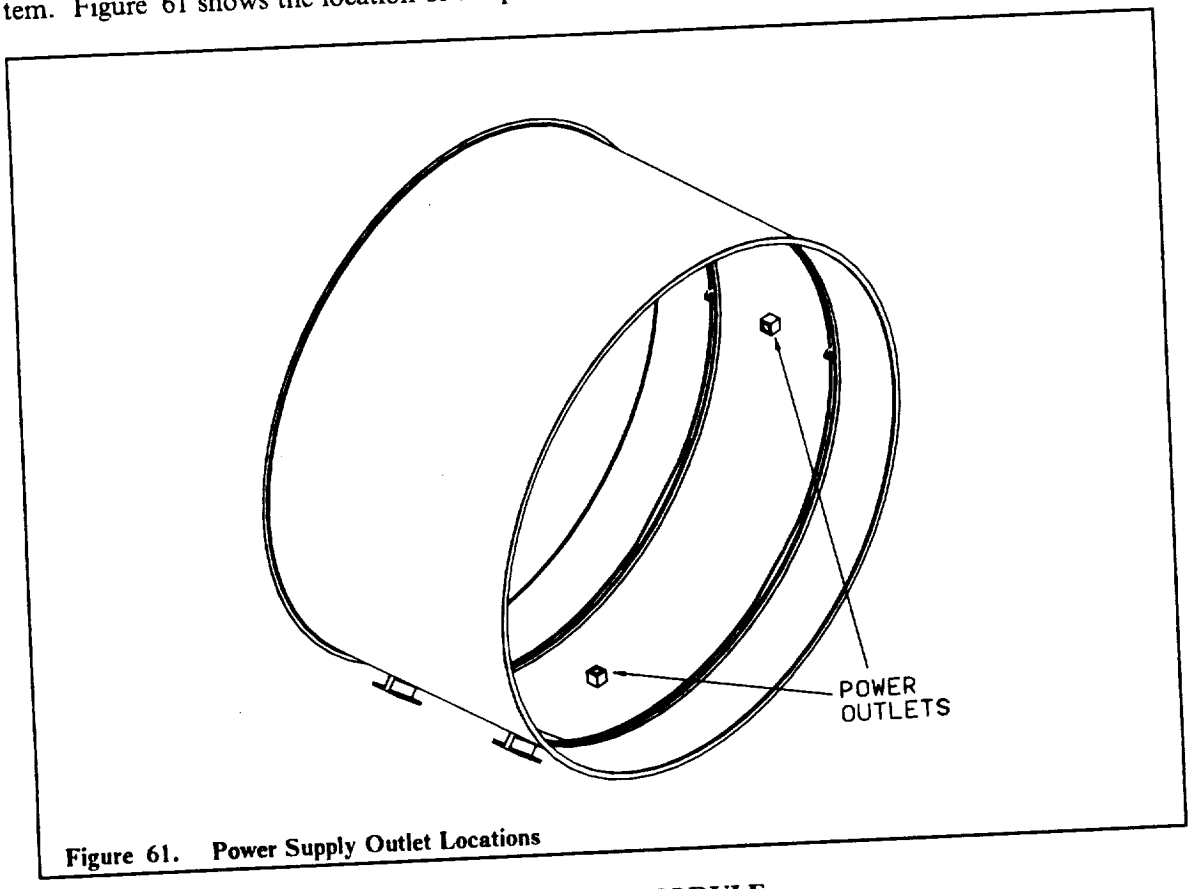

Figure 61. Power Supply Outlet Locations

MOUNTING OF PAYLOAD WITHIN CARGO MODULE

The interior of each cargo module has four payload attachment points located on each of the two internal stringers. Each payload will be required to have its own corresponding attachment points, and must also be fastened to at least two of the attachment points on each stringer. This insures a solid connection between the payload and the cargo module. Figure 62 on page 73 shows the location of the attachment points.

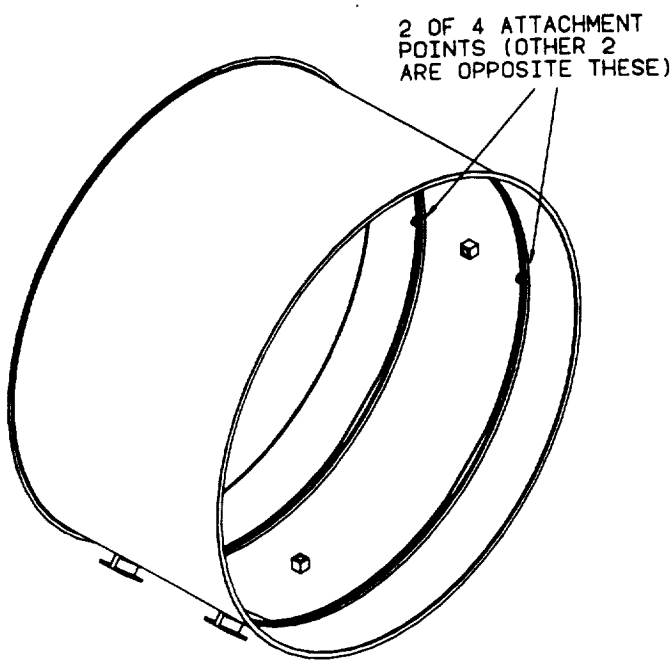

Figure 62. Payload Attachment Point Locations

ASSEMBLY AND DELIVERY TO SPACE

The cargo module's simple design allows it to be assembled in space. Individual components such as the skin, hubs, and stringers are fabricated on the ground and transported into space by the Space Shuttle. These components are then welded together in space to form the completed cargo module. Since cargo modules are reusable, only a small number (on the order of three or four) must be constructed.

INSTALLATION/REMOVAL

The cargo module design simplifies the task of installation and removal of the mission module. After being assembled, the mission module is positioned above the appropriate rail mounting point and lowered into place. Small errors in positioning are automatically corrected as the module is completely lowered. Upon contact the feet are bolted to the rails. The removal procedure is even simpler. The bolts are undone to release the feet from the rails, and the mission module is raised away from the vehicle. Robot arms may grasp the cargo module at any of eight externally distributed grasping hooks.

MASS BREAKDOWN

Table 14 on page 74 shows a mass breakdown of all cargo module components. The estimated mass for one cargo module is 556 lbm.

Table 14. Mass Estimate for Cargo Module

ITEM	MASS (lbm)
Protection Layers	48.2
End support rings (2)	48.5
Internal stringers (2)	102.2
End stringers (2)	64.0
End Cover	42.8
Support ribs (4)	14.8
Feet (4)	74.9
Cylinder skin	149.0
Wiring/Power Outlets (2)	1.0
Grasping Hooks	2.0
TOTAL MASS	556.4

4.4 CREW MODULE

The crew module was developed so that three people may be transported essentially as passengers aboard the ASTV. Should a crew be necessary, one or more crew modules could be mounted to the vehicle in place of a corresponding number of cargo modules. Each crew module can support three adults for 48 hours with the capability for one full repressurization. The crew is transported in an ideal earth atmosphere for a round trip time of 14 hours 39 minutes.

The overall crew module consists of 3 seats, a set of guidance and communication controls, overhead storage racks, space suit storage, and a lavatory. The controls allow the vehicle to be manually controlled in case of a guidance system failure. Figure 63 and Figure 64 on page 75 show the crew module layout.

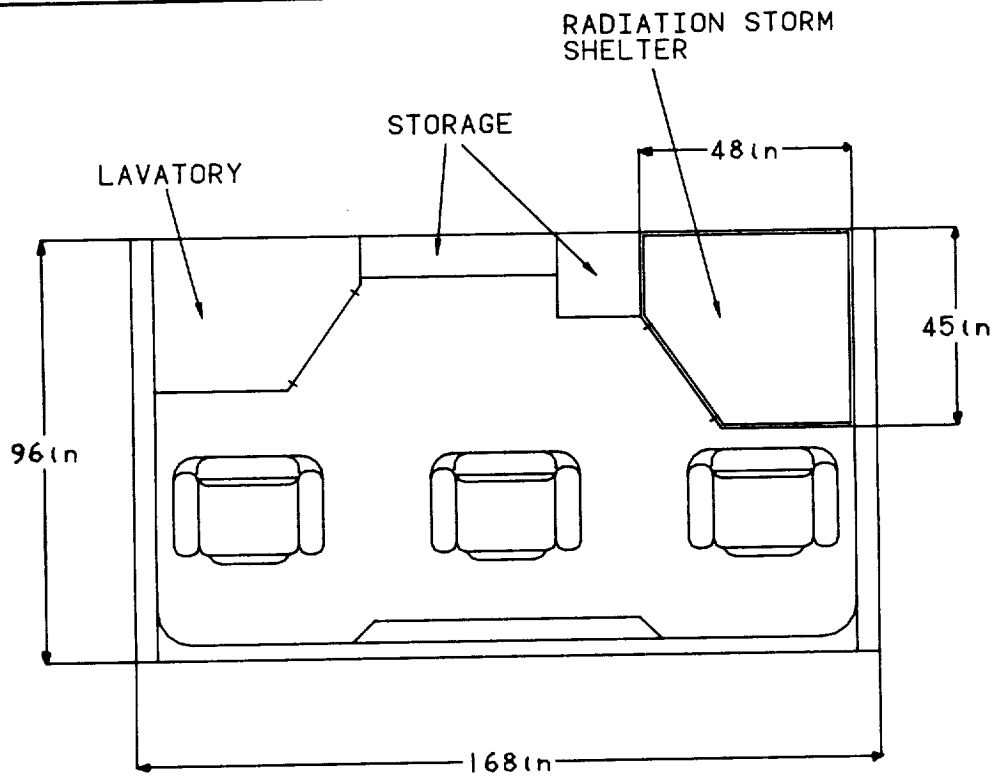

Figure 63. Crew Module Layout - Top View

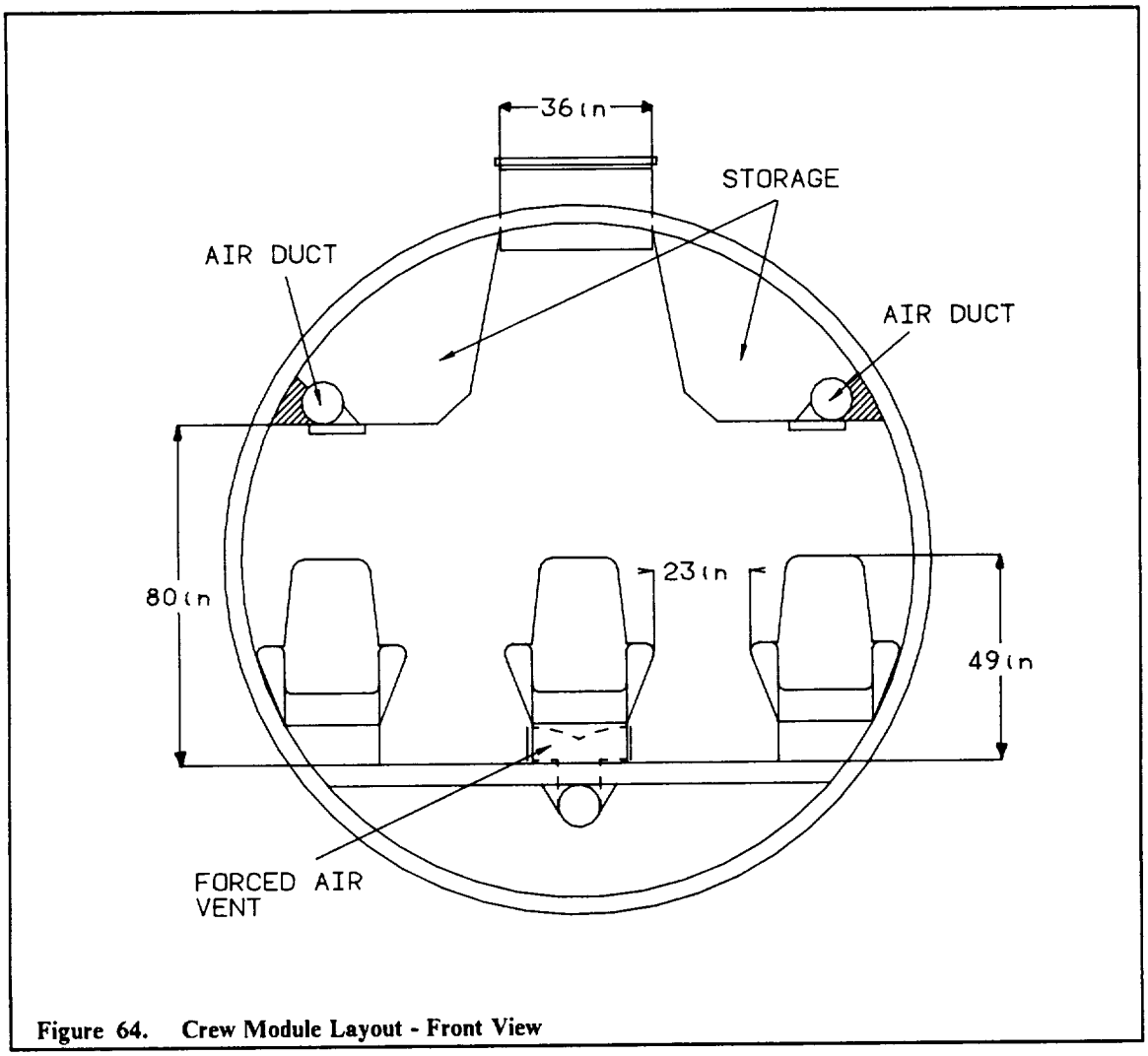

Figure 64. Crew Module Layout - Front View

4.4.1 DIMENSIONS/CONSTRUCTION

The crew module dimensions are the same as the cargo module dimensions to accommodate the cargo module stacking feature. The crew module structure is made of aluminum alloy 2014-T6 ($\rho = 0.101$ lb/ft^3) and developed using a stress analysis which assumed a maximum loading of 4 g's. The crew module is cylindrically shaped so that it may be transported by the Space Shuttle. It is 14 feet in diameter and 8 feet long (see Figure 65 on page 77 and Figure 66 on page 78). It will have a 0.25 inch thick aluminum deck to secure equipment under the 4 g loading. The structure also consists of two C 5x9 aluminum alloy end stringers (as referenced to the W and C classifications for beams), one centered W 4x13 stringer, three W 4x13 beams which run lengthwise, and three W 4x13 beams which also run lengthwise and are used below the deck as machinery mounts. The skin is made of a sandwich type construction composed of an inner airtight shell 0.02 inches thick. The inner skin thickness was calculated assuming an interior pressure of 14.7 psi and a factor of safety of 1.44. The exterior skin is made of 0.01 inch thick aluminum. Sandwiched between the inner and exterior skin is 4.16 inches of insulation and meteorite protection.

Table 15. Weight Summary of Crew Module

STRUCTURE	No.	LENGTH (ft)	TOTAL LENGTH (ft)	AREA (ft^2)	TOTAL VOLUME (ft^3)
C 5x9	2	43.980	87.96	0.018	1.613
S 5x14.75	3	11.489	34.50	0.030	1.039
S 5x14.75	1	8.000	8.00	0.030	0.240
W 4x13	1	43.980	43.98	0.027	1.169
W 4x13	8	8.000	64.00	0.027	1.728

Structure Mass	1,006.0 lbm
Mass of Inner Skin (Thickness = 0.02 in)	96.3 lbm
Mass of Exteroir Skin (Thickness = 0.01 in)	50.7 lbm
Other Weight Estimates	
Thermal/Radiation/Impact Protection	235.0 lbm
Avionics and Controls	200.0 lbm
Crew 3x175 lbm	525.0 lbm
Aluminum Deck Plate (t = .25 in)	330.0 lbm
Seats 3x100 lbm	300.0 lbm
Air Tanks	250.0 lbm
Air Ducting	60.0 lbm
Air Recirculation Machinery	60.0 lbm
Radiation Storm Shelter	773.0 lbm
Interior -Overhead	75.0 lbm
-Lavatory, Plumbing, Pump	80.0 lbm
-Onboard Water	100.0 lbm
-Misc (Space Suits, Lights etc.)	500.0 lbm
TOTAL	4,891.0 lbm

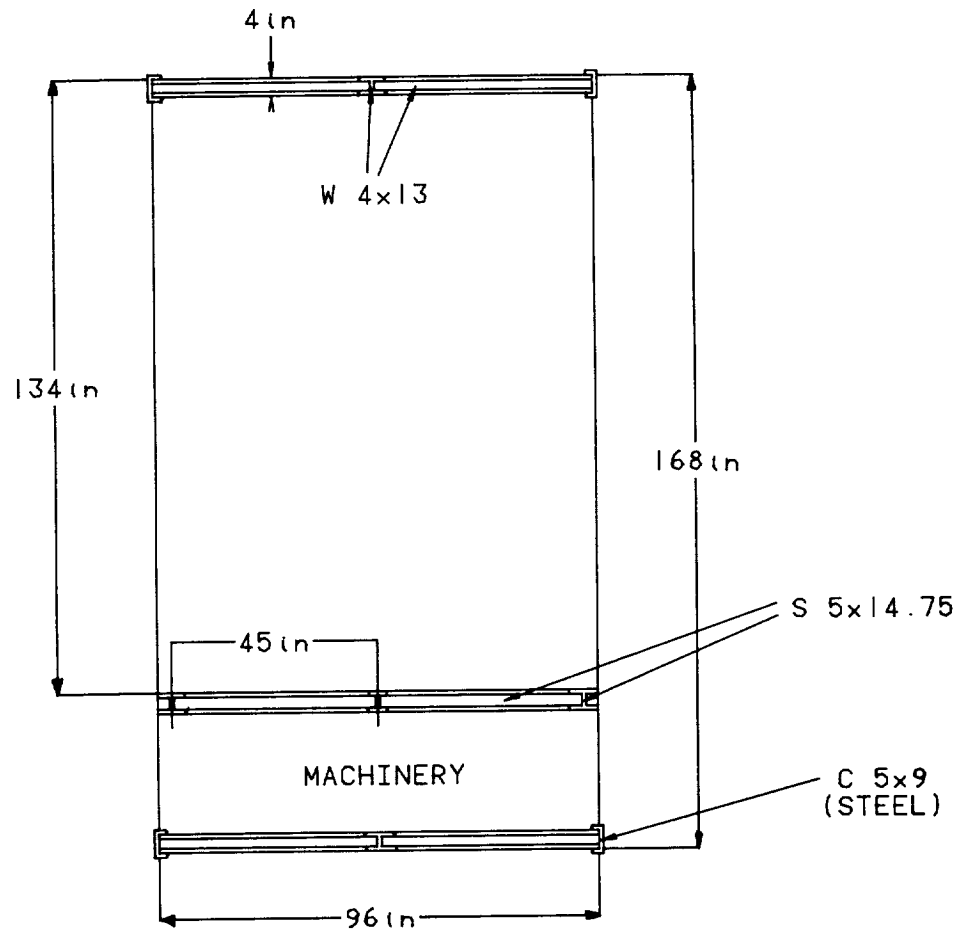

Figure 65. Crew Module Structure - Side View

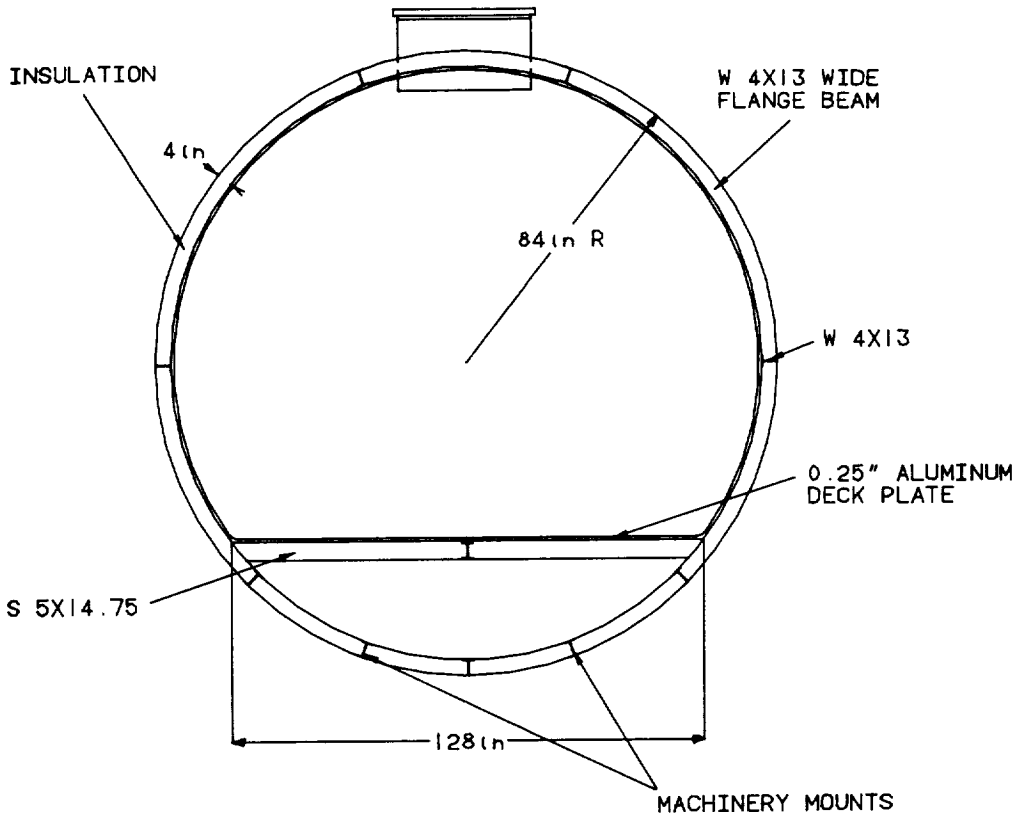

Figure 66. Crew Module Structure - Front View

4.4.2 LIFE SUPPORT

The environmental control and life support system (ECLS) chosen for the crew module requires equipment for the following tasks:

1) Cabin Atmosphere Revitalization Section (ARS) for personnel and equipment.
2) Atmosphere Storage and Control.

The ECLS is designed to provide a suitable environment for the crew of three within the following parameters:

Temperature----------70° ± 5° F
Total Pressure--------10 - 14.7 psi
O_2 Partial Pressure---3.5 ± .2 psi
Diluent----------Nitrogen
CO_2 Partial Press.-----8 mm Hg max
Relative Humidity-----50 ± 10%

Crew Metabolic Parameters

O_2 Consumption----------2.07 lbm/man-day
CO_2 Output----------2.12 lbm/man-day
Water Consumption----------6.125 lbm/man-day

Wash Water----------26.3 lbm/man-day

Respiration and Perspiration

Perspiration Output----------3.08 lbm/man-day
Heat Output (Sensible)----------7,730 Btu/man-day
Heat Output (Latent)----------3,230 Btu/man-day

The ARS is further broken into two main subsystems:

1. Active Thermal Control
   - -Freon Coolant Loop
   - -Space Radiator
   - -Avionics Cooling

2. Atmospheric Revitalization
   - -Atmospheric Revitalization
   - -Atmospheric Pressure Control
   - -Avionics Cooling

Thermal control for the mission is provided by one Freon-21 loop, two air-water-Freon loops, and one water to Freon loop. Heat generated by the crew as well as heat from the air circulation machinery is dissipated through a 650 lbm/hr air loop which is designed to remove 3,660 Btu/hr from the module. In addition to cooling the crew and machinery, the crew module air loop will also remove 8,300 Btu/hr from the one avionics package on board the module for a total heat transfer of 11,960 Btu/hr. The heat is the transferred to a water loop using a stainless steel air to water heat exchanger. A second air loop is provided for the avionics cooling which removes heat from the below deck avionics at 5,200 Btu/hr using an air flow of 875 lbm/hr. The heat from this second air loop is also transferred to the water loop using a heat exchanger. The final avionics cooling is provided by a water loop which cools coldplates mounted to the shelves of the avionics bay. The coldplates remove 2,833.3 Btu/hr and circulate water at 100 lbm/hr.

The total heat rejected to main water loop is approximately 20,000 Btu/hr at a flow rate of 426 lbm/hr. The heat is then transferred from the water loop to a Freon-21 loop via a heat exchanger. Finally the heat is dissipated into space by a set of space radiators located on the module.

The cabin air cooling system is triply redundant with three heat exchangers and three ducted fans, each one capable of 650 lbm/hr. The avionics package air loop and the coldplate water loop are doubly redundant given that there are two more avionics packages on board the vehicle.

The ARS also provides trace contaminant, CO_2, humidity, and odor control. Air from the cabin is drawn into the cabin air fan assembly through a filter debris trap by one of two redundant fans at 150 cfm. The air is then drawn through the CO_2, trace contaminant, and odor assembly. The assembly contains two CO_2 and odor control cartridges composed of lithium hydroxide, activated charcoal, and purafil. The cartridges are expendable and accessible from the cabin for replacement every 15 hours. The cabin temperature is controlled by passing the air through and/or around a humidity control assembly where the air is cooled below the dew point in the heat exchanger. The dry air is returned to the cabin while the condensate is removed from the heat exchanger and stored for removal at LEO or GEO.

The cabin atmosphere simulates an ideal earth atmosphere. The temperature and pressure are 75°F and 14.7 psi respectively. The cabin atmosphere is composed of 78% nitrogen and 21% oxygen. This mixture meets the crew requirements, reduces the risk of fire or equipment failure and aids in equipment cooling. Carbon dioxide is controlled to 0.03% and catalysts are used to remove carbon monoxide. An extra supply of 39.90 lbm of oxygen and 89.5 lbm of nitrogen is also carried on board. This amount of air allows for a full repressurization of the module and meets the 7 lbm air/day leakage and the 2.07 lbm O_2/man-day consumption rates for forty-eight hours. A trip from LEO to GEO and back to LEO takes 14 hours and 39 minutes. The extra gas is carried for repressurization purposes should the crew have to leave the module in an emergency or for a repair without having a docking airlock available. In the event of a solar flare, the radiation protection on the outside of the module may not be sufficient. In this case the three crew members enter the

storm shelter shown in Figure 63 on page 74. The storm shelter is made of 0.866 inch thick aluminum. This additional shielding provides ample radiation protection during an abnormally large solar event. Drinking water as well as wash water for the crew is a by-product of energy production in the fuel cells. The water is stored on board in a fresh water storage tank.

Table 16. Tanks

	OXYGEN TANK	HYDROGEN TANK	DIMENSION
Disposable Tanks:			
Tank Radius	4.396	6.115	ft
Skin Thickness	0.009	0.013	in
Skin Mass	29.430	78.450	lbm
Stringers:			
Width (w)	1.000	1.000	in
Height (h)	1.000	1.000	in
Thickness (t)	0.109	0.018	in
Thickness at connection point	1.160	0.117	in
Hole/Pin Radius	0.304	0.125	in
Total Mass	13.300	3.100	lbm
Baffle Width (w)	6.844	9.422	in
Ejection Rocket:			
Burning Surface Area	1.963	4.507	in^2
Throat Area	0.223	0.512	in^2
Exit Area	1.733	3.980	in^2
Burn Rate	0.480	0.480	in/sec
Fuel Mass	0.120	0.275	lbm
Structure Mass	42.730	81.550	lbm
Permanent Tanks:			
Tank radius	1.065	1.479	ft
Skin thickness	0.073	0.031	in
Skin Mass	13.859	11.143	lbm
Stringer Mass	2.338	0.273	lbm

4.5 PROPELLANT TANKS

In order to reduce overall mission costs a disposable propellant tank configuration was designed. With this configuration, the propellant tanks extend over the outer edges of the aerobrake. This allows for the aerobrake to be smaller and less massive, and hence yields a savings in propellant. Just prior to entry through the atmosphere the tanks would be ejected away from the spacecraft and allowed to burn up on their entry into the atmosphere. At this point, small permanent tanks would take over the remaining propellant requirements. The ejection system for the propellant tanks consists of four releasable connection points that connect the tank to the main structure and a solid fuel rocket that boosts the tank away from the spacecraft. A comparison between a solenoid ejection system and a rocket ejection system was done and it was found that the rocket system would be more reliable, less massive and less expensive.

4.5.1 DISPOSABLE TANKS

CALCULATION OF COMPONENT DIMENSIONS

The main tank components consist of the skin, stringers, impact and thermal protection, and internal baffles. The material used for these components is an aluminum lithium alloy (2090-T8E41) with a tensile yield strength of 87 ksi, a shear yield strength of 43.5 ksi, and a density

of 0.092 lbm/in^3. In the calculations it was assumed that the maximum propellant mass of each loaded tank would be 4257.89 lbm for the hydrogen tank and 25310.19 lbm for the oxygen tank. It was also assumed that the maximum acceleration would be 2 g's at the time of maximum loading and the gauge pressure of each tank would be 20 psi. This reflects the negligible pressure due to loading. Mission propellant requirements led to a hydrogen tank of 6.1146 ft radius and an oxygen tank of 4.3956 ft radius. Stress calculations that were done to arrive at the existing dimensions are presented below:

Tank thickness (using hoop stress analysis):

$$\sigma = pr/2t$$

O_2: $t = 0.0061$ in
H_2: $t = 0.0084$ in

where p is the gauge pressure, σ is the normal stress, r is the radius of the tank and t is the thickness of the tank.

Skin Mass:

$$M = 4\pi r^2 t\rho$$

O_2: $M = 19.62$ lbm
H_2: $M = 52.30$ lbm

where ρ is the density of the material.

"T" Stringer dimensions (using normal stress calculations):

$$\sigma = P/A$$

O_2: $A = 0.11450$ in^2
H_2: $A = 0.02447$ in^2

where P is one quarter of the total force produced at 2 g's since there are essentially four stringers in the cross section and A is the cross sectional area of the stringer. It is assumed that the width w and the height h of the stringers are equal at one inch. This gives the following thicknesses:

O_2: $t = 0.07275$ in
H_2: $t = 0.01224$ in

Pin cross-section area at connection point:

$$\tau = F/2A$$

O_2: $A = 0.2909$ in^2, $r = 0.3043$ in
H_2: $A = 0.0489$ in^2, $r = 0.1248$ in

where τ is the yield shear strength, F is the force on each pin, and A is the cross sectional area of the pin. The thicknesses in the height portion of the stringers were recalculated at the connection holes in the following manner to prevent tearing of the stringers:

$$K = \sigma max/\sigma ave$$
$$d = D - 2r$$
$$\sigma ave = P/A$$

where D is the total width at the hole, r is the radius of the hole, P is the force, and A is the cross sectional area of the stringer.

O_2: $r/d = 0.7538$, $K = 2.08$, $\sigma ave = 41826.9$ psi, $A = 0.3026$ in^2, $t = 0.7731$ in

H_2: $r/d = 0.1636$, $K = 2.39$

$\sigma ave = 36401.7$ psi $A = 0.05848$ in^2

$t = 0.0779$ in

After these calculations were complete a factor of safety of 1.5 was applied to arrive at the final dimensions and masses listed in Table 15 on page 76.

BOOSTER ROCKET DIMENSIONS

After the tank mass was calculated, a booster rocket was designed that would eject the tank far enough away so as not to interfere with the spaceship on the rest of its mission. The selected fuel grain used is an end-burning type since this would give a constant thrust throughout the burn. It was estimated that the thrust would be twice the mass of the tanks and the burn time would be two seconds. This would put the tanks 128.8 ft away at a velocity of 128.8 ft/sec. The trajectory would be at a 45° angle to the raked plane of the aerobrake and almost perpendicular to the thrust line. An extra stringer reaching one quarter of the way around the tank is added to support the thrust of the booster rocket, as seen in Figure 67. It was assumed that the exit pressure would equal 14.7 psi, and that the chamber pressure would equal 1000 psi. The solid fuel used is ALT-161, and has the following combustion properties:

Chamber temperature	= 3,660 R
γ	= 1.27
MW	= 30
density	= 110 lbm/ft^3
burn rate	= 0.48 in/sec @ -320° F
n	= 0.745
R	= 1,658.7 lbf^2-s^2/lbm^2

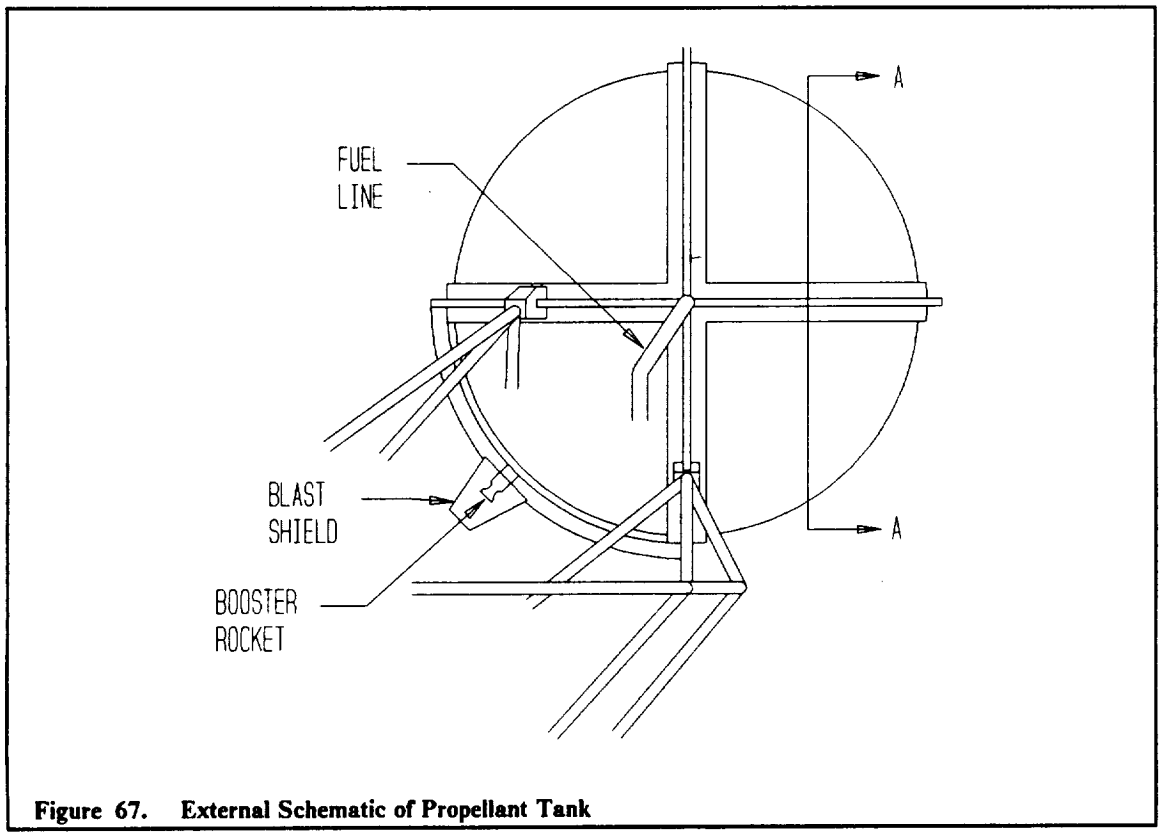

Figure 67. External Schematic of Propellant Tank

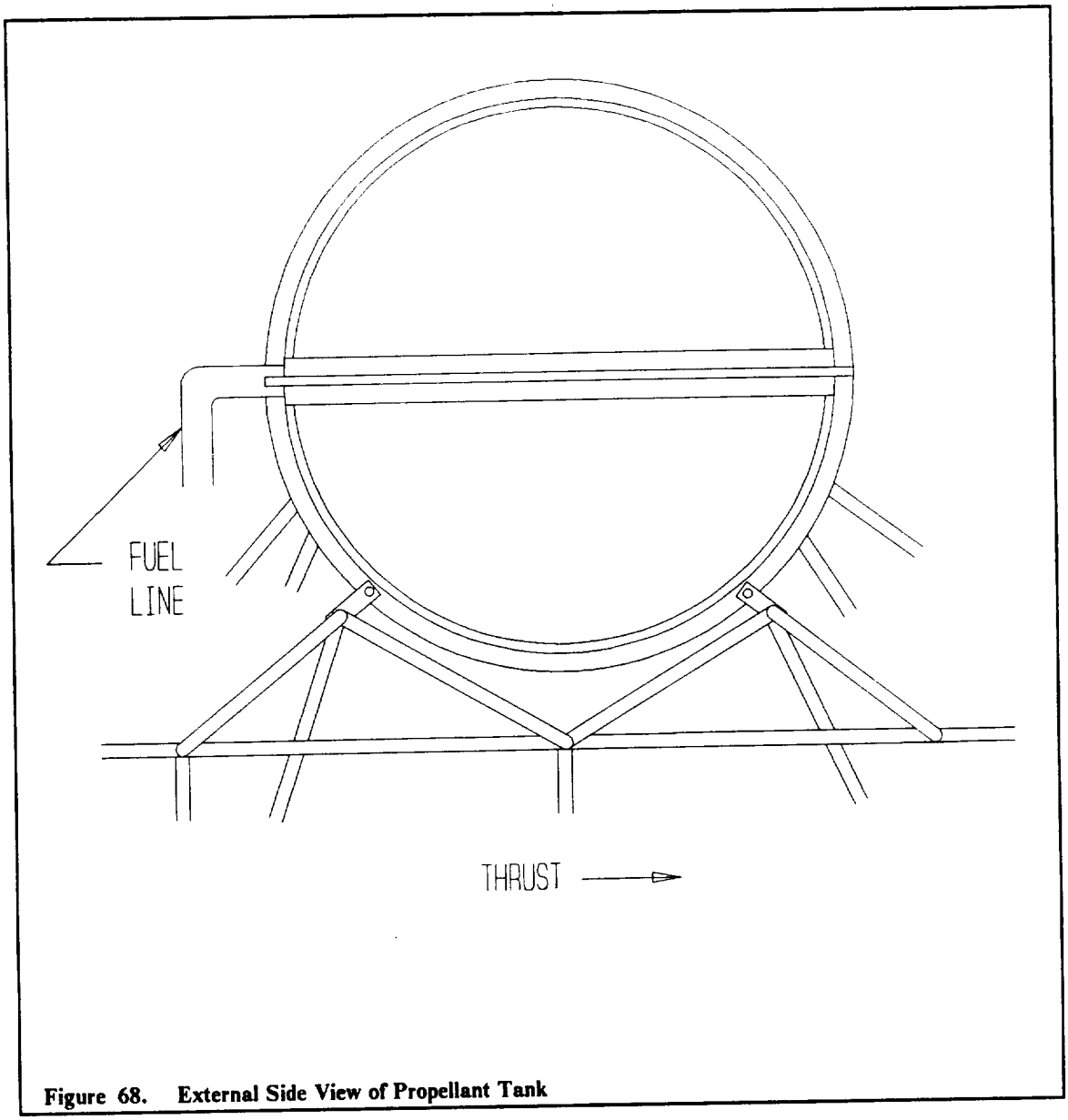

Figure 68. External Side View of Propellant Tank

The dimensions of the booster rockets were arrived at using ideal, isentropic equations. From these results the final dimensions in Table 15 on page 76 were calculated for each of the booster rockets assuming the structure mass plus the insulation mass of the oxygen tank is 186.8 lbm and the hydrogen tank is 429.0 lbm.

BAFFLES

Three ring baffles are added inside each propellant tank to reduce the amount of sloshing within the tank. The baffles are oriented perpendicular to the line of thrust since this is the primary direction of the sloshing. This can be seen in the section shown in Figure 69 on page 84. The three ring baffle was found to reduce the sloshing most effectively. In addition, a w/R ratio of 0.125 was most effective in terms of dampening versus weight of the baffles. This corresponds to the dimensions given in Table 16 on page 80.

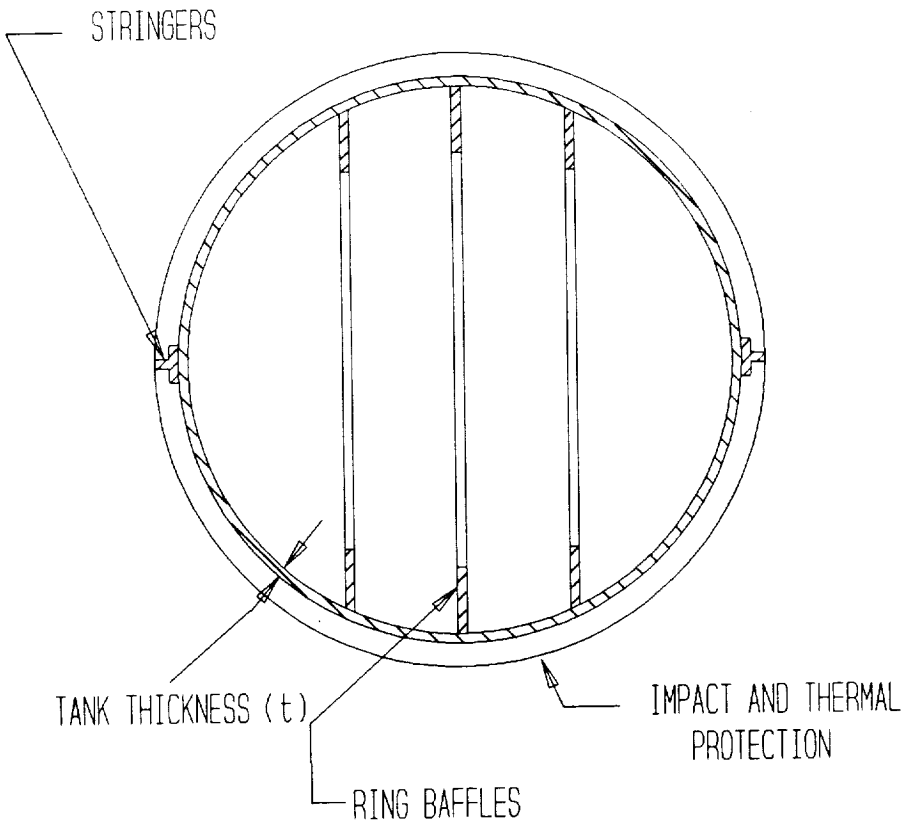

Figure 69. Tank Section View A-A

TANK RELEASE MECHANISM

The tank release mechanism consists mainly of four connection points, two of which are located between the aerobrake and the tank and, the other two located between the mission module and the tank. All connection points attach to the stringers of the aerobrake. A clamp is attached to the stringer by an exploding bolt as seen in Figure 70 on page 85. The bolts are made from a hardened steel such as 4340 steel since this material produces a clean fracture and allows the bolt to release more easily. A comparison of the solenoid-pin mechanism versus the exploding bolt mechanism was made and it was found that the exploding bolt mechanism was more reliable and required less power. Just before tank ejection, the bolts are detonated, allowing the clamp to open up and free the tank from the spacecraft.

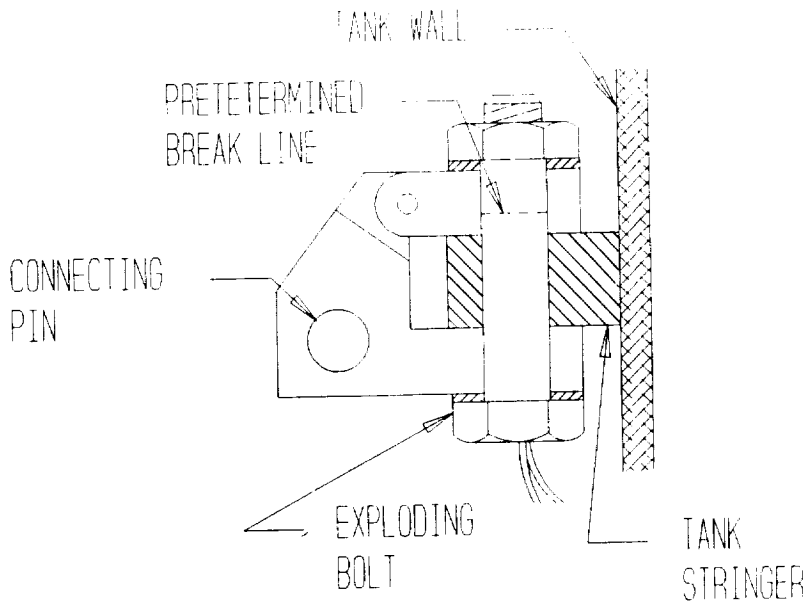

Figure 70. Tank Release Mechanism

4.5.2 PERMANENT TANKS

Ten small tanks supply the spacecraft with propellant to complete the mission after release of the disposable tanks. Five of these are oxygen and five are hydrogen. They are oriented so that the propellant exit is closest to the engine side of the vehicle. Thrusting therefore aids in extracting propellant. There is also a helium filled bladder to pressurize the propellant. This serves to pump the propellant to the engines and greatly reduces sloshing within the tanks. It also serves to pump propellant to the engines when the spacecraft is not thrusting. The schematic of this configuration can be seen in Figure 71 on page 86. The internal pressure of the tanks is 500 psi. Each oxygen tank has an empty mass of 137.4 lbm, and each hydrogen tank has an empty mass of 22.8 lbm. The same calculations that were done for the disposable tanks were done for the permanent tanks to arrive at the dimensions listed in Table 16 on page 80. The stringer size is consistent with the corresponding disposable tanks since the permanent tanks have longer expected lifetimes.

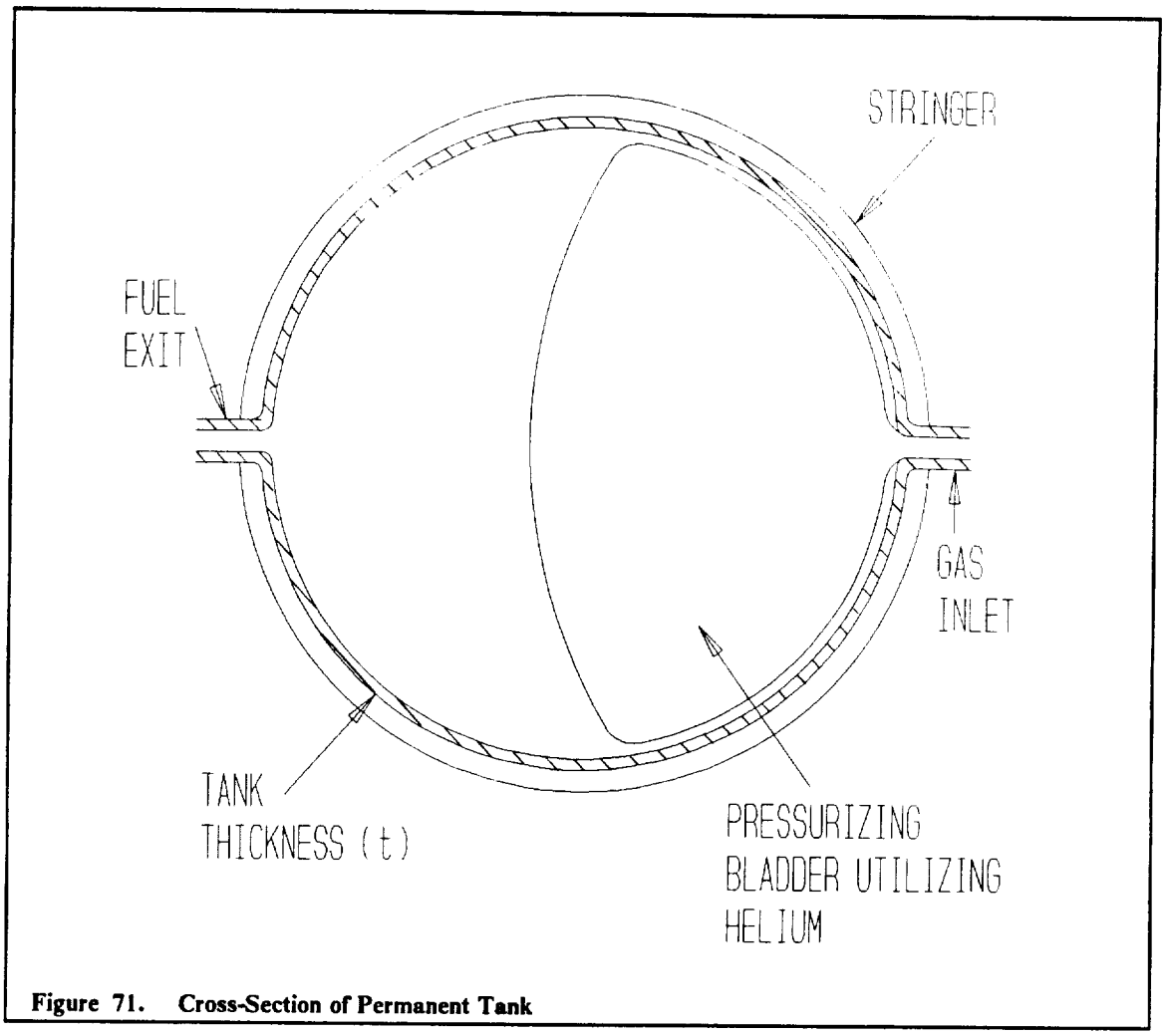

Figure 71. Cross-Section of Permanent Tank

4.5.3 INSULATION

The multilayer insulation thickness required for the tanks was determined by allowing for one percent boiloff. Boiloff is the propellant component that is vaporized within the tank due to heat flux. This measure is conservative for any particular mission where boiloff below 5% may be tolerated.

The maximum heat flux which may be transferred into the tanks is determined partly by the heat flux due to solar radiation on the exposed surface of the tank. The temperature of the tank surface can then be determined using the Stefan-Boltzman Law.

The calculated insulation thickness for the various tanks is shown in Table 17 on page 87. The actual amount of insulation required will be slightly greater due to the heat transfer that occurs because of piping. This amount, however, will not significantly increase the total mass of insulation.

4.5.4 IMPACT PROTECTION

Table 17 on page 87 gives the thicknesses for radiation shielding, impact protection material and insulation for each component, along with the total insulation mass for each component. Radi-

ation protection is supplied by the stainless steel foils that compose part of the MLI, and impact protection is also supplied by both the foils as well as by the spacer material (Nextel).

The required shielding thickness was determined using the Ames criterion:

$$t = 2.7\times10^{-6}(AT/P)^{1/3}$$

where

A - surface area
T - mission duration (sec)
P - probability of no penetration

The result yields a thickness for one sheet of aluminum; however, the chosen design uses several layers which can reduce the thickness needed. Hence, an improvement of 20% in thickness was assumed. A factor of safety of 1.5 was also imposed and the results are as given in the following table.

Table 17. Tank Shielding and Insulation

COMPONENT	SHIELDING (in)	INSULATION (in)	MASS (lbm)
Main O_2 tank	0.02	0.319	2 x 144.1
Main H_2 tank	0.025	0.397	2 x 347.4
Permanent O_2 tank	0.006	0.100	4 x 1.38
Permanent H_2 tank	0.008	0.124	4 x 3.329

Total Mass for Tank Protection and Insulation = 1002 lbm

REFERENCES

1. Abramson, H.N., *The Dynamic Behavior of Liquids in Moving Containers,* U.S. Government Printing Office, Washington D.C., 1966.
2. Brauer, K.O., *Handbook of Pyrotechnics.* , New York, Chemical Publishing Company, 1974.
3. Beer, F.P., and Johnston, E.R. Jr., *Mechanics of Materials*, New York, McGraw-Hill, 1981.
4. Beer, F.P., and Johnston, E.R. Jr., *Vector Mechanics for Engineers: Statics and Dynamics*, New York, McGraw-Hill, 1984.
5. Cooper, L. and Scheer, D, *Status of Advanced Propulsion for Space-Based Orbital Transfer Vehicle*, Great Britain, Acta Astronautica, 1987.
6. Collins, J.A., *Failure of Materials in Mechanical Design: Analysis and Prevention*, New York, John Wiley and Sons. 1981.
7. Hill, P.G., and Peterson, C.R., *Mechanics and Thermodynamics of Propulsion*, Reading, MA. Addison-Wesley Publishing Co., 1970.
8. Jones, J.B. and Hawkins, G.A., *Engineering Thermodynamics*, New York, John Wiley and Sons, 1986.
9. Lubin, George, ed., *Handbook of Composites*, Van Nostrand Reinhold Comp. Inc. 1982.
10. Murphy, Joe, "PC-STRAN, A 1-, 2- or 3-Dimensional STRuctural ANalysis Program For the IBM Personal Computer", Version 3.50, tm Joe Murphy.

5. RCS SYSTEM

INTRODUCTION

The RCS system is designed for three main purposes. The first is the reorienting of the vehicle after it leaves LEO or GEO so that the thrusting acceleration will be in the correct direction. The second purpose of the RCS is to provide small changes in roll, pitch, and yaw during the aerobraking phase to achieve different lifting characteristics. The third duty of the RCS is to provide small translational and rotational changes to position the craft for docking.

5.1 MOMENTS OF INERTIA

The table below lists the mass and moments of inertia for the ASTV.

Table 18. Mass and Moments of Inertia

	With Propellant	Without Propellant
Total Mass:	85,083 lbm	34,457 lbm
Moments of Inertia:		
Ixx	9,671,275.00 lbm-ft^2	574,673.80 lbm-ft^2
Iyy	2,553,844.00 lbm-ft^2	985,919.10 lbm-ft^2
Izz	9,761,294.00 lbm-ft^2	4,357.40 lbm-ft^2
Ixy	-120.80 lbm-ft^2	-120.80 lbm-ft^2
Iyz	29,845.60 lbm-ft^2	29,845.60 lbm-ft^2
Ixz	-140,038.00 lbm-ft^2	36,974.08 lbm-ft^2
Center of Gravity Position:		
X	14.64 ft	18.83 ft
Y	0.00 ft	0.00 ft
Z	5.71 ft	4.98 ft

5.2 SIZES

The dimensions for the two types of thrusters are shown in Table 19 on page 90. These values were obtained by using the NOTS program.

C-2

Table 19. RCS Dimensions

RCS	EXIT DIA (in)	THROAT DIA (in)	LENGTH (in)
60 lbf	6.20	0.390	9.58
10 lbf	2.53	0.160	3.91

5.3 PROPELLANT TYPE

Liquid hydrogen/liquid oxygen was chosen as the RCS propellant over hydrazine for several reasons (see Table 20). The most important reason is the integration with the main propulsion system which also uses LO_2/LH_2. By using the same type of propellant, the RCS can feed off of the main tanks thus eliminating the need for separate tanks.

Table 20. Fuel Type Considerations

CONSIDERATION	HYDRAZINE	LO_2/LH_2
Handling Safety		+
ISP	+	
Integration with given system		+

5.4 LOCATIONS

The reaction control system is configured to provide the maximum possible moment arm for each thruster. Roll is controlled by RCS groups D and B (see Figure 72 on page 91), Groups D and B each have two upward firing 60 lbf rockets, two upward firing 10 lbf rockets, two downward firing 60 lbf rockets, two downward firing 10 lbf rockets, and four fore and aft firing 60 lbf rockets (see Figure 73 on page 92 and Figure 74 on page 92). The two different types of vertical firing roll thrusters are to provide appropriate roll rates (see Table 21 on page 91) depending upon the propellant tanks on board. During the aerobraking phase the craft will experience 4,237 ft-lbf torque for every 1° of roll. The maximum roll moment which can be attained by using the RCS is 1,960 ft-lbf or 0.46 degrees.

The pitch controls are located at A and C (see Figure 72 on page 91). Each cluster consists of two upward firing 60 lbf rockets and two downward firing 60 lbf rockets. Also on this cluster but not related to pitch control are four side firing 60 lbf rockets, four side firing 10 lbf rockets, and one outward firing 10 lbf rocket (see Figure 73 on page 92 and Figure 74 on page 92). During aerobraking the craft will experience 4,508 ft-lbf of torque for every one degree change in pitch. The maximum pitch moment available through the RCS is 2,220 ft-lbf of torque which can produce a pitch change of 0.49°.

The yaw controls are also mounted in the front and rear RCS packages. As mentioned earlier the packages contain two left firing and two right firing 60 lbf rockets as well as two left firing and two right firing 10 lbf rockets (Figure 73 on page 92 and Figure 74 on page 92). The yaw rates for different combinations of thrusters and vehicle weights are given for nonaerobraking flight (Table 21 on page 91). During the aerobraking phase the craft experiences a yaw restoring force of 170 ft-lbf per degree of yaw. The maximum available yaw force from the RCS is 2,590 ft-lbf for a total yaw angle of 15.2°. The RCS is set up as a doubly redundant system. For example, only two of the four 60 lbf thrusters are need to provide sufficient roll force during aerobraking and free flight. Furthermore, all thruster firing is accomplished in pairs to cancel any extraneous moments arising from the thruster locations not on the CG axis. The RCS packages can also be retracted behind the skirt when not in use (see Figure 75 on page 93).

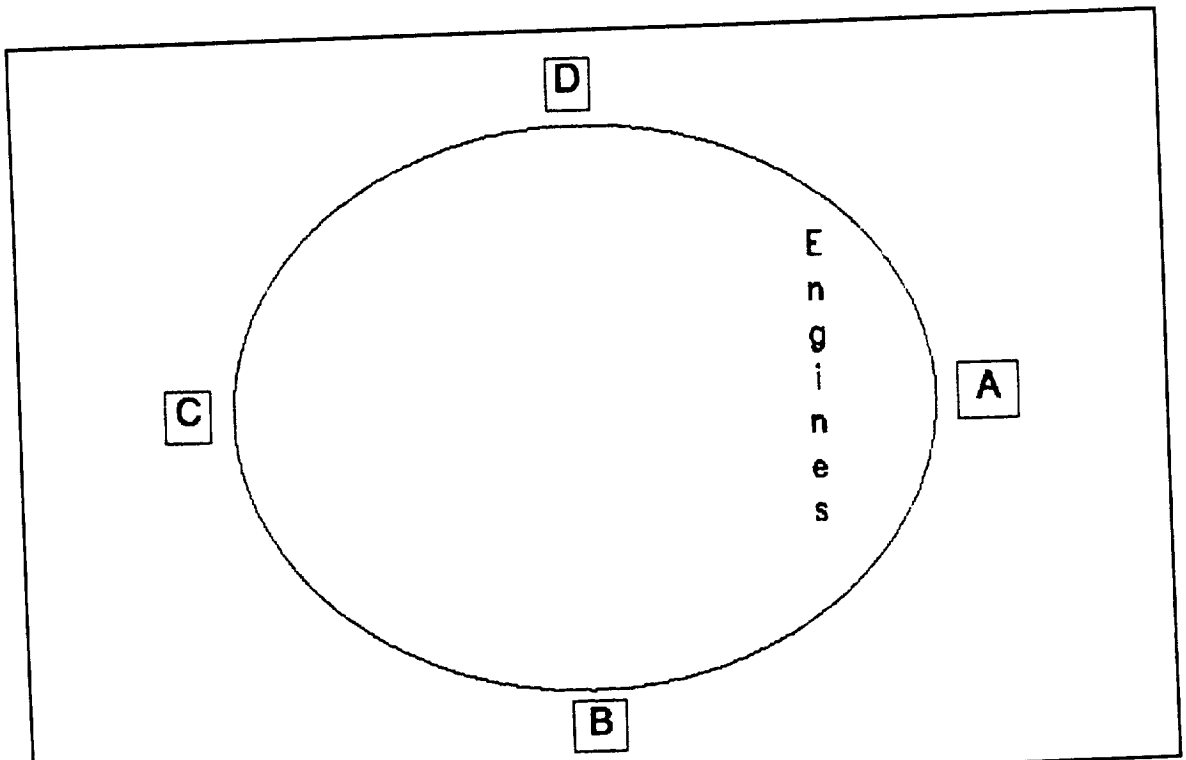

Figure 72. RCS Locations

Table 21. RCS Angular and Linear Acceleration

Pure Translation

Direction	Possible Thruster	Acceleration (ft/s²) w/ fuel	w/o fuel
x	1/60 lbf	0.0007	0.00174
	2/60 lbf	0.0014	0.00348
	3/60 lbf	0.0021	0.0052
y	2/60 lbf	0.0014	0.00348
	2/10 + 2/60 lbf	0.0016	0.004
z	2/60 lbf	0.0014	0.00348
	4/60 lbf	0.0028	0.0067

Pure Rotation

Motion	Possible Thruster	Rate (deg/s²) w/fuel	w/o fuel
roll	2/10 lbf	0.053	0.894
	2/60 lbf	0.320	5.363
pitch	2/60 lbf	1.600	4.125
yaw	2/10 lbf	0.070	2.734
	2/60 lbf	0.419	16.404

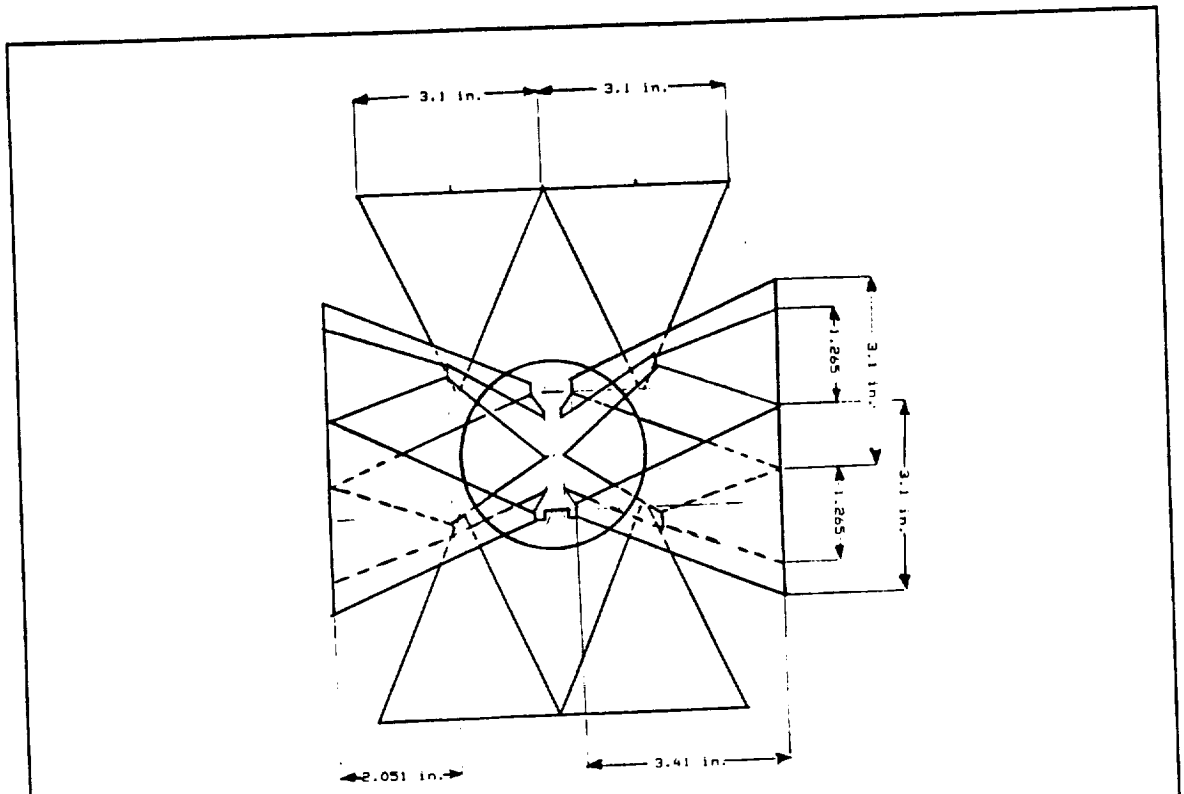

Figure 73. RCS Package View 1

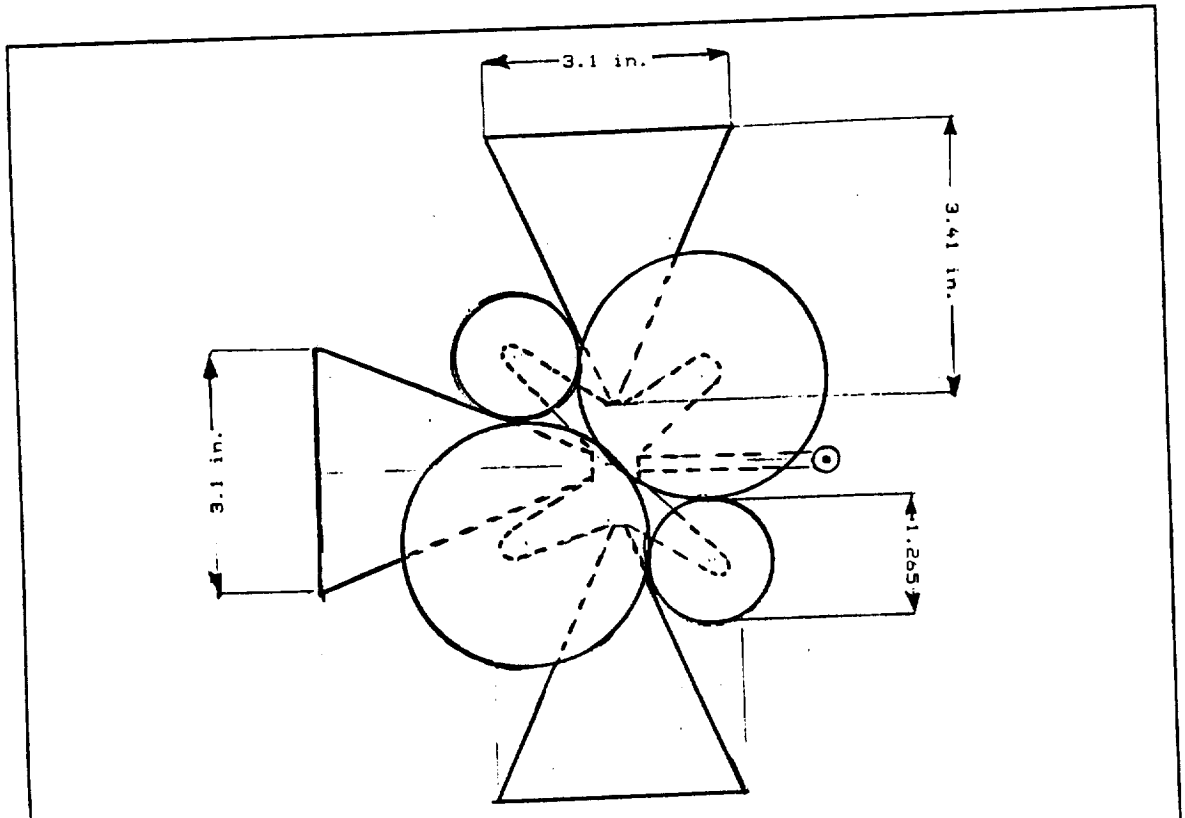

Figure 74. RCS Package View 2

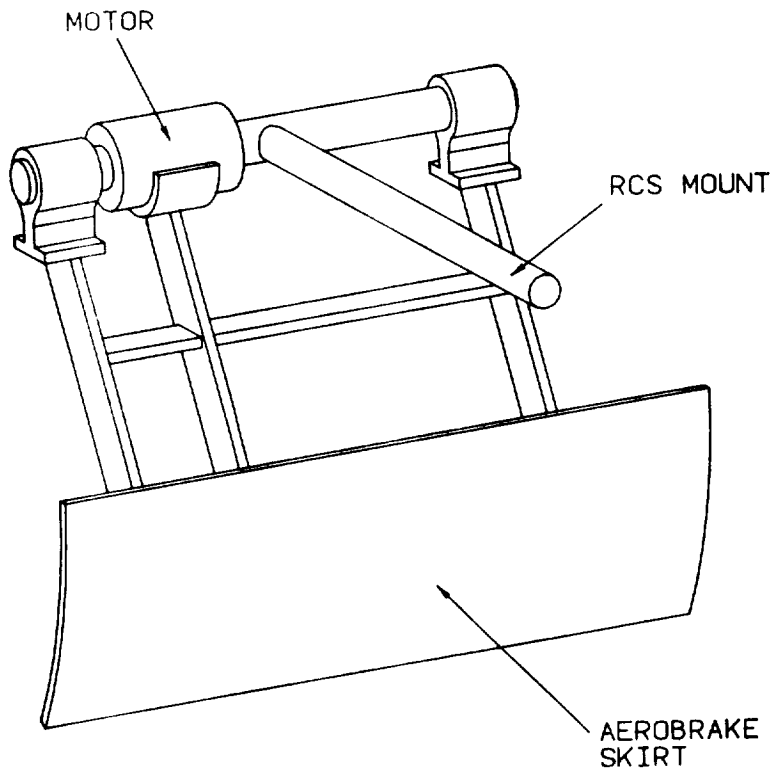

Figure 75. RCS Retractor

5.5 PROPELLANT REQUIREMENTS

The amount of propellant required by the reaction control system was determined from the total burn time for each size control (60 lbf, 10 lbf). An Isp of 472 sec and an oxidizer to fuel ratio of 6:1 was used. The simple relations between these quantities allowed the total propellant mass to be found:

- $Isp = F/(mdot \times g_0)$
- $(mdot)oxy = mdot/(r+1)$
- $(mdot)fuel = mdot/(r+1)$
- $mdot(tp) = \{(mdot)oxy + (mdot)fuel\}tp = m(oxy) + m(fuel) = m(tot)$

The 10 permanent tanks of the ASTV hold all of the propellant (LO_2/LH_2) required for the RCS, as well as the propellant necessary for the last burns of the main engines and the propellant reserve. This combination yields a total oxidizer mass of 1,750.25 lbm and a total fuel mass of 287.30 lbm. These tanks are pressurized with helium gas to eliminate the need for a turbopump system.

A simplified analysis of this pressure feed system, assuming an adiabatic expansion for the helium gas, was performed for the desired tank pressures ($P(LO_2) = P(LH_2) = 500$ psi). Due to uncertainties in heating and cooling effects on tank and pipe walls and liquid propellants, 10% excess propellant is carried on board. This same excess is also allowed for the helium gas to account for variations in ambient temperature and gas absorption by the propellant. The expansion of the high pressure gas may be assumed to proceed slowly due to the short pulse nature of the RCS. Thus the helium was assumed to be at a constant temperature of 68°F. From similar calculations and experimental results the pressure of the gas was allowed to be seven times that of the propellant

tank, with a minimum pressure of 1.3×P(tank)(due to regulator). Due to the difference in oxidizer and fuel tank pressures, calculations were made for one helium gas tank that would pressurize the entire system of permanent tanks. The responsibility of maintaining correct tank pressures is taken care of by pressure regulators.

The total mass of helium required is found to be 34.77 lbm for propellant volumes of:

- oxidizer per tank = 4.919 ft^3
- fuel per tank = 12.963 ft^3

These volumes are determined from the masses found earlier and the respective densities of oxidizer and fuel. Using the mass of helium required for the limiting pressure of the propellant tanks, the necessary gas tank volume was found to be 17.26 ft^3. In order to reduce weight, two pressure bottle was designed with composite tank technology. For the operating pressure of 3,500 psi, two cylindrical tanks 72 in long x 17 in diameter will be used. The gas bottles will have two, axially opposed ports and consist of an Aluminum 6061-T6 liner with IM-6 carbon fiber overwrap. This configuration assumes a burst pressure of 7,000 psi. Although the term "burst" is used, the gas bottle is designed to leak before actual rupture would occur.

REFERENCES

1. Sutton, George P., *Rocket Propulsion Elements 5th ed.*, John Wiley and Sons, Inc. 1986.

2. Pearce, T.M., Neverman, D.A., Darms, F.J., Morris, E.E., *Composite Fiber/Metal Space Station Tankage--Applications, Material/ Process/Design Trades, And Subscale Manufacturing/ Test Results*, AIAA, 1987.

3. Morris, E.E., Darms, F.J., Lynn, V., *Lower Cost, High-Performance Composite Fiber/Metal Tanks for Spacecraft*, AIAA-86-1694.

6. GUIDANCE, NAVIGATION AND CONTROL

6.1 REQUIREMENTS

Important criteria for the guidance and control system of the ASTV include:

- acquiring long-term celestial references
- maintaining spacecraft attitude throughout cruise periods
- reorienting the vehicle to perform maneuvers such as midcourse correction and orbital insertion
- maintaining control of the spacecraft during periods of occultation of celestial references
- providing attitude stabilization and thrust impulse control

Docking and rendezvous capabilities are also important aspects of the guidance system.

6.2 MAIN COMPONENTS

The guidance, navigation, and control (GN&C) system provides control for the ASTV through the use of the Reaction Control System discussed in the previous chapter. The navigation is performed by an autonomous inertial system having minimum interfaces with the ground or space stations.

The actual components consist of an inertial measurement unit, control electronics and a star tracker. The weight estimations and a brief function description of each component are shown in Table 22 on page 97. An onboard computer carries out all necessary computations to perform the mission without ground support.

Roll attitude is maintained by using a gimballed star tracker. The gimballing allows the star tracker to be used at varying altitudes by increasing its field of view.

The vehicle's attitude is maintained by the inertial reference system during periods of occultations. Orientation measurements are made by gyroscopes in this inertial system. Both rate gyros and rate-integrating gyros are used. Rate gyros measure the craft's angular rates and are part of a feedback system for either spin rate control or attitude stabilization. Rate-integrating gyros measure the vehicle's angular displacements directly.

The control electronics provide an interface between the central computer and the RCS, and switching for power management.

There is double redundancy of all components during the manned mission.

Table 22. GN&C Main Equipment

COMPONENT	MASS (lbm)	FUNCTION
Inertial measurement unit	42	provide angular displacement and linear velocity information.
Star tracker	17	provide attitude update
Control electronics	45	provide interface to RCS

7. POWER SYSTEMS, COMMUNICATIONS AND DATA MANAGEMENT

INTRODUCTION

The communication subsystem is responsible for transmitting and receiving information. This information comes from the GN&C subsystem as well as the other subsystems and sensors located throughout the vehicle. This data is collected and processed by the data management system and then relayed to the ground, the Space Station, and/or the Space Shuttle. These systems require electrical power and it is the responsibility of the electrical power subsystem to provide, control and distribute this power.

7.1 POWER SYSTEMS

The power system must provide power to all the ASTV subsystems such as guidance, navigation, control, communications, data management and processing, propulsion, the crew module, and the payload if necessary. These sources include the launch pad via umbilical connections in the Space Shuttle, the Space Station while docked, or internal sources during its mission to and from the GeoShack. The power system is also responsible for the distribution and control of the power.

The internal power is provided by two fuel cells, each rated at 4.0 kW. The cells are fueled by liquid oxygen and liquid hydrogen drawn from the permanent tanks at a fuel to oxidizer ratio of 8:1. LO_2/LH_2 cells were selected because of their proven performance and reliability. Both cells operate simultaneously; however each is capable of carrying the full load in case the other one fails. A third fuel cell is added for the manned mission to provide triple redundancy. The two cell configuration provides the necessary equipment to accommodate the third fuel cell, thus reducing time and cost to upgrade the craft to manned conditions. Also on board are two nickel/hydrogen (Ni/H) batteries to provide smoothing during transition between cells.

Table 23 on page 99 lists the components of the electrical power subsystem and their respective quantities and masses for the manned mission. The fuel cell system is listed with its respective parts. As it turns out, it is more cost effective to configure the vehicle for unmanned missions with two fuel cells and enough hardware to connect a third cell quickly. With the addition of the third fuel cell, double the number of valves and add an additional heat exchanger and a set of pumps. This brings the system to its required redundancy level for manned missions.

The distribution and control system provides interfacing with all other vehicle subsystems, switching capabilities between internal and external power sources and the wiring network connecting the subsystems together. The power distribution units are responsible for relay switching functions which control various components of the communications and GN&C subsystems. The power transfer unit switches the vehicle power supply from internal to external sources. The wiring network then links all subsystems together in the onboard computer. The control of all these systems is maintained by the onboard computer which will be discussed later in this chapter.

Table 24 on page 99 lists all major electrical subsystems and their respective power usages (Ref. Boeing). Using a 48 hour mission duration (worse case, normal mission time 15 hours) the energy usage was computed. From this, the average usage was found to be 3.6 kW which led to the choice of a 4.0 kW fuel cell size.

Most of the equipment will be mounted in the structure under the mission module. This location was chosen since most of the electronic equipment is near the crew module. Locating the fuel cells and communications equipment close together reduces the amount of cabling and thus the risk of failure.

Table 23. Electrical Power Subsystem Components(Manned Mission)

SUBSYSTEM COMPONENT	QUANTITY	MASS
Fuel Cell System		
Fuel Cell	3	120.0
Relief Valve	8	0.5
Solenoid Valve	4	0.5
Disconnects	2	0.5
Accumulator	2	3.0
Pump	3	4.0
Heat Exchanger	2	9.0
Radiator	1	52.0
Coolant Pump	2	10.0
Lines/Fittings	—	10.0
Coolant Plumbing	—	10.0
Coolant	—	6.0
Ni/H Battery	2	60.0
Distribution and Control		
Power Distribution Unit	2	40.0
Energy Control Unit	1	31.0
Power Transfer Unit	2	20.0
Wire Harness/Cables	—	200.0
TOTAL MASS		912.0

Table 24. Power Requirements

SUBSYSTEM	POWER (watts)	DURATION (hours)	ENERGY (watt-hours)
Guidance and Navigation	215	48.0	10,320.0
Communications	146	48.0	7,008.0
Data Handling	801	48.0	38,448.0
Instrumentation			
Engine coast	25	47.5	1,187.5
Engine burn	50	0.5	25.0
Propulsion			
Engine coast	30	47.5	1,425.0
Engine burn	700	0.5	350.0
Crew Module	1800	48.0	86,400.0
Payload	200	48.0	9,600.0
Emergency	100	48.0	4,800.0
Losses (5%)			7,700.0
Miscellaneous (5%)			7,700.0
TOTAL (watt-hours)			174,963.5

7.2 COMMUNICATIONS AND DATA MANAGEMENT

7.2.1 COMMUNICATIONS

The communications subsystem is responsible for transmitting and receiving information from the ground, Space Station, and/or the Space Shuttle. Also communications with the payload must be supported. The information will include video and sound as well as data.

The communication is achieved by ground systems or space systems. Ground based systems communicate directly to the Earth via an Earth-based Antenna System (EAS). This is not the primary means of communications due to the large amounts of interferance with the atmosphere. Also, high frequencies encounter more interference while low frequencies require larger antennas. The space-based system works with antennas based in space, e.g. Space Station, Space Shuttle and satellites. To accomplish global and continuous communications, the vehicle will rely on the Tracking Data Relay Satellite System (TDRSS). This system utilizes satellites whose positions are know as a function of time in order to communicate with the Space Station and Earth no matter where it is.

The frequencies and rates of communication play an important role in determining a communications system. The S-band and K-band were investigated. The S-band is capable of receiving/transmitting various combinations of data including video, voice, and telemetered data. This is accomplished in two transmit/receive rates, transmit 192 kilobits per second (kbps) and receive 72 kbps or transmit 64 kbps and receive 32 kbps.

The K-band, like the S-band, is also capable of transmitting/receiving in two different modes. The first transmitts up to 52 megabits per second (Mbps) while the second mode transmitts at a rate of 7 Mbps. Reception of data is at 2 Mbps. The K-band has a feature that the S-band does not. It can double as a radar tracking unit. While one antenna is being used for communication, the other can be used for radar. Moving targets can be tracked to a range of 345 miles while stationary targets are tracked to 15 miles. This radar is effective to within 100 feet. K-band communications are in the 13,000 to 15,000 MHz range. Due to its versatility and higher volume capabilities, the K-band system was chosen.

The vehicle communicates via two omni antennas, a transponder, a power amplifier, a diplexer, an RF switch, and a network of cables. Each omni antenna provides hemispherical coverage and switches between the two automatically depending on the signal strength at each. A second pair is added for the manned mission to provide redundancy. The amplifier as well as the transponder are configured to operate in the K-band range of 13,000 to 15,000 MHz.

7.2.2 DATA MANAGEMENT

Data management is incorporated into the onboard computer system. This system of four (five for manned missions) main components is responsible for the acquisition and processing of data obtained from various sensors on the vehicle, as well as receiving and transmitting pertinent information to and from the Earth, Space Shuttle, and/or the Space Station.

Each of the main components is called a data management unit (DMU). Each has its own processors that incorporates double redundancy. This is the cost optimum configuration and includes all necessary hardware needed to upgrade the entire system to triple redundancy for manned missions easily. Cabling to critical areas is also redundant.

Each DMU is responsible for collecting and formatting data and monitoring a specific area or subsystem. Communications and telemetry formatting is the responsibility of DMU #1, while

DMU #2 takes care of the guidance, navigation and control operations. The power subsystem is monitored and controlled by DMU #3. DMU #4 accomplishes the control and monitor of the propulsion subsystem. DMU #5 provides redundant components and is added for the manned mission only.

With the addition of the crew module, more electronics are added. The astronauts will be able to interface with the on board computer and have access to the data generated by the vehicle subsystems. Interfacing will be accomplished with laptop-like computers currently used in the Space Shuttle. Data will be stored on erasable optical disks due to their radiation resistance and ability to store video and audio data without using magnetic tape.

Table 25 lists the components, quantity, and estimated power requirements for the communications and data management subsystems.

Table 25. Communications and Data Handling

COMPONENT	QUANTITY	POWER (watts)	MASS (lbm)
Communications			
Transponder	2	36	14.0
RF Power Amplifier	2	110	13.0
Diplexer	2	-	2.0
RF Switch	2	-	0.5
Omni Antenna	4	-	1.5
Wiring	-	-	40.0
Data Handling			
Data Management Unit #1	1	127	34.0
Data Management Unit #2	1	216	64.0
Data Management Unit #3	1	202	45.0
Data Management Unit #4	1	156	40.0
Data Management Unit #5	1	100	44.0
Fiber Optics	-	-	40.0
Instrumentation			
Propellant Electronics	1	25	15.0
Propellant sensors	-	-	20.0
Subsystems Monitors	-	25	90.0
TOTAL MASS			497.0

REFERENCES

1. Boeing Aerospace Co., *Orbital Transfer Vehicle Concept Definition and System Analysis Study, Final Report, Vol II, Book 2,* D180-29108-2-2 Contract NAS8-36107, December 1986.

8. DOCKING TO SPACE STATION, ASSEMBLY, AND MAINTENANCE

8.1 DOCKING

The docking system for the vehicle has three main requirements. The first is to hold the vehicle steady in relation to the station. The second is the ability to remove the modules from the craft and place them aboard the Space Shuttle, the space station, or another ASTV. The third requirement is that the docking equipment be able to connect an airlock to the crew module.

The docking system is based around a set of moveable robotic arms at the space station. There will be two arms to grasp the vehicle on either side of the engines to hold the craft steady. A third overhead arm will be used for extraction of the modules and placement of the airlock. Each arm is extendable and can rotate about three axes. The arms will connect with modules, airlock, and vehicle via the four point connector shown in Figure 76 on page 104. The four point system allows for a moment to be exerted about any axis thereby giving the operator more control in close quarters.

8.2 HANGAR AT SPACE STATION

The facilities at LEO include a hangar at the bottom of the dual keel Space Station. The hangar provides protection on five sides with the bottom open. The hangar is 115 ft by 148 ft when viewed from the open side and will be 98 ft long. This gives ample space for the storage of 2 ASTV's, storage tanks, payloads, and ASTV components such as aerobrakes and spare engines.

The hangar is expected to give shielding from the space environment, including micrometeoroid and radiation protection.

8.3 GENERAL COST ANALYSIS

The cost life cycle of the entire mission will involve eight general steps. These are identification of need, preliminary design, detail design, development, production and construction, support, and finally phaseout.

The first step, identification of need, is the process of determining a solution to some challenge. It involves defining objectives and the steps for achieving them. For this project, mission requirements are proposed and refined for the ASTV.

The preliminary design investigates performance factors, design factors, and effectiveness requirements. All the alternatives are considered and the trade-offs are evaluated. Computational analysis and tests are performed based on the research. This leads to an initial concept. Physical models help to verify the design.

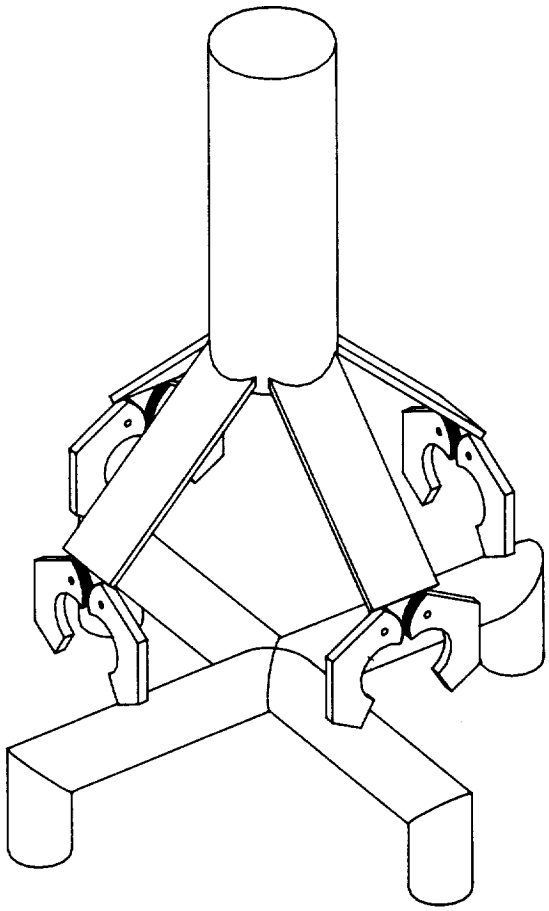

Figure 76. Four Point Docking Grapple

The detailed design involves a component-by-component analysis in which prototypes are built and evaluated. System logistic support requirements are established. The prototypes are refined until these requirements are met.

The vehicle construction must be of modular design to allow delivery to and assembly in orbit. Additional costs will arise from these necessary design modifications. It is projected to take approximately four space shuttle missions to deliver all components.

Further costs include mission support. This will involve providing the propellant, the disposable tanks, life support systems, and general maintenance.

At the end of the service life, the vehicle must be disposed of in a safe and effective manner. This would allow for a more efficient and state of the art vehicle to replace it. The disposal or phaseout stage would involves inserting the craft into an orbit 100 miles above GEO. This would be done once all the salvageable systems were retained for further use after testing and repairs have been made.

SUMMARY

An aerobraking space transfer vehicle (ASTV) has been designed for the purpose of delivering crew and payloads between low Earth orbit and geosynchronous Earth orbit. It will rendezvous with the Space Station at low Earth orbit and with the proposed Geosynchronous Operations Support Center (GeoShack) at GEO. Missions encompassed by the vehicle design include 1) deliver 6,000 lbm roundtrip; 2) deliver 20,000 lbm to GeoShack and return empty; 3) deliver 28,000 lbm to GeoShack and dispose vehicle into a higher orbit. These three missions provide a basis for a wide variety of other missions.

The empty craft mass is estimated to be 11,860 lbm, which yields a maximum propellant requirement of 62,960 lbm for the second mission. The ASTV is 37 feet long, 30 feet wide, and 20 feet high (including payload). The vehicle frame consists of 181 grahite epoxy truss members which are rigidly connected via aluminum endfittings. The frame may be split into three sections for delivery into space. The rigid aerobrake attaches to this main vehicle truss structure. Thermal protection is provided by a 0.337 inch thick multilayer insulation consisting of alternating layers of Nextel cloth and stainless steel foil.

The ASTV is configured with two LO_2/LH_2 engines located side-by-side at the front of the vehicle and thrusting parallel to the top of the aerobrake. Each engine is rated at 15,000 lbf vacuum thrust and incorporates an extendable nozzle to achieve a compact design. The engines are expected to achieve a specific impulse close to 500 seconds. Thrust may be vectored along two rotational degrees of freedom. Before reentry the engines are rotated away from the wake into stowed position. Four sets of reaction control rockets distributed along the aerobrake perimeter provide vehicle control.

Propellant for all but the final impulse is stored in four disposable tanks; one pair (r = 4.4 ft) stores oxygen and the other pair (r = 6.1 ft) stores hydrogen. These tanks are ejected from the vehicle prior to entry into the atmosphere using solid fuel rockets. Five permanent oxygen (r = 0.77 ft) and five permanent hydrogen (r = 1.07 ft) store propellant for the remainder of each mission.

The mission payload is mounted in cargo modules; up to three such modules can be joined together to form one 24 foot long cargo module. A crew module can also be incorporated in place of one of the cargo modules. The crew module provides up to 48 hours of life support for three crew members. The modules attach to the frame at variable positions along two rails to allow for proper CG positoning.

Appendix A. : FLIGHT PLAN ANALYSIS

This section describes the Flight Profile for an ASTV mission. The analysis is for the delivery of a 20,000 lbm payload to GEO, and the ASTV returning to LEO with no payload (Mission 2). The following chart summarizes the requirements of the flight.

Event	Time h:m:s	ΔV ft/s	Mass lbm	Comments
ASTV performs separation	00:00:00	20.0	94274.3	ASTV begins separation from Space Station. ΔV is sufficient to protect the station from all hazards associated with ASTV separation. Impulse applied at nodal crossing.
Coast Period	00:00:02		94157.9	Coast to equator to position for next impulse
ASTV insertion into GEO transfer orbit	00:45:31	7938.0	94157.9	ASTV begins burn which places it on a transfer ellipse arriving at the GEO altitude.
	00:55:43		57654.8	Impulse to take ASTV to GEO is complete, coast to mid-course.
Mid-course corrections applied	03:34:05		57654.8	Mid-course corrections performed if required by orbital position. Continue transfer to GEO altitude.
Circularize and change planes	06:12:26	6000.2	57654.8	Impulse applied which changes orbital planes and circularizes the orbit at GEO.
	06:17:26		39793.9	Impulse is complete, coast to dock with station at GEO
Docking Maneuvers	06:17:26		39793.9	Required impulses applied to dock with station at GEO.

GEOSYNCHRONOUS OPERATIONS

The specific activities and duration of this phase is a variable depending upon the requirements and operations associated with the deployment of the payload from the ASTV. During this time, any life support systems will be supplied by the station at GEO. The mass of the ASTV is decreased by 20,000 lbm as the payload is delivered (current mass of the ASTV is now 19,793.9 lbm).

Event	Time h:m:s	ΔV ft/s	Mass lbm	Comments
ASTV performs separation	00:00:00	20.0	19793.9	ASTV performs separation from GEO station. ΔV is sufficient to the station from all hazards associated with ASTV separation. Coast to near the nodal crossing.
Impulse to take ASTV to Phasing Orbit	00:00:01	5894.2	19769.4	This impulse takes the ASTV on a transfer ellipse to a target perigee of 52.54 mi., orbital plane is changed from 0.0° to 26.3°.
	00:01:42		13734.7	Impulse is complete coast to mid-course corrections.
Mid-course corrections applied	02:37:13		13734.7	Mid-course corrections performed if required by orbital position. Once applied, coast to atmospheric entry,
Release disposable tanks	05:00:00		12558.1	Disposable tanks are jettisoned away from the ASTV before it begins the aerobraking maneuver. Any fuel left in the tanks is discarded.
Coast to Atmosphere (400,000 ft)	05:09:27		12558.1	ASTV enters atmosphere with γ = -4.0° and a speed of 33,818.2 ft/s, aerodynamic braking and maneuvering begin.
Exit Atmosphere	05:12:37		12558.1	Exit atmosphere with γ = 4.0° and a speed of 26,127.6 ft/s.
Circularize at Phasing Orbit	05:56:27	448	12558.1	ASTV burns to circularize at a phasing orbit altitude of 350 mi.
	05:56:33		12215.2	Impulse is complete, coast at phasing altitude
Coast at Phasing Orbit	06:07:53		12215.2	At this altitude, complete approximately one orbit while making any necessary corrections after atmospheric flight.
	07:32:28		12215.2	Orbit at phasing altitude is complete, prepare to transfer to LEO.
ASTV insertion into LEO transfer orbit	07:32:28	221.0	12215.2	Impulse takes the ASTV along a transfer ellipse arriving at LEO, applied at the proper time to meet space station at LEO.
	07:32:31		12049.6	Impulse is complete, coast to LEO.
Circularize at LEO	08:19:14	222.9	12049.6	Circularize orbit at LEO, prepare to dock with the space station.
	08:19:17		11884.7	Impulse is complete.
Docking Maneuvers	08:19:17		11884.7	Required impulses applied to dock with space station.